Universität für Bodenkultur Wien

University of Natural Resources and Life Sciences, Vienna

Department of Water, Atmosphere and Environment

Institute of Hydraulics and Rural Water Management

Master Thesis

DEVELOPING WATER EROSION PREDICTION TECHNOLOGY FOR NEW ZEALAND

by

Hanna Schilcher

0840822

Supervisor: PhD Andreas Klik

Co-supervisor: PhD Thomas Cochrane

September, 2015

ACKNOWLEDGEMENTS

To accomplish a thesis like this, a lot of support, patience and allocation of equipment is required. The experimental, modeling and most of the writing was executed at the University of Canterbury in Christchurch for four months. Afterwards it was completed at the University of Natural Resources and Life Sciences in Vienna.

First of all I appreciate the encouragement and backing of my family and friends who assisted me during all stages and facilitated the fulfillment of my thesis.

Secondly I express my gratitude to my supervisor Andreas Klik, who enabled the whole project. Furthermore, I appreciate his support and patience at the University of Life Science.

Thirdly I want to thank my co-supervisor Tom Cochrane for his adjuvant assistance during the whole experimental period. Additionally he arranged the appropriation of all requirements at the University of Canterbury and the support of the employees at the department of Civil and Natural Resources Engineering. Here I directly mention Peter McGuigan and Ian Sheppard.

TABLE OF CONTENTS

LIST OF TABLES

LIST OF FIGURES

ABSTRACT

Several existing erosion model programs offer different methods for erosion modeling. Erosion strongly depends on the soil material, the climate, slope and land management and use. The WEPP (Water Erosion Prediction Project) models soil erosion as a process of interrill and rill detachment and transport. For that assumption a rill and interrill erodibility parameter need to be defined for the area of interest. These parameters can be described as soil properties in terms of resistance against soil erosion, but they are not readily definable for each soil texture. A lot of values are derived from the experiments carried out in the United States to develop the WEPP model. (Laflen, Elliot, Simanton, Holzhey, & Kohl, 1991) and (Elliot et al. 1989) With those experiments it was possible to describe the rill and interrill erodibility of a broad range of different soils. These experiments were used to suggest equations which calculate the rill and interrill erodibility. They are based on other soil properties such as soil texture, organic matter content and bulk density. The WEPP model uses those equations if the input data are not available.

This thesis explains methods how to obtain the erodibility with laboratory experiments which are carried out at laboratory of the University of Canterbury, Christchurch, NZ. Two separate attempts are used to derive interrill and rill erodibility and critical shear strength of two soil samples. The soil samples originate from the Loess depositions at the Banks Peninsula, New Zealand.

With the experimental results and the grain size distributions the applicability of the WEPP model is tested. It is based on the equation which WEPP provides for interrill and rill erodibility and the critical shear stress. According to the interrill experiment it shows an increasing divergence with steeper slopes. The differences resulting from the experimental and modeled rill erodibility, yield to new empirical equation which is valid for a defined range of soil textures.

1 INTRODUCTION

1.1 Research Question and Interest

The aim of this thesis is to develop a modified water erosion prediction technology for New Zealand. Already in the 1960s erosion was recognized to be one of the great threats of New Zealand's prosperity/welfare/economic vitality. 70 percent of New Zealand consists out of hills and high country. In the late 1930s about two-thirds of these areas were affected by erosion. Control measures in order to reduce erosion on farmlands for the future have been started to been set up (Reed & Reed, 1960). But nowadays the rate of soil formation is still exceeded by the rate of erosion causing depletion of soil resources and productive potential. The inequality between soil-formation and soil erosion is often a result of human activities. The increase of global population and the concomitant demands for food, shelter and increasing standard living expectations lead to faster depletion processes and larger areas. The problem for soil erosion is not necessarily at its large range though. The average erosion rates compensate the maximum and minimum values. There can be wide parts barely affected by erosion but some minor parts which effectuate the most of the proportion of the total erosion (Toy, Foster, & Renard, 2002).

The development and management of effective erosion control programs demand understanding of erosion processes, accurate measurement and estimation methods and acquirement of erosion-control techniques (Toy et al., 2002). Although measurements have been made and still need to be done for some individual farms and catchments, it is not economical to observe the current situation and propose the best management practice for all locations on the Earth's surfaces seperartely. Therefore appropriate assessments, evaluations and predictive tools have been developed over the last 30 years. The models have not been tested of all possible circumstances and so they are only applicable for a limited range of conditions, concerning scale and the most influencing erosion factors such as climate, soil, slope and land use (Morgan & Nearing, 2011).

The most widely known and accepted method is the usage of the empirical United Soil Loss Equation (USLE). It was first introduced in 1965 and is based on a regression analysis of data from hundreds of experimental plots of the United States Department of Agriculture (USDA) Soil Conservation Service. It later got modified into the Revised Universal Loss Equation

(RUSLE) in 1997. They both compute the average annual soil loss from field areas triggered by rill and sheet erosion from rainfall and runoff corresponding to:

$$A = R * K * L * S * C * P \qquad 1\text{-}1$$

A… Potential long-term average annual soil loss (t ha^{-1})

R … Rainfall-Runoff erosivity factor (MJ mm (ha yr h)$^{-1}$)

K … Soil erodibility factor (t ha h (ha MJ mm)$^{-1}$)

L … Slope length factor (-)

S … Slop steepness factor (-)

C … Cover-Management factor (-)

P … Support practice factor (-)

(Wischmeier and Smith 1978)

The product gives an estimation of soil loss at the end of a slope as it was defined for the observed area. But it does not access deposition by overland flow or channel flow, nor gully flow or stream channel erosion. It can be applied for sheet and rill erosion where the boundary condition fit into the range of the equations (Dissmeyer & Foster, 1980) and (Morgan and Nearing 2011). These statistically based equations are proven and utilized for long-term averages and predictions, but for short-term periods or events more detailed information is required. Beside that and other theoretical and practical reasons, process-based erosion prediction models have attracted attention. With the ability to describe temporal and spatial distribution and the extrapolation possibility, a large range of situations can be covered (Yan, Yu, Lei, Zhang, & Qu, 2008) and (Nearing et al. 1989).

The process orientated Water Erosion Prediction Project (WEPP) is designed to replace the USLE for routine assessment of soil erosion. It was initiated in 1985 and carried out by the United States Department of Agriculture (USDA) Agricultural Research Service (ARS). The model separates water erosion into interrill and rill components and with the combined results the total erosion is calculated. It enables a great diversity of climates and additionally the WEPP has improved considerations of topography and the seasonal changes in crop growth, soil moisture and residue cover.

For the separate consideration of interrill and rill erodibility of the model, the existing determination of the susceptibility of soil to rill and interrill erosion were not adequate. Hence

a new set of equations had to be defined. The development of those was started by implementing a field research project to measure different erodibility of soils in the United States. With these experiments, the interrill and rill erodibility could be defined for a huge range of soils from the United States. Furthermore, equations were generated for calculating the interrill erodibility (K_i), the rill erodibility (K_r) and the critical shear stress (τ_c) in dependence on the soil properties such as sand, silt, clay and organic matter content (Elliott, Liebenow, Laflen, & Kohl, 1989). The WEPP model uses those equations if the input parameters are not known for the observed soil. Previous studies have shown that these generated values do not always lead to satisfying results (Romero, Stroosnijder, & Baigorria, 2007).

1.2 Objective

The primary objective of this study is to obtain experimental interrill and rill erodibility parameters for the soils which have been collected at the Banks Peninsula. Therefore, two different methods, one for interrill and one for rill erodibility estimation, are executed. For each of them a separate construction is set up in the laboratory.

The second objective is to test the Water Erosion Prediction Project (WEPP) for applicability for those soils and current conditions. The ideal intent was to achieve results for many different soil types of New Zealand. As this has turned out to exceed the range of this thesis, it focuses on the loess soil of the Banks Peninsula in Canterbury. This region is chosen because loess is known to be highly influenced by erosion (Shi & Shao, 2000) and there are several other ongoing projects concerning erosion at the Banks Peninsula, for which the results of this thesis might be useful for.

The interrill and rill erosion should be simulated on defined soil material in the laboratory with the application of a rainfall simulator and an artificial created inflow, respectively. After the experimental values are derived, they will be compared with the values resulting from the WEPP model.

2 BACKGROUND

Erosion can be defined as the movements of sediment and associated pollutants over the landscape and into water bodies (Morgan & Nearing, 2011) . Erosion can either be caused by wind or water. Erosion due to wind is a function which depends on the amount of detached sediment and the transport capacity of the wind but it is not further discussed in this study. Water erosion occurs when the forces acting on the soil are greater than the resisting forces.

The resisting forces which act against water erosion can be described with soil properties but they are highly influenced by topography, land use and land cover and the soil material itself. The topography can be described as geometry of the land surface. It can either be uniform or non-uniform. The important variables are slope length, slope steepness and the shape in profile and plan view. The increase of erosion along the length of uniform hill slopes is the result of the runoff accumulation. Also the augmentation of erosion is proportional with the increase of steepness. Non-uniform slopes like a concave-shaped hill form presents erosion uphill and sedimentation downhill compared to a convex slope where the erosion significantly increases with the length of the slope.

Land use has high influence on erosion and refers to general land use and land management which is applied. The type of vegetation is primarily defined by climate and soil, but the amount of vegetation is influenced by the management. Soil disturbances and bare soil are strongly affected by soil erosion because vegetation effects both, forces applied to the soil and resistance of the soil (Toy et al., 2002).

Soil properties depend on bedrock, pedogenic processes and human activities. Weathering, soil-forming processes and deposition of organic matter are the result of long term alteration. Changes over short time are mainly influenced by the variation of climatic condition and anthropogenic influence (Schaetzl & Anderson, 2005).

As the soil properties of the upper earth surface layer are essential parameters which have to be defined in this study, a short overview of the different components is given hereafter:

- Soil Texture

In general, clastic rock particles in a soil can be divided into fine earth fraction (<2 mm) and in a coarser fraction. Geologists commonly use the phi scale to describe the sizes of the particles (Schaetzl & Anderson, 2005) , whereas pedologists express the particle sizes in mm or µm. The fine earth fraction can be divided into 12 soil classes which are defined by the percentage of particles included, differentiated by their size into sand, silt and clay (Soil Survey Division Staff, 1993) and (Tan, 2005).

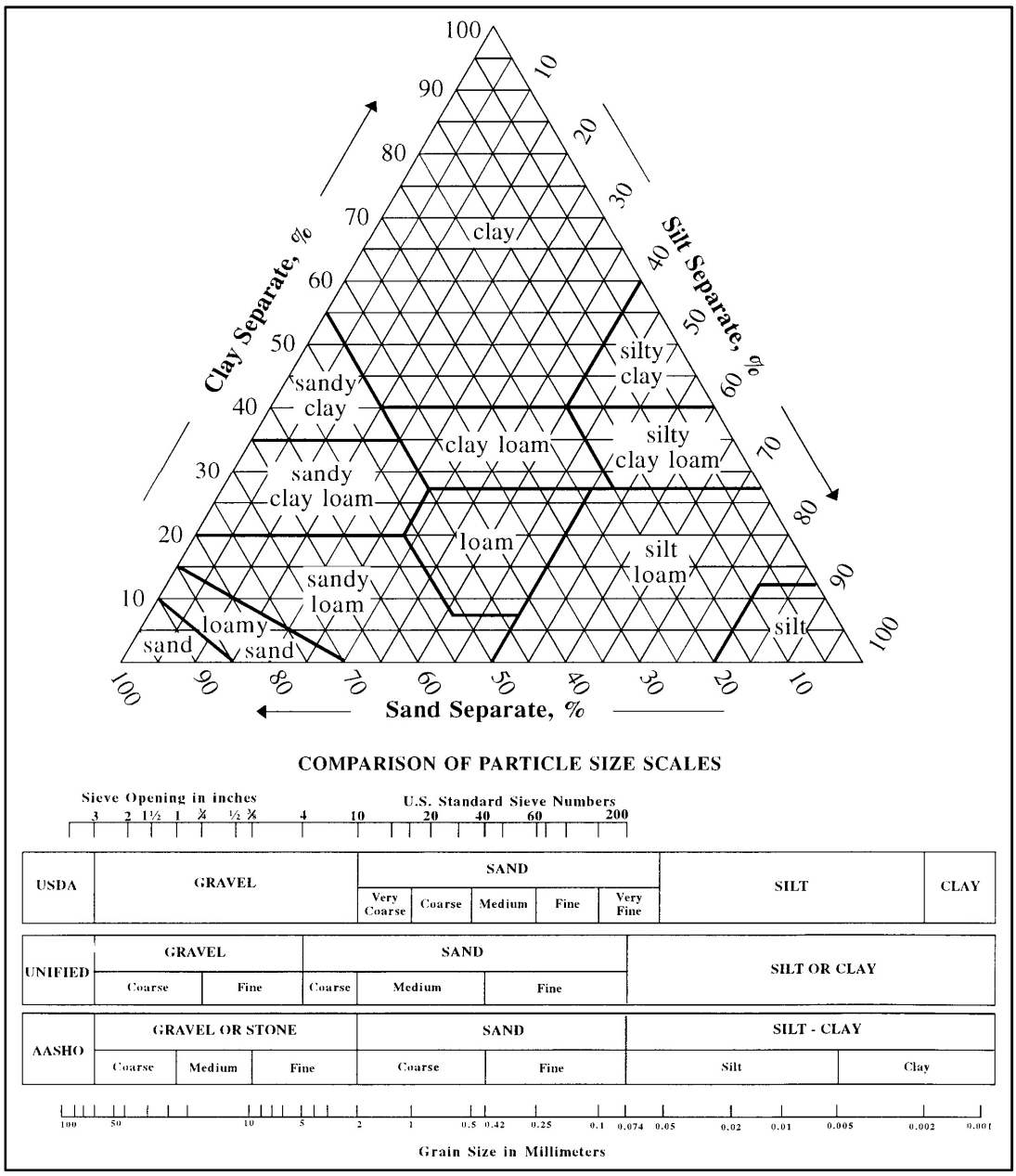

Figure 1. Soil Texture Classification. (Soil Survey Division Staff, 1993)

With analysis of the relative proportion of sand, silt and clay, the soil texture can be specified in its inorganic components. The organic matter, which is defined as organic fraction derived from living organism, is typically less than 5 percent. It accumulates in the upper layer and is the main energy source for macro- and microorganism and the processing of soil organisms releases vital plant nutrients like nitrogen and phosphorus (Rose, 2004).

- Soil Erodibility

Not to be mistaken for the term "soil erosion", "soil erodibility" is defined as the properties of the soil which cannot be readily defined or calculated (Bryan, 1968). Soil erodibility is the inverse of the soil resistance to erosion. The most influencing parameter is the soil texture. It is also affected by the soil organic matter content and the structure of the soil. The structure describes the arrangement of the soil aggregates within the soil and present binding agents which can be expressed in cation exchange capacity. These and more soil parameters are later described in Chapter 3.1.

As the erodibility of a soil is characterized by its resistance, it depends on the type of the occurring driving force. Soil erodibility can be divided into "interrill erodibilty" or "interrill erodibility factor" where the raindrops which are reaching the surface is the main driving force. The other phenomenon is "rill erodibility" or "rill erodibility factor" which is characterized by the discharge flowing down on the surface (Wischmeier & Smith, 1978). Their determination method and equations will be described in Chapter 2.1.

- Soil Shear Stress

The critical shear stress (τ_c) can be considered as a measure of soil resistance to erosion by flowing water. It is assumed that it has to be exceeded before soil particles start moving and therefore it is an important parameter considering rill erosion. It is used as governing detachment by runoff in several models (Léonard & Richard, 2004).

Beside the soil texture, the interrill and rill erodibility and the critical shear stress, soil parameter such as organic matter, particle size distribution, water content, effective hydraulic conductivity, bulk density and cation exchange capacity will be described in Chapter 3.1.

2.1 Interrill- and Rill erosion

Water soil erosion can be subdivided based on the spatial context and their topographic position within a watershed. Erosion can occur in open channels or pipes. There is one

classification possibility to define the erosion occurring on overland areas, based on their spatial context. It can be divided into two different phenomena. The erosion appearing in the small rill areas is defined as rill erosion, where the detachment is mainly driven by surface runoff. The traditional definition of rills is that they are channels which are so small that they get destroyed by normal tillage operations and formation will start at different location. The flow pattern of those rills is influenced by plant systems, roots, debris, rocks and local deposition provoking an uneven surface. The areas between these rills are identified as inter-rill areas, where the rainfall falling on the soil surface is the driving force. Another classification possibility is the sheet and rill erosion. They are likely used in the same context as rill and inter-rill erosion, but the difference between sheet and rill erosion is not their spatial position. Sheet erosion is a uniform removal from soil of the surface and recognized to be the first erosion process. With increasing erosion rill formation will start and rill erosion is assumed to begin. With progressing action gully erosion can start, which indicates deep carved channels (Toy et al., 2002). The processes and the forces occurring due to interrill and rill erosion will be described more detailed in Chapters 2.1.1 and 2.1.2 and their calculation and modeling methods which are applied in this study will be elucidated in Chapter 3.3.

2.1.1 Interrill erosion

The main driving force generating erosion due to water is rainfall. The erosion process and amount varies a lot with changing topography, land use and cover and is depends on soil properties. Water erosion can be evoked by raindrops falling on the soil which is considered as main force triggering interrill erosion. It is influenced by the size of the raindrops and intensity and duration of the rainfall. When the raindrops fall directly on the bare soil surface, it can break down the soil structure of the upper particles (surface seal). Therefore the resistance of the soil surface is reduced and transportation of the particles is more likely to occur (Rose, 2004).

With a rainfall simulator, the process and characteristics of natural rainfall can be successfully simulated. A rainfall simulator is an ideal tool for rebuilding soil infiltration, soil erosion and other relative field researches. If there is no strong influence of wind, the rainfall intensity, raindrop distribution, terminal velocity, rainfall energy, spatial distribution of raindrops and validity of rainfall areas are known. There are different types of rainfall simulators, all should be light enough to be transported and suitable for field conditions (Metzinger, n.d.).

In this thesis, a rainfall simulator is used to perform interrill erosion on soil in a laboratory. The force introduced due to the precipitation is rainfall erosivity, which depends on rainfall amount, rainfall intensity and kinetic energy. By concentrating on the most influencing factors (amount and intensity), an estimation of the total erosivity of a storm event (for raindrop impact) can be made by multiplying erosion per unit rainfall (measured with rainfall intensity) with rainfall amount. The total kinetic energy is proportional to the total amount of rainfall in a storm event (Toy et al., 2002).

The interrill detachment rate (D_i) can be simulated by using a rainfall simulator and is calculated with the following equations:

$$D_i = K_i * I^2 \qquad 2\text{-}1$$

Further investigations, comparison and collection of other studies led to a modification, where the slope was added to the equation:

$$D_i = K_i * I^2 * S_f \qquad 2\text{-}2$$

D_i… Interrill detachment rate (kg $m^{-2}s^{-1}$)

K_i… Interrill erodibility constant, (kg s m^{-4})

I… Rainfall intensity (m s^{-1})

S_f… Slope factor (-)

For lower slopes interrill transport limits erosion and higher slopes raindrop detachment is limiting interrill erosion (Foster, Meyer, & Onstad, 1977), this is included into the equations with:

$$S_f = 1.05 - 0.85 * \exp(-4 \sin(\alpha)) \qquad 2\text{-}3$$

α… Slope angle (°)

(Elliot et al. 1989).

2.1.2 Rill erosion

The runoff flowing over the soil surface is the driving force for rill erosion. Once the runoff has started, the occurring processes can be distinguished into detachment, entrainment, transport and deposition of the soil particles. The capacity of runoff transporting material depends on the transportability, which is related to the particle size and density of the material

and the occurring shear stress of the flow. Before particles begin to move, a critical value of the shear stress has to be exceeded (Rose, 2004).

The erosion can either be commenced due to the raindrops falling on the surface or by overland flow. The effect of raindrops can be very significant in shallow flows. The impact and splash of a raindrop can augment the sediment concentration in the flow (Rose, 2004). Focusing on overland flow there are two prerequisite conditions which lead to surface runoff causing soil erosion. Either the soil is saturated or the rainfall intensity transcends the infiltration capacity of the upper soil layer. The infiltration capacity is the maximum rate of water that can be uptaken by the soil (Toy et al., 2002). Once surface runoff has started, there are different movements sediments can undergo. After detaching, sedimentation is possible again. But if they have been detached from their origin place once, the cohesion between the particles is much smaller and it is likelier that they get moved again (Rose, 2004).

The description of soil erosion processes occurring due to overland flow, are very similar to erosion in stream beds. This has led to use sediment transport equations to describe flow characteristics and movements of soil erosion (Hairsine & Rose, 1992a). The mixture of water and sediments flowing down the surface introduces a force called shear stress (τ).

The ability of the flowing liquid to erode soil is named stream power (Ω) and is the product of the shear stress and the flowing velocity. Flow driven soil erosion occurs when the stream power exceeds a certain threshold of the soil:

$$\Omega = \tau * v \qquad 2\text{-}4$$

Ω… Stream power (N m^{-1} s^{-1})

v… Velocity (m s^{-1})

τ… Shear stress (N m^{-2})

(Rose, 2004) and (Hairsine & Rose, 1992b).

The shear stress depends on the density of the flowing medium (ρ), the acceleration gravity (g), the hydraulic radius (R) and the inclination of the slope (α):

$$\tau = \rho g R sin(\alpha) \qquad 2\text{-}5$$

τ… Shear stress (N m^{-2})

ρ… Density (kg m^{-3})

g… Acceleration of gravity = 9.81 m s^{-2}

R… Hydraulic radius (m)

α… Slope

How long or far the particles are transported is influenced by their own settling velocity, resulting from the particle size and density. The amount of soil which gets detached is affected by the sediment concentration of the water flowing down. Therefore the net soil detachment is calculated as:

$$D_f = D_c * \frac{1 - G}{T_c} \qquad 2\text{-}6$$

D_f… Net detachment rate (kg s^{-1} m^{-2})

D_c… Soil detachment capacity (kg s^{-1} m^{-2})

G… Sediment load in rill (kg m^{-1} s^{-1})

T_c… Transport capacity (kg m^{-1} s^{-1})

For clear water flowing down the bed a linear regression fit can be assumed, where $G = 0$ and $\frac{1-G}{T_c} = 1$.The rill detachment capacity describes the maximum detachment rate that occurs when there is no sediment in the water. This results to:

$$D_c = K_r * (\tau - \tau_c) \qquad 2\text{-}7$$

K_r… Rill erodibility (s m^{-1})

τ_c… Critical shear stress (N m^{-2})

(Bjorneberg et al. 2010).

2.2 Water Erosion Prediction Technologies

Different model types have been developed which can be distinguished between physically based, stochastic and empirical models. Physically based models describe the processes are involved in the model and take the laws of conservation of mass and energy in account. Stochastic based models use the statistical characteristics of existing data to bring out synthetic sequences of data. They can be used for generating input sequences for physical and empirical models if the available periods of observation are short. Empirical based models deploy statistically significant relationships between assumed important variables for a reasonable data base. They can be subdivided into black-box (based on input- and output

studies), grey box (some details of the processes are considered) and white box model (where the whole system operations are known) (Morgan & Nearing, 2011).

Process based models provide several major advantages over empirically based erosion prediction technology such as the capability to estimate spatial and temporal distributions of soil loss. They can be extrapolated to a broad range of conditions (Nearing, Foster, Lane, & Finker, 1989).

2.2.1 Water Erosion Prediction Project

The Water Erosion Prediction Project is a processed-based model, which was initiated by Dr. George R. Foster with the intent to replace the empirically based Universal Soil Loss Equation for typical agricultural land. To develop the model and to gain data for model parameterization, a core team of scientists was formed. They contrived the basic hydrologic and erosion logic and implemented field experiments (Elliott et al., 1989) and (Laflen et al., 1991). In 1995 they documented and validated WEPP was released at a Soil Water Conservation Society symposium in Des Moines, Iowa (Flanagan & Livingston, 1995). Since then there are ongoing developments of the model, its interface and database, validation and application. However the effort of the accomplished works never reached the level of the initial project.

WEPP is a distributed parameter model that can be operated in hill slope profiles or watershed configurations. The recommended length of a hillslope is 1 to ~ 100 m, however it can also be used with slopes of lengths of several hundreds of meters. For smaller watersheds up to 260 ha it gives satisfying results on sediment yield. Larger regions can be successfully simulated where a great risk of runoff and soil loss subsists. It submits simulation of major processes of overland flow, sheet and rill erosion, erosion from small channels and ephemeral gullies. The hydrological processes used and simulated in the model are surface and subsurface water movement, including percolation, deep seepage, sub surface lateral flow and demarcating impervious subsurface layers.

This study focuses only on the simulation of single hill slope profiles where the output of the model is the total amount of precipitation in mm, the runoff in mm, the soil loss in kg m^{-2} and the sediment yield in t ha^{-1}.

The four basic input files are slope, soil, management and climate. Despite WEPP provides a huge range of existing data files from the United States, new input files can be created or

uploaded. To get the desired climate file, there are different possibilities and requisites to use data from existing rainfall events. The application range varies from single storm events to very long rain periods. Climate input data can also be modified to approximate the impacts due to climate change on future climate by varying frequency, amounts and intensities of precipitation or different temperature. For creating a single storm event, storm depth, storm duration and intensity information is required.

The management file is characterized by the land use, according to the growing period of the vegetation and its seasonal management.

To describe the hillslope file, length and slope of the area can be defined.

The soil file is generated due to soil texture, organic matter, cation exchange capacity, soil depth and if existing, different layers. It is possible to define the albedo and the initial water content of the soil. A restriction layer can supplementary be defined with its saturated hydraulic conductivity and with an anisotropy ratio, which defines the ratio between the lateral and vertical flow. In addition to these the interrill erodibility (K_i), rill erodibility (K_r), critical shear strength (τ_c) and effective hydraulic conductivity (k_{feff}) can be either manually added or automatically calculated by the model. For single storm event simulation, the initial water saturation level is crucial to define as WEPP uses it for adjustment of the infiltration (effective hydraulic conductivity) and erodibility parameters.

WEPP provides parameters for the baseline soil erodibility. The estimation represents values for cropland that is freshly tilled and without crop residues. Rangeland is considered as fully consolidated and where all surface residues are removed. Based on erodibility experiments carried out in the United States, following equations are provided for the automatically executed estimation of K_i, K_r and τ_c (Flanagan, Frankenberger, & Ascough, 2012):

For cropland soil containing more than 30% sand:

$$K_i = 2728000 + 192100 * VFS \qquad 2\text{-}8$$

$$K_r = 0.00197 + 0.00030 * VFS + 0.03863 * EXP(-1.84 * ORGMAT) \qquad 2\text{-}9$$

$$\tau_c = 2.67 + 0.065 * \mathrm{CLAY} - 0.058 * \mathrm{VFS} \qquad 2\text{-}10$$

VFS… Percentage of very fine sand

CLAY… Percentage of clay

$ORGMAT$… Percentage of organic matter in the surface

These equations require a value for VFS less than 40% (otherwise 40 % should be used). The value for ORGMAT needs to be greater than 0.35% (if it is lower use 0.35%). For CLAY the value must be less than 40% (if higher 40% is applied).

If the cropland soil contains less than 30% sand:

$$K_i = 6054000 - 55130 * CLAY \quad 2\text{-}11$$

$$K_r = 0.0069 + 0.134 * EXP(-0.20 * \mathrm{CLAY}) \quad 2\text{-}12$$

$$\tau_c = 3.5 \quad 2\text{-}13$$

Here CLAY must be greater 10%. If differently, 10% is utilized.

For rangeland soils the baseline erodibility equations are:

$$K_i = 1810000 - 19100 * SAND - 63270 * ORGMAT - 846000 * \theta_{fc} \quad 2\text{-}14$$

$$K_r = [0.000024 * CLAY - 0.000088 * ORGMAT - 0.00088 * BD_{dry} - 0.00048 * \mathrm{ROOT10}] + 0.00017 \quad 2\text{-}15$$

$$\tau_c = 3.23 - 0.056 * \mathrm{SAND} - 0.244 * \mathrm{ORGMAT} + 0.9 * \mathrm{BD}_{dry} \quad 2\text{-}16$$

θ_{fc}… Volumetric water content at 0.033MPa ($m^3\ m^{-3}$)

BD_{dry}… Bulk density ($g\ cm^{-3}$)

ROOT10… Total biomass within upper 10 cm ($kg\ m^{-2}$)

WEPP user's summary suggests values for K_i between $1x10^4$ and $2x10^6$ kg s m^{-4}, for K_r a range is defined between $1x10^{-4}$ and $6x10^{-4}$ and τ_c can vary between 1.5 and 6.0 Pa (Flanagan and Livingston 1995b).

Those parameters are used to determine the total erosion which is composed out of interrill and rill erosion and described in the WEPP as the following:

$$\frac{dG}{dx} = D_f + D_i$$

dG... Sediment load (kg s^{-1} m^{-1})

x... Downslope distance (m)

D_i... Interrill sediment delivery to the rill (kg s^{-1} m^{-2})

D_f... Rill erosion rate (kg s^{-1} m^{-2})

The interrill erosion modeling is based on the equations which are previous described in Chapter 2.1.1 for the interrill erosion. It is modified to the following equation:

$$D_i = K_{iadj} * I_e * \sigma_{ir} * SDR_{RR} * F_{nozzle} * \left(\frac{R_S}{w}\right) \quad \textit{2-17}$$

K_{iadj}... Adjusted interrill erodibility

I_e... Effective rainfall intensity (m s^{-1})

σ_{ir}... Interrill runoff rate (m s^{-1})

SDR_{RR}... Sediment delivery ratio

F_{nozzle}... Adjustment factor for sprinkler irrigation Nozzle

R_s... Spacing of the rills (m)

w... Rill width (m)

For the rill modeling WEPP applies a modification of the DuBoys channel scour equation (Equation 2-7). Graf (1971) and Meyer and Foster (1972) showed that the rill detachment depends on the sediment concentration of the flowing medium. With increasing concentration a decreasing detachment was recognized. Therefore WEPP includes algorithms which incorporate the sediment load of the discharge. Rill erosion is modeled with:

$$D_f = D_c \left(1 - \frac{G}{T_c}\right) \quad \textit{2-18}$$

$D_c(x)$…Rill detachment capacity by rill flow (kg m^{-2} s^{-1})

$T_c(x)$... Sediment transport capacity in the rill (kg m^{-1} s^{-1})

$$D_c = K_r(\tau_f - \tau_c) \quad \textit{2-19}$$

K_r… Rill erodibility parameter (s m^{-1})

τ_f… Flow shear stress (N m^{-2})

τ_c… Rill detachment treshold parameter, critical shear stress (N m^{-2})

When sediment load, G is greater than sediment transport capacity, T_c net deposition in a rill is calculated with:

$$D_f = \frac{\beta\, V_f}{q}(T_c - G)$$

V_f... Effective fall velocity for sediment (m s^{-1})

q... Flow discharge per unit width (m^2 s^{-1})

β... Raindrop-induced turbulence coefficient

The coefficient β is designated a value of 0.5 for drops which impact rill flows. In case of snow melt of furrow irrigation a value of 1.0 is assigned.

(Flanagan, Nearing, Lane, Risse, & Finkner, 1995)

3 METHODOLOGY

The next chapter describes firstly the soil testing methods which are fulfilled to describe the soil properties. Secondly the experimental setups and techniques are delineated. Thirdly the calculation practices are explained.

3.1 Soil Testing

Six different soil characteristics are determined and redescribed in the following paragraphs.

3.1.1 Removal and determination of Organic Matter

The removal of organic matter can either be used for the determination of its content or it can be an essential pretreatment for followed soil testing methods. Depending on the post procedures, there are different methods for the removal of the organic content (Dane, 2002). It can be physically removed by heating or eliminated with chemical reagents such as hydrogen peroxide (H_2O_2), which is the suggested standard oxidant for pre-treatment of a particle size analysis.

If concentrated hydrogen peroxide (30% or 50%) is used, the concentration should be diluted to a 3 % solution with distilled water before applying on the soil samples. The soil is placed in small cylindrical vessels, where the solution can be infused easily. By adding the solution, foaming will start. This has to be done continually until the frothing has stopped. The samples can be heated up to 90°C to accelerate the time of completion. Once the digestion process has terminated, the sample has to be dried at 105°C, cooled in a desiccator and weight. Then the organic matter content is gravimetrically determined in the following way:

$$OM = \frac{M_i - M_f}{M_i} * 100 \qquad 3\text{-}1$$

OM… Organic matter Content (%)

M_i… initial Mass (g)

M_f… final Mass (g)

It has to be taken in consideration that it might take up to a week or more to achieve complete removal of the organic matter. It can be fastened up by warming the samples. By not taking a characteristic amount of soil, the result can be highly influenced.

Another widely used method is the loss-on-ignition method. The idea is to destruct all organic matter by heating. With the difference between the initial and the final sample weight, the total organic matter can be calculated. The temperature should be kept between 350 and 440 °C so that the inorganic carbonates stay within the sample. This method is not convenient for pretreatment of some soil texture analysis as the ashes of the burned materials can have high influence on the soil distribution. Both methods require a water/ moisture correction before calculating the organic matter content (Schumacher, 2002).

3.1.2 Soil texture analysis

There are different methods to obtain the soil texture. A rough estimation can be achieved by a "feel" of the sample. By rubbing a sample between the thumb and forefinger, clayed soils form a ribbon, sandy soils feel gritty and silt imparts smoothly. The accuracy of the field method strongly depends on skills and experiences of the sampler (Schaetzl & Anderson, 2005).The laboratory method is an indirect method, where the soil texture is conducted through the quantitative determination of soil separates. It is called the particle size distribution or mechanical analysis. The procedure consists of two steps.

First a complete dispersion of the soil sample is required to disrupt the aggregates into the individual particles. Therefore, a chemical reagent, such as NaOH (sodium hydroxide) or NaPO3 (sodium metaphosphate) is used.

The second step is the sedimentation. The different grain size diameters indicate the settling velocities, which are explained by the law of Stokes. Based on the law of Stokes the Bouyoucos Hydrometer measures the amount of particles in suspension in grams. It is applicable for soil fraction of sand, silt and clay. A previous sieving of the soil sample should be applied not to disrupt the results and estimate the larger particle fractions. It is assumed that:

Sand, all particles > 0.06 mm settle after 40 seconds

Silt, particles between 0.06-0.02 mm will settle after 6 hours

With the results, the mass percentage of each fraction can be defined (Tan, 2005).

Another recent method is the application of laser light scattering (diffraction). It uses the principle that particles of a given size diffract light at a certain angle. The smaller the particles, the larger the angle. The limitation of the usage depends on the width of the laser beam and the capable measuring of the scattering angle. The result is the distribution of particle size

spheres with equivalent cross sectional area. One limitation is that particles with diameters close to the wavelength of the light, do not diffract the light (Dane, 2002). If the material includes coarser fractions which are not in the range of these instruments, a separation with sieves with accurate mesh sizes should be preceded. As the soil texture is a crucial parameter, both methods are applied. The laser light scattering is realized with a particle size analyzer (PSA). The available model is a Horiba LA-950V2, which is able to capture particles ranging from 0.01 to 3000 µm. It can be run with dry or wet samples. To attain the particle size distribution for the sample material the wet test was chosen because of the pre-treatment with hydrogen peroxide. The result of the one analysis is obtained in a few minutes after the test, but several tests have to be carried out to ensure the characteristic of the soil. For each soil three wet samples are put into the Particle Size Analyzer. To get the average value for one sample out of at 3 samples, between 3 and 7 tests had to be made. The same material is kept in the sample chamber, but with different setting mode of the analyzer, different results are experienced. The influence of varying circulation speed of the pump, which supplies the machine, the influence of different ultrasonic operation, which can break down aggregates and the influence of varying agitation speeds, is observed.

3.1.3 Methods for analyzing the water content

There are several direct and indirect methods to obtain the water content of a soil The water content itself can be distinguished in total soil moisture content and available water content, which is the amount of water held by soil between field capacity and wilting point (Tan, 2005). Direct methods utilize separation or removal of water from the soil to obtain the removed amount of water. It can be fulfilled by heating, extraction and replacement by solvent or chemical reaction. The amount of removed water can therefore be shown in the change of mass after treatment. Indirect methods reason the water content from physical or chemical properties of the soil, such as the dielectric constant, electrical conductivity, heat capacity, hydrogen content and magnetic susceptibility. The indirect methods are less destructive, but the accuracy depends on strength of the relationship between the measured property and the volumetric water content.

Traditionally, the water content is expressed as ratio or percentage of the soil. It has to be clarified whether the relation is described as a ratio of two masses or of two volumes. The mass-based gravimetric water content is related to the volume-based water content as follows:

$$\Theta_V = \frac{\rho_b}{\rho_w} * \Theta_m \qquad 3\text{-}2$$

Θ_V… volumetric water content (m^3/m^3)

ρ_b… bulk density (kg/m^3)

ρ_w… bulk density (kg/m^3)

Θ_m… mass basis gravimetric water content (kg/kg)

(Black, 1965)

The initial water content is captured with an EC-5 Soil Moisture Sensor from Decagon Devices. Although the measurement is based on the dielectric constant of the soils, the shown value on the display is the volumetric water content (Decagon Devices, 2013).

3.1.4 Infiltration and hydraulic conductivity

Infiltration is the first process where water starts entering the soil from the surface. The infiltration rate is measured in length unit per time and is affected by the soil texture and pore size, the percentage of swelling clay and the organic matter content of the surface. It depends likewise on the mode of alimentation and on its vegetation cover. A varying influencing factor is the initial soil water content. Once the water has infiltrated and is moving vertical through the soil, it is called percolation (Musy & Higy, 2011) and (Decagon Devices, 2007). Various parameters can be obtained by measuring the infiltration, depending on the applied device and practice (Musy & Higy, 2011). For this thesis the desired parameter is the effective hydraulic conductivity. The hydraulic conductivity describes the ability of the bulk soil to transit water (Delleur, 2007).

For obtaining the hydraulic conductivity, a minidisk infiltrometer is a handy applicable measuring instrument which can be applied in the field or in the laboratory. In this study, the hydraulic conductivity is measured with the soil samples which are used for the erosion simulation. The method is based on the measurement of the infiltrating water volume in a certain time inside a cylinder. The water can infiltrate into the soil through a porous sintered stainless steel disc. It can be manually adjusted with a negative pressure to ensure that the water cannot flow through macro pores or cracks. The preserved parameter is the water volume changing over time. Depending on the soil properties and especially soil texture, reasonable time intervals have to be chosen and different Van Genuchten parameters are used

for the calculation. To compute the hydraulic conductivity with a minidisc infiltrometer, the following method is proposed by (R. D. Zhang, 1997)(R. D. Zhang, 1997)(Zhang 1997)(R. D. Zhang, 1997):

$$I = C_1 \mathrm{t} + C_2\sqrt{t} \qquad 3\text{-}3$$

I… Cummulative Infiltration (cm)

C_1… Parameter for hydraulic conductivity (m s^{-1})

C_2… Parameter for soil sorptivity (m s^{-1})

t… Time (s)

$$k = \frac{\mathrm{C}_1}{A} \qquad 3\text{-}4$$

k… hydraulic conductivity (m s^{-1})

A… Value relating van Genuchten parameters for given soil types

$$A = \frac{11.65(n^{0.1} - 1)\exp\left(2.92(\mathrm{n} - 1.9)\alpha h_0\right)}{(\alpha r_0)^{0.91}} \quad n \geq 1.9$$

$$n \geq 1.9 \qquad 3\text{-}5$$

$$A = \frac{11.65(n^{0.1} - 1)\exp\left(7.5(\mathrm{n} - 1.9)\alpha h_0\right)}{(\alpha r_0)^{0.91}} \quad n < 1.9 \qquad 3\text{-}6$$

$$n < 1.9 \qquad 3\text{-}6$$

α… Van Genuchten parameter listed in Table 1

n… Van Genuchten parameter listed in Table 1

r_0… Disk radius (cm)

h_0… Suction (cm)

The twelve texture classes are obtained from (Carsel & Parrish, 1988). The van Genuchten Parameter are presented in Table 1:

Table 1. Van Genuchten paramaeter values.

			h_o						
	α		-0.5	-1	-2	-3	-4	-5	-6
Texture		n	A						
sand	0.145	2.68	2.84	2.40	1.73	1.24	0.89	0.64	0.46
loamy sand	0.124	2.28	2.99	2.79	2.43	2.12	1.84	1.61	1.40
sandy loam	0.075	1.89	3.88	3.89	3.91	3.93	3.95	3.98	4.00
loam	0.036	1.56	5.46	5.72	6.27	6.87	7.53	8.25	9.05
silt	0.016	1.37	7.92	8.18	8.71	9.29	9.90	10.55	11.24
silt loam	0.020	1.41	7.10	7.37	7.93	8.53	9.19	9.89	10.64
sandy clay loam	0.059	1.48	3.21	3.52	4.24	5.11	6.15	7.41	8.92
clay loam	0.019	1.31	5.86	6.11	6.64	7.23	7.86	8.55	9.30
silty clay loam	0.010	1.23	7.89	8.09	8.51	8.95	9.41	9.90	10.41
sandy clay	0.027	1.23	3.34	3.57	4.09	4.68	5.36	6.14	7.04
silty clay	0.005	1.09	6.08	6.17	6.36	6.56	6.76	6.97	7.18
clay	0.008	1.09	4.00	4.10	4.30	4.51	4.74	4.98	5.22

(Decagon Devices, 2007)

3.1.5 Bulk Density

The bulk density is determined by the cylindrical core method. The soil cores are taken from the simulation containers after all the experiments are finished. With the known volume of the soil sample inside the cylinder and the weight of the dried soil mass, the bulk density can be defined with:

$$\rho_{bulk} = \frac{m_{dry}}{V_{tot}} \qquad 3\text{-}7$$

ρ_{bulk}… Bulk density (g cm^{-3})

m_{dry}… Mass of dried soil (g)

V_{tot}… Volume of sample before drying (cm^2)

(Dohrmann, 2006)

3.1.6 Cation Exchange Capacity (CEC)

Cation exchange capacity is the quantity of cations adsorbed on soil particles per unit of mass of the soil under chemically neutral conditions (milliequivalents/100 grams of soil). (WEPP HELP) It is a soil property which describes the ability to hold and release various elements and compounds. It is highly influenced by the content of clay and organic matter (Dohrmann 2006). The determination is carried out by the Hill Laboratory.

3.2 Experimental set up and procedure

As the WEPP model assumes no surface crop residues for rangeland and farmland to calculate the soil baseline, interrill erodibility (Ki), rill erodibility (Kr) and critical shear stress (τ_c), bare soil is used for all experiments. The first step of both erosion experiments is the soil preparation followed by the adjustment of the driving forces, which are rainfall for interrill erosion and a discharge for rill erosion. Once those are set up, the simulation can be run with different inclinations. The output of the experiments is the eroded material, which is collected during each trial and used for further calculations.

3.2.1 Interrill Erosion

The experimental interrill erosion can be sectioned into three parts. The first is the rainfall calibration, which is only run once and the derived values are used for all following simulations. The second part is the soil preparation. Three soil containers with the material from Caton Bay and three containers with the material from Okana valley are needed. The third one is the rill experiment itself.

Rainfall Calibration

The raindrops falling on the surface introduce the main driving forces for interrill erosion, a rainfall simulator is utilized to obtain spatial rainfall. The rainfall simulator had to be put on its right position so that it can stay there for the following simulation months. The model specification is VeeJet 80100[1].

The available rainfall intensities cover a range from 9.5 m h^{-1} up to 99.0 m h^{-1}, depending on the height and operating pressure a variation is possible. With increasing pressure the drop size gets reduced and therefore the velocity as well. It is segmented into 5 steps which can either be single or double switched and operated at 6 psi.(View my documents Rainfall Simulator Specifications) To get the corresponding intensity to the observed area calibrations are carried out.

The RUSLE model uses the maximum 30 minutes intensity (i_{30}) (mm h^{-1}) for calculating the rainfall erosivity (Renard, Foster, Weesies, McCool, & Yoder, 1997). As it is used for the RUSLE it was tried to get the maximum intensity for a 30 minutes period (i_{30}) of the site area.

[1] Design based on Norton Ladder Rainfall Simulator Developed by USDA- ARS.NSERL at Purdure University-West Lafayette, Indiana

According to the National Climate data base the maximum 30 minutes intensity of the Okuti[2] measuring station between 2000 and 2013 varied between 9 mm and 24.1 mm. The first calibration is used to assimilate the operating rainfall intensity to the appropriate rainfall intensity of the catchment. The calibration started at the medium intensity of the rainfall simulator. The empty containers with the same size as the interrill containers are weighed and placed on defined positions. Then rainfall is introduced and collected for 10 minutes. The full containers are weighed again. With the difference of the two weights, the mass of water is known. By dividing it by the surface and the time step, the intensity is computed. To gain the intensity of the region where the soil is taken from, it has to be reduced. This procedure is fulfilled four times until the result is satisfying. The chosen intensity is at step 1 single operating and its mean value is 18.9 m h^{-1}. Each step was run twice for 10 minutes and then the average was taken as intensity for each position.

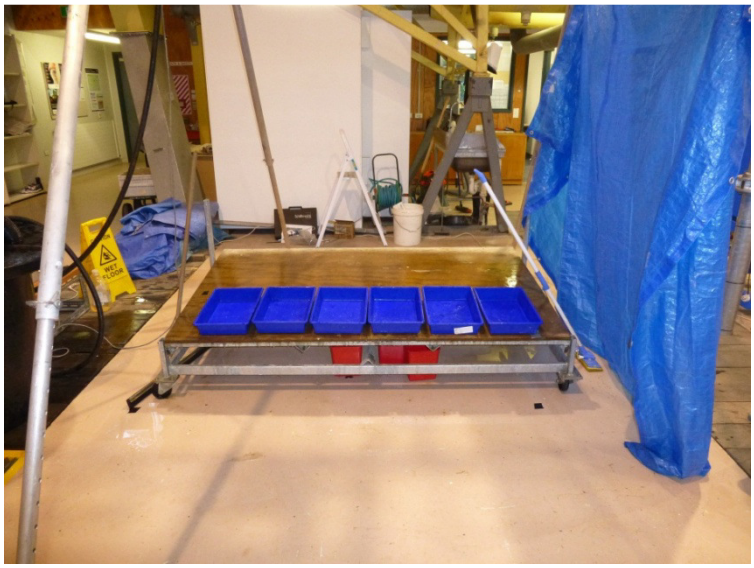

Figure 2. Container placement for first rainfall simulator calibration.

The second calibration is used to show the variation along the cross section. It varies between 17.5 m h^{-1} and 24.6 m h^{-1}, which has to be considered for the further calculations. The result of the second calibration is shown in Figure 3

The containers are numbered from 1 to 6 from left to right and their varying intensity is shown in Figure 3.

[2] Closest rainfall measuring station of the study area.

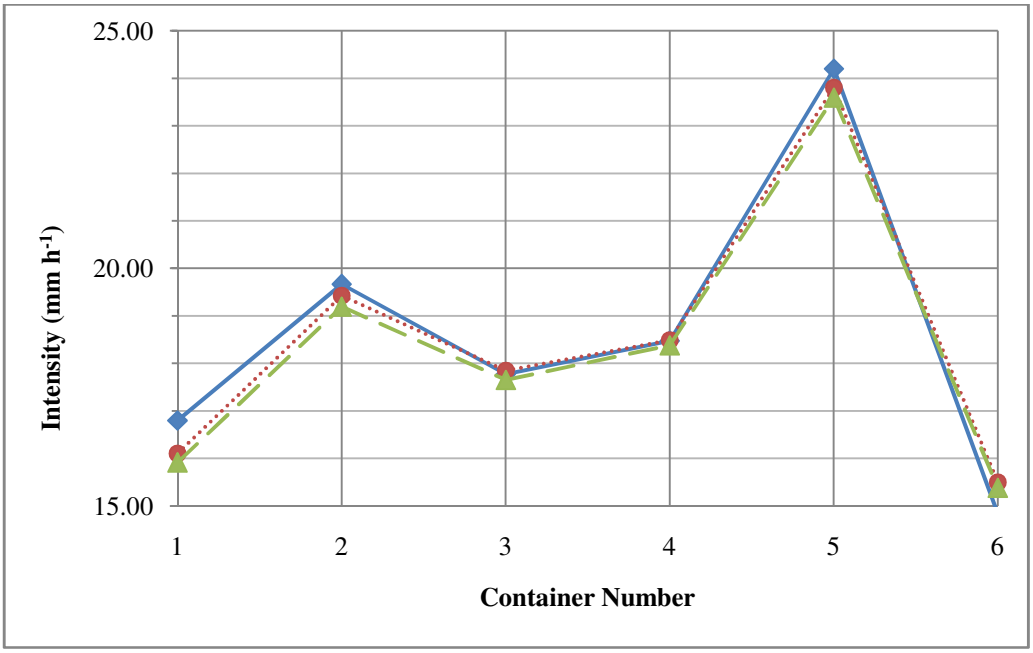

Figure 3. Spatially variing intensity of rainfall simulator obtained from three trials at step 1 single operating.

Three positions are used for the later interrill simulations. The chosen container positions are number 2 with a mean intensity of 19.31 m h^{-1}, position number 3 with a mean intensity of 17.72 m h^{-1} and number 4 with a mean intensity of 18.43 m h^{-1}. The calibration was executed for 10 minutes. The average intensity of those three values is 18.49 m h^{-1}.

Soil and Container Preparation

The vascular for the interrill erosion is a rectangular (37 x 24.5cm) tray with modifications. To prevent impoundment in the container, small pillars are attached to the bottom to higher it. Additionally, some holes are drilled in order to enable seepage. Coverage with geotextile is necessary to hold the soil particles back. Once the drainage system is completed, the soil can be put on top of it. At one of the narrow sides a funnel was attached to facilitate the collection of the eroding material and water flowing down. Covering the funnel was necessary during the rainfall to prevent disruption of the measured water amount. After trying several different methods for attaching the funnel to the container, it is put underneath the edge of the container and the other sides are raised with silicate to minimize splash erosion to the sides. The whole arrangement is put into a second same sized container where the infiltrating water can be captured. The lower vessel is equipped with a small hose on the lower narrow side, to prevent overflow. It is necessary that the constructions are properly connected and leaking is impended to assure the collection of the whole material. The connection of the funnels was firstly done

with silicone, but to shorten the drying period it is replaced by tape. For each material three containers are prepared.

Figure 4. Empty inner soil containers.

To ensure equal condition for all containers the collected soil is unified by putting it through a sieve with a mesh opening of 5 mm. Then the containers are filled with the material and ready to be used for the experiments.

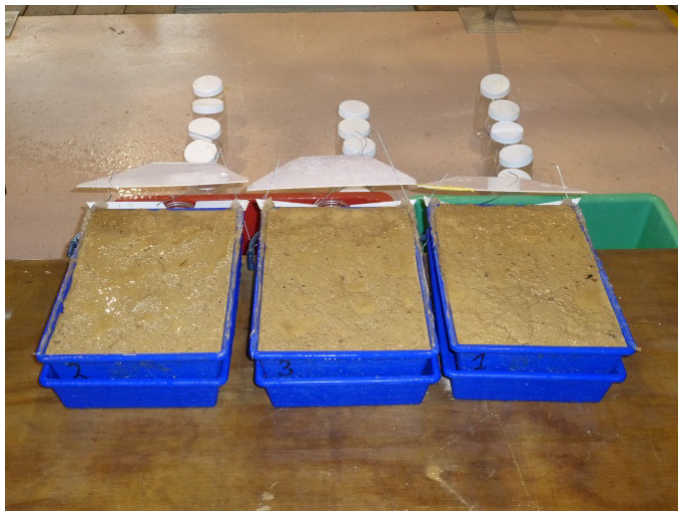

Figure 5. Prepared soil containers.

3.2.1.1 Experiment

The below described practice is conducted for the material collected in the Okana valley and the material from Caton Bay. The whole experimental work is implemented in the laboratory.

The aim of the attempt is to calculate the interrill erodibility. The required parameter can be defined by collecting the material during the implemented rainfall at the lower end of the funnel of each container. One run delivers the eroded material plus the runoff of three

containers which are placed on position 2, 3 and 4 (Figure 1). The experiment is executed three times to obtain three values for three different inclinations. The lowest is set up to 5 degrees, the medium at an inclination of 15 degrees and the steepest was put on approximately 30 degrees. As the soil surface changed due to the rainfall, the slope varies slightly. The inclination is measured before and after each trial at the upper, middle and lower part of the container. One trial lasts between 80 at 110 minutes. The collection containers are changed in a 10 minutes interval until the discharge is recognized as stable. The procedure can be delineated into following steps:

a) Ensure enough empty, weighed and labeled containers for capturing the material.
b) Put the three soil containers on the right position where the intensity was calibrated.
c) Measure the water content of the soil.
d) Adjust the requisite inclination to each container and measure it on the surface.
e) Cover the collection channel and place the gathering buckets underneath.
f) Switch on motor and pump of rainfall simulator.
g) Check the present water pressure.
h) Start the simulation and the chronograph.
i) Change the capturing container every 10 minutes.
j) Dry the containers outside, take weight and close them.
k) Finish simulation when discharge is constant for three collection intervals.
l) Measure the inclination of the soil.
m) Measure the water content of the soil.
n) Measure the infiltration.
o) Bring all the containers in the laboratory to dry the collected material.
p) Label and weigh the new containers which are appropriate to put into the drying furnace.
q) Transfer the samples into the new container and make sure all the particles have been decanted.
r) Dry the material.
s) Take it out after 24 to 48 h until the water is evaporated and weigh them again.

Each container delivers six values for its inclination and its water content. Additionally, depending on the experimental time, Between 8 to 11 values for the total amount of water and sediment running down are recorded. The experiment is run until six stable values for the

discharge are obtained. If an outlier is observed, it is not taken in consideration. After the drying process, the sediment can be weighed and the calculation of the sediment loss can be executed. Further calculation explained in Chapter 3.3. The setup scene is shown in Figure 6.

Figure 6. Picture taken during an interrill simulation experiment.

3.2.2 Rill Erosion

Although there are significant differences between the interrill erosion and rill erosion, the set up and procedures can be divided into the same chapters.

3.2.2.1 Rainfall Simulations

As it is used for previous rill erosion experiments (Hairsine & Rose, 1992b) no direct rainfall was executed. Other experiments show that rainfall does not affect sediment transport for slopes greater than 9% this might be caused due to the high flow velocity at those slope steepnesses (Moss, Walker, & Hutka, 1979). As rill erosion is mainly initiated due to the shear stress of water running over the soil surface, the rainfall was not simulated with the rainfall simulator. Rill erosion is induced by an artificial inflow. The water is taken out of the main water supply system. From there it is conducted in a hose into a discharge measuring device, then leading it to the upper end of the rill container. There it runs through a divider to make the flow as laminar as possible. Before it touches the soil surface it flows over a small plastic

disc to inhibit vertical erosion. To get a homogenous runoff over the whole cross section, a discharge around 40 ml s^{-1} is introduced. Variations between 37.1 and 42.9 ml s^{-1} are observed. The different discharges are documented for each experiment.

3.2.2.2 Soil Preperation

For both soils, only one container is prepared. The rill erosion vessel is particularly designed for this project. As the WEPP model assumes a rectangular rill channel (Flanagan et al. 2012) for calculating flow depth and flow shear stress, a 1.5m x 0.10m x 0.10m (lxhxw) rill with one completely and one half closed end was shaped out of polypropylen. At the opened end, a funnel is attached to assembly the runoff and the eroded material (Figure 7). In difference to the interrill erosion, there is no drainage system required neither a use for a funnel coverage. The rill erosion is induced by an artificial inflow. For the rill experiment only one test is run at a time and one trial takes between four and eleven minutes. The first attempts are conducted in a slope of about 5 degrees. To get more values for a higher shear stress, the slope was steepened up 17 degrees. There are seven tests run for the material from Caton Bay. Three runs at 5 degrees and four runs at 17 degrees. For the Okana material the change of an inclination from 5 degrees to 17 degrees, did not show the expected detachment rate. That is the reason why three tests out of nine are executed at a slope of 30 degrees. The steps for one run are explained as following and are used for both materials:

a) Put the discharge to the requested flow rate to ensure equilibrium for the run.
b) Weigh the empty collection containers and numbered them.
c) Place them in the right order on the lower end of the rill.
d) Measure the length of the rill and its inclination.
e) Start the stopwatch when putting the diverter where the constant discharge is coming out from on the plastic disc.
f) Write down the discharge for the collection container.
g) Measure the velocity with another clock watch and a tracer for one capturing period.
h) Change the collection bucket after the requested interval.
i) Repeat step f), g) and h) so that at least until 3 minutes of discharge are introduced to the soil.
j) Remove the discharge from the rill.
k) Measure the inclination of the whole length.

l) Read the volume of the discharge from the scale of the collection container or if there is no scale mark the level with an appropriate pen.
m) Weigh the full containers
n) Dry the containers
o) Weigh the dried containers

This was carried out for each run. Because of the long drying period of the first trials, whose discharge was collected in a 60 seconds interval and yield to approximately 2.5 liters, the collection time was shortened. The first two or three capturing vessels are still kept for 60 seconds to get equilibrium, but afterwards the assembly beakers get changed after 20 seconds which constitute an amount of 900 milliliter. A second person had to be present for capturing all the prerequisite values. For illustrating a picture can be seen in Figure 7.As space in the drying oven was a limiting factor, it was not possible to do more than three runs in a week. To ensure natural condition in the rill, the whole rill was covered with clingfilm during the drying procedures of the collected material. All the documented values can be found in the Appendix B.

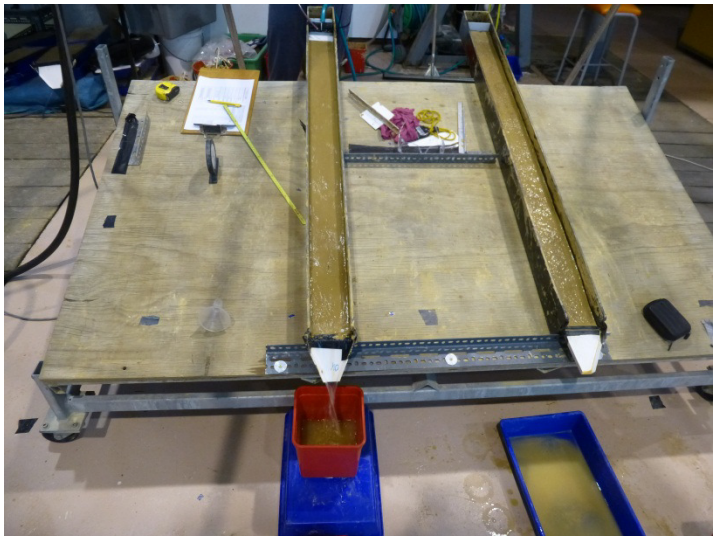

Figure 7. Picture during a rill erosion experiment.

3.3 Calculation Procedures

As two different approaches lead to the interrill and rill erodibility their determination is described in two separated steps. Within one step first the experimental and then the modeled approach is described.

3.3.1 Interrill Erodibility

After all the steps of laboratory methods are fulfilled it is possible to calculate the interrill erodibility factor with Equation 2-2 (Elliott et al., 1989). The difference is that the experiment provides the interrill detachment rate (Di) and therefore the interrill erodibility factor (Ki) can be computed. WEPP suggests interrill erodibility factors which are calculated with equations from Chapter 2.2.1 and with those it calculates the detachment rate (kg m^{-2} s^{-1}) and inherent soil loss for the observes storm event and area.

Estimation of experimental derived interrill erodibility:

The first attempt was defined as that the interill detachment rate is equal to the interrill erodibility factor times the square of the intensity:

$$D_i = K_i I^2 \qquad 3\text{-}8$$

Further investigations, comparison and collection of other studies lead to a modification by introducing the slope factor (S_f) to the equation:

$$D_i = K_i I^2 S_f \qquad 3\text{-}9$$

D_i… Interrill detachment rate (kg $m^{-2}s^{-1}$)

K_i… Interrill erodibility constant, (kg s m^{-4})

I… Rainfall intensity (m s^{-1})

S_f… Slope factor (-)

For lower slopes interrill transport limits erosion and higher slopes raindrop detachment is limiting interrill erosion (Foster et al. 1976). It was defined as:

$$S_f = 1.05 - 0.85 * \exp(-4 \sin(\alpha)) \qquad 3\text{-}10$$

α… Slope angle (°)

(Elliot et al. 1989)

Each run, mainly characterized by its slope, provides the measurements of three soil containers. These are placed under the simulated rain for a certain period. For each container the intensity, the initial and final inclination (which varies because of the uneven surface) and water content, as well as discharge and sediment loss for all the captured intervals are measured.

With the measured mass of the eroded sediments the interrill detachment rate (Di) can be calculated by dividing the mass of the sediment in kilo grams for each interval by its interval in seconds and the soil surface in square meter.

With the measured slopes the average slope of one trial is calculated and further the slope factor (Sf) with Equation 3-10. As the intensity is already given by the former calibration of the rainfall simulator, the interrill erodibility factor (Ki) can be computed with Equation 3-9. The soil loss is then computed by multiplying the each detachment rate (Di) with the capturing interval (10 minutes) and sum up the last six values to get the soil loss for the rain duration of 60 minutes. This is done for both soils. The result is one soil loss value and one soil erodibility value for each soil at the low, medium and steep slope.

Calculation of WEPP Interrill Erodibility

To obtain the soil loss of an event with WEPP, all four input parameter (Climate, Management, Slope and Soil) have to be defined. The attempt is to get model values for the soil loss for each inclination which later on can be compared with the value from the experiment.

For the climate input, a single storm event is created with the duration of one hour, based on the interrill experiments. The storm amount is calculated by multiplying the average intensity of the experiment by the duration of the event. The maximum intensity is taken from the highest average intensity which was implemented regarding the three containers which are run in parallel at one run. The duration to peak intensity is set to zero because it was permanently introduced.

The management file is set to continuous fallow. These two input files stayed the same over the whole modeling period.

Two slope files are created for each run. The first one is uniform and defined by the average of all measured inclination of the 3 containers from one run. The second is divided into three sections, consisting of the average of the upper, the middle and the lower section of the three containers from one trial.

Several soil files are created to define the soils properties with different input parameters. The Albedo is taken as given from the WEPP program with 0.23. The initial saturation is assumed as 100 % resulting from the experiments which show a constant discharge - and detachment

rate for the last 60 minutes. Rill erodibility is calculated by WEPP and the Critical shear is set to 50 Pa to eliminate rill erosion (Flanagan et al., 2012).

The organic matter content and the cation exchange capacity are taken from the test results of Hill Laboratories.

The main varying input parameters for the interrill erosion are two different values for the interrill erodibility paramter. One is calculated by the model itself (autoKi) where WEPP uses the equations from Chapter 2.2.1. The other value is the result of the average out of the last six interrill erodibility factors (calKi) calculated with the experimental detachment rate. The other distinguishing parameter is the grain size distribution. As the soil texture analysis is realized with different procedures, there are two different grainsize distributions derived. One is analyzed with the Horiba Particle Size Analyzer (self) and the other is characterized by the results of the Hill Laboratories carried out by Eurofins (lab). These lead to four different soil input files for the Caton material and the Okana material.

With the created input files, simulations are run and afterwards the soil loss from the simulation is compared with the soil loss from the experiments. WEPP also derives a runoff in mm for the storm event, which can be used for adjustments. WEPP calculates the discharge depending on the rainfall and influenced by the initial water content and the effective hydraulic conductivity of the soil. By modifying one of those two parameters, different soil loss from simulations can be achieved.

3.3.2 Rill Erodibility

With the data derived from the rill experiment, the rill erodibility based on the experiment could by calculated. To obtain the WEPP model suggested rill erodibility, the soil properties are the only needed parameters,

Estimation of experimental derived rill erodibility:

The description of soil erosion processes occurring due to overland flow, are very similar to sediment transport in stream beds. This has led to use sediment transport equations to describe flow characteristics and movements of soil erosion (Hairsine and Rose 1992a). The mixture of water and sediments flowing down the surface introduces a force called shear stress (τ), it depends on the density of the flowing medium (ρ), the acceleration gravity (g), the hydraulic radius (R) and the inclination of the slope (α):

$$\tau = \rho g R sin(\alpha) \quad 3\text{-}11$$

τ… Shear stress (N m^{-2})

ρ… Density (kg m^{-3})

g… Acceleration of gravity = 9.81 m s^{-2}

R… Hydraulic radius (m)

α… Slope

$$R = \frac{A}{P} \quad 3\text{-}12$$

A… Cross section of flowing water (m^2)

P… Perimeter of flowing water (m)

The transportation of the particles is also influenced by their own settling velocity, that depends on the particle size and density. The amount of soils which gets detached is also affected by the sediment concentration of the water flowing down. Net soil detachment is calculated as:

$$D_f = D_c \frac{1 - G}{T_c} \quad 3\text{-}13$$

D_f… Net detachment rate (kg s^{-1} m^{-2})

D_c… Soil detachment capacity (kg s^{-1} m^{-2})

G… Sediment load in rill (kg m^{-1} s^{-1})

T_c… Transport capacity (kg m^{-1} s^{-1})

For clear water flowing down the bed a linear regression fit can be assumed, where G = 0 and $\frac{1-G}{T_c}$ = 1. This results to:

$$D_c = K_r(\tau - \tau_c) \quad 3\text{-}14$$

K_r… Rill erodibility (s m^{-1})$^{-a}$

τ_c… Critical shear (N m^{-2})

(Bjorneberg et al. 2010)

With available data the linear regression can be formed as:

$$D_c = a + b\tau \quad 3\text{-}15$$

$b = K_r$

$\frac{a}{b} = \tau_c$

(Cochrane, 1995).

Same approach as it is used for the interrill erosion estimation, the rill detachment capacity (Dc) is gained by dividing the dried eroded soil mass of a known collected interval, by its interval and the surface of the rill. Only the last 3 values of the experiment are taken in consideration as they are identified as stable. The average out of these three values yields to the rill detachment capacity of each experiment. If not the whole surface is contributing to the discharge, it has to be taken in consideration for all the calculations where the width of the channel is involved.

Two attempts are made for calculating the hydraulic shear. Both are based on Equation 3-11. The first one uses the measured height of the flowing water to calculate the hydraulic radius. The height is captured with a general meter. The second one derives the height by dividing the recorded discharge by the measured flowing velocity and the channel width. With the average of the initial and final measured slope the two hydraulic shear stresses can be calculated for one average detachment capacity of one experiment.

By plotting all the measured rill detachment rates (kg m^{-2} s^{-1}) against their inherent hydraulic shear (Pa) a linear regression can be fitted. The intercept with the horizontal axis is noticed as the critical shear (τ_c) and the slope is the rill erodibility (Kr).

Calculation of WEPP Rill Erodibility

Rill erodibility is not directly simulated with the WEPP model. To obtain the rill detachment rate (K_r) and the critical shear strength (τ_c) Equations 2-12 and 2-13 are used for Cropland and 2-15 and 2-16 are used for Rangeland conditions. Although the site area is characterized as rangeland, it has to be proven if one is more convenient than the other for the bare observed material. Each calculation is carried out for the soil texture determined with the PSA and the hydrometer analysis from the Hill Laboratories. This leads to four rill erodibility values (Kr) and four critical shear stress (τ_c) for the Caton and the Okana material.

4 RESULTS

4.1 Soil Properties

The results emerging from soil properties are necessary to define the input parameters for the WEPP model. The soil characteristics of the material collected at Caton Bay and at the Okana valley have to be specified. The results obtained from the two different analyzing methods lead to a new approach as they deviate from the expectations.

Before the results of the Hill Laboratories were available, a clear difference in the clay and sand content of the two collected material is analyzed with the particle size analyzer with precious organic matter removal. The obtained results arisen from the PSA are characterized in Table 2 and named “Caton” for the material from Caton Bay and “Okana” for the material from the Okana valley. To approve the output of the machine, the soil samples are sent to a laboratory to be proven as a lot of further calculations are based on those. The later received results from Hill Laboratories show an almost identical soil texture for the Caton and the Okana material. The analysis is carried out with a Hydrometer and preceded organic matter removal and sieving methods. Their discernible difference in the soil texture is that the material from the Okana catchment has 1 percent more silt and 1 percent less clay than the Caton material. Therefore a new soil with common properties is created by using the averages of the results arising from the Hill Laboratory analysis. It is called “General” and characterized in Table 2.

The percentage of the soil fractions of Caton Bay and Okana sample is the average value of all representative particle size analysis of the Horiba Particle Size Analyzer (PSA). The results of the PSA are the percentage of a certain range of diameters which are reflected and their cumulative values. To obtain the percentage of clay, silt and sand according to the USDA[3] limits, linear interpolation is used. One distribution of one sample is shown in Figure 8 and all the others can be found in the Appendix C.

[3] USDA, U.S. Department of Agriculture

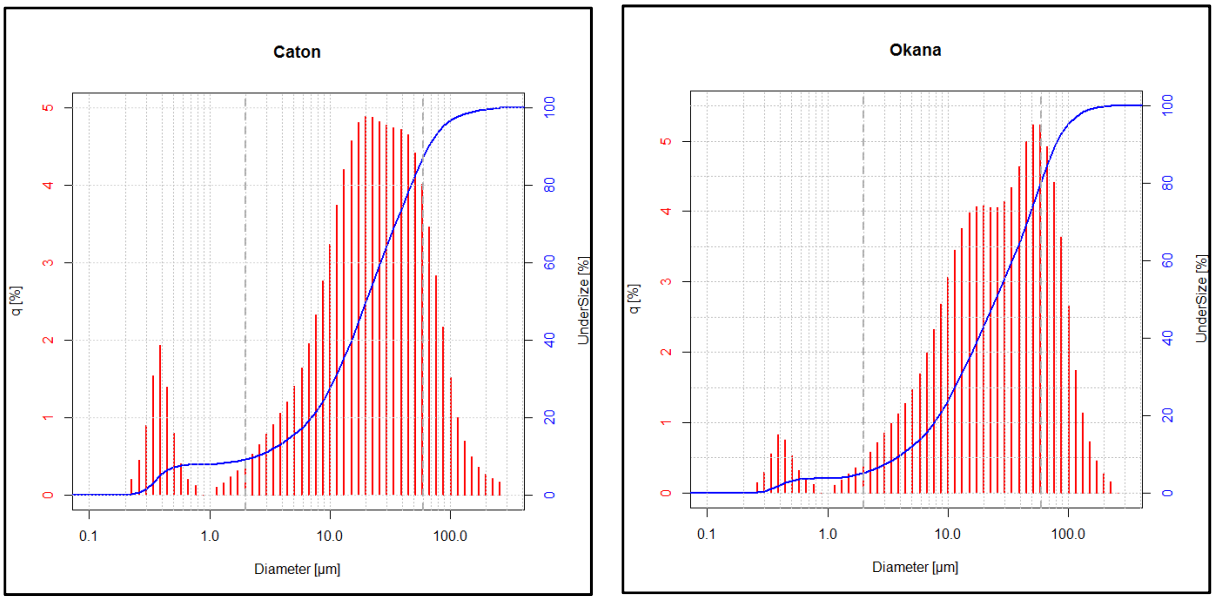

Figure 8. Grain size distribution of one soil sample from Caton Bay(left) and the Okana valley(right).

The Content of Organic Matter (OM) and the Cation Exchange Capacity (CEC) are carried out by Hill Laboratories. The effective hydraulic conductivity is derived from a Minidisc Infiltrometer. Several tests are run. One trial leads to the hydraulic conductivity (kf_{eff}) of the soil from Caton Bay and the kf_{eff} value for the Okana soil was gained by using the average of two attempts. All values and the progression can be found in the Appendix C.

Table 2. Soil properties of the investigated material.

Caton			**Okana**			**General**		
Clay	**9.75**	%	Clay	**5.89**	%	Clay	**21.5**	%
Silt	**80.65**	%	Silt	**75.95**	%	Silt	**66.5**	%
Sand	**9.6**	%	Sand	**18.16**	%	Sand	**12**	%
OM	**1.9**	%	OM	**1.60**	%	OM	**1.75**	%
CEC	**18**	me $(100g)^{-1}$	CEC	**14.00**	me $(100g)^{-1}$	CEC	**16**	me $(100g)^{-1}$
k_{feff}	**0.61**	mm h^{-1}	k_{feff}	**0.69**	mm h^{-1}	k_{feff}	**0.65**	mm h^{-1}

4.2 Interrill Erosion

To present the results of the interrill erodibility the two soils (Caton and Okana) are considered separately. Starting with the result of the experiments, then showing the results of the WEPP modeling and finally showing the comparison of both. As the grain size distribution does not influence the experimental processes, the different textures lead not to various results. Whereas the varying grain size distribution derived from the PSA and the hydrometer method can influence the result of the WEPP Model. For that reason in the WEPP simulation two soils are considered for Caton and Okana material, one characterized with the self-determined soil texture (self) and one created from the laboratory (lab) results. It has to be mentioned that the soils determined by the hill laboratories lead to one common file which is separately compared with the Caton Material and the Okana Material. The present intensities are shown in Table 3:

Table 3. Varying intensities of the rainfall simulator

	Container left	Container middle	Container right	Average
Intensity (mm h^{-1})	19.31	17.72	18.43	18.49

4.2.1 Caton Bay:

In the next step the results from the interrill experiment, the interrill modeling and the comparison of these results are expressed.

Interrill Experiment:

To illustrate the progressively received results, two different graphs are shown leading to the experimental results of interrill detachment rate (D_i) and interrill erodibility (K_i). These graphs are received for the low, middle and steep slope. To exemplify why the duration of 60 minutes is taken for further calculation, the progress of the discharge (Q) and the interrill detachment rate (D_i) are presented in Figure 9 and Figure 10.

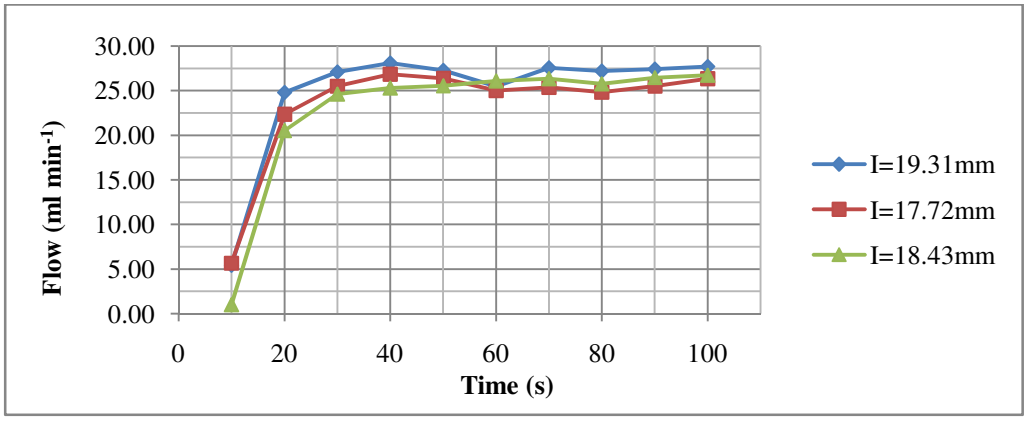

Figure 9. Progress of discharge of three soil container with Caton bay material at a slope of 13°

With the measured mass of the eroded sediments, obtained after drying and weighing, the interrill detachment rate can be plotted over the time:

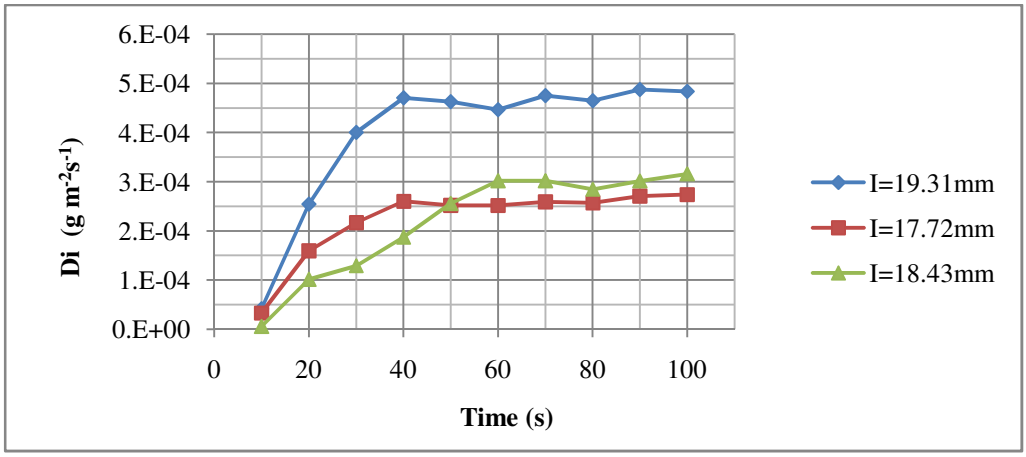

Figure 10. Detachment rate at a slope of 13° of Caton Bay material.

With the average value of the initial and final inclination of the three containers, the interrill erodibility (K_i) can be calculated. In addition to the average inclination of one container also the average of the upper, middle and lower part is calculated and shown in Table 4:

Table 4. Different Inclination of the experiments run with Material from Caton's Bay.

	1st Experiment	2nd Experiment	3rd Experiment
Average(°)	4.67	13.00	26.44
Upper(°)	4.50	13.50	26.50
Middle(°)	5.50	14.00	29.50
Lower(°)	4.50	12.50	25.00

According to equations in Chapter 3.2.1 the interrill erodibility parameter can be calculated shown in Figure 11:

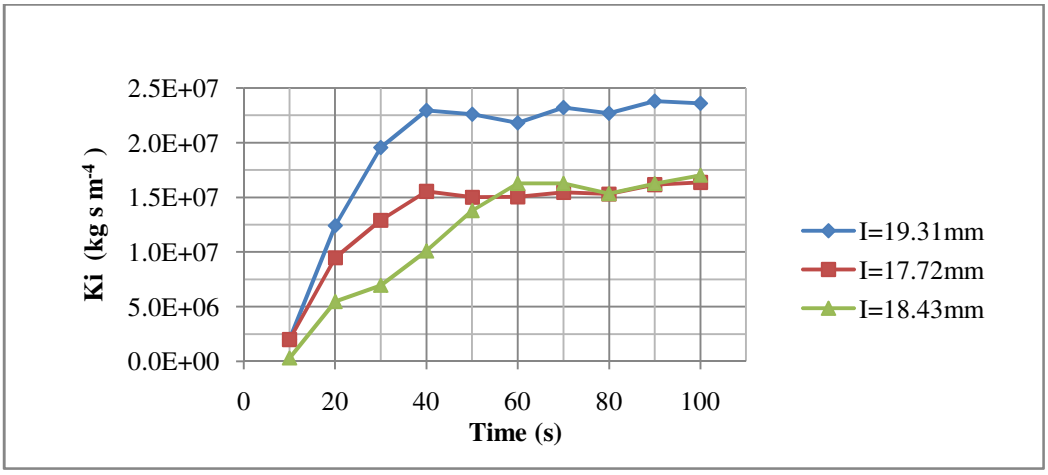

Figure 11: Progress of interrill erodibility (K_i) over time at inclination of 13°, showing the different soil containers of Caton Bay.

Showing the Progression of this experiment might lead to the assumption of a strong influence of the intensity. By incorporating all 3 experiments no clear dependence between detachment rate and intensity can be observed. This can also be caused by the small scale variations of the intensity. All the results from the other simulations can be found in the Appendix A. However, the increase of soil loss with augmenting slope is definitely noticeable and the average values of the last 6 results are shown in Table 5. The average of each soil container leads to a minimum, average and maximum values for each slope. Only one average discharge is calculated for one slope.

Table 5. Average soil loss values for the material collected at Caton Bay

	measured soil loss (kg m^{-2} h^{-1})			Q (mm)
Slope (°)	Min	Average	Max	Average
4.67	0.156	0.187	0.218	14.27
13.00	0.939	1.230	1.692	16.93
26.44	1.933	2.233	2.467	15.06

To obtain a representative Ki value, also only the last six measurements of each run are taken in consideration. This six values lead to a total experiment period of 60 minutes for the later modeling. The average out of these six values is computed for each soil container. So each container provides one value which leads to three values for one slope. The highest and lowest average value are used to create the range of the soil loss for each inclination shown in Figure 12. The trend line results out of the average of these three values. The values obtained are presented in Table 6:

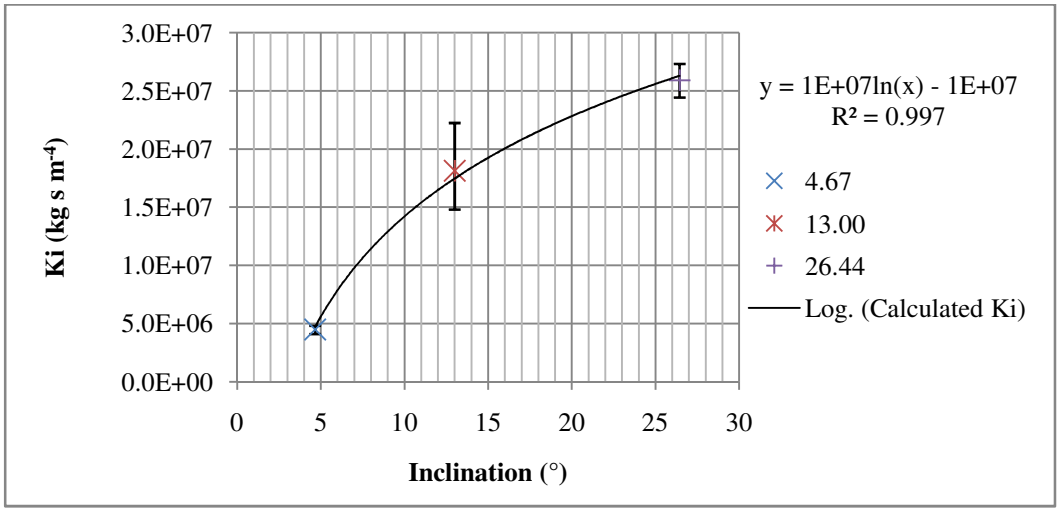

Figure 12: Experimental derived interrill erodibility factor (Ki) for Caton Mateial.

Table 6. Average interrill erodibility values for Caton Material calculated with experimental data.

Caton	calculated Ki (kg s m^{-4})		
Slope	Min	Average	Max
4.67	4.04E+06	4.49E+06	4.75E+06
13.00	1.56E+07	1.81E+07	2.30E+07
26.44	2.43E+07	2.59E+07	2.72E+07

Interrill Modeling

The different created input files for the WEPP model lead to different soil losses. Four different soil files for each slope are created. Two for the soil characteristics derived with the PSA (self), one with the experimental calculated (cal.Ki) value and one with WEPP auto-calculated (auto.Ki) value. Same is done for the Hydrometer soil texture (lab). Two slope files for each inclination are created. A uniform and a segmented profile are set up. The storm event with the intensity of 18.49 mm and the duration of one 1 h as well as the continuous fallow land management file are kept constantly. The values obtained are shown in Figure 13. The results are 8 different values for each slope. The abbreviations are explained in Table 7 .

Table 7: Explication of short forms

self.calKi	Soil Texture from PSA and Ki value from experiments
lab.calKi	Soil Texture from Hill Lab. and Ki value from experiments
self.autoKi	Soil Texture from PSA and Ki value from WEPP model
lab.autoKi	Soil Texture from Hill Lab and Ki value from WEPP model
...+devSL	stands for segmented (deviating) slope
...+uniSL	stands for uniform Slope

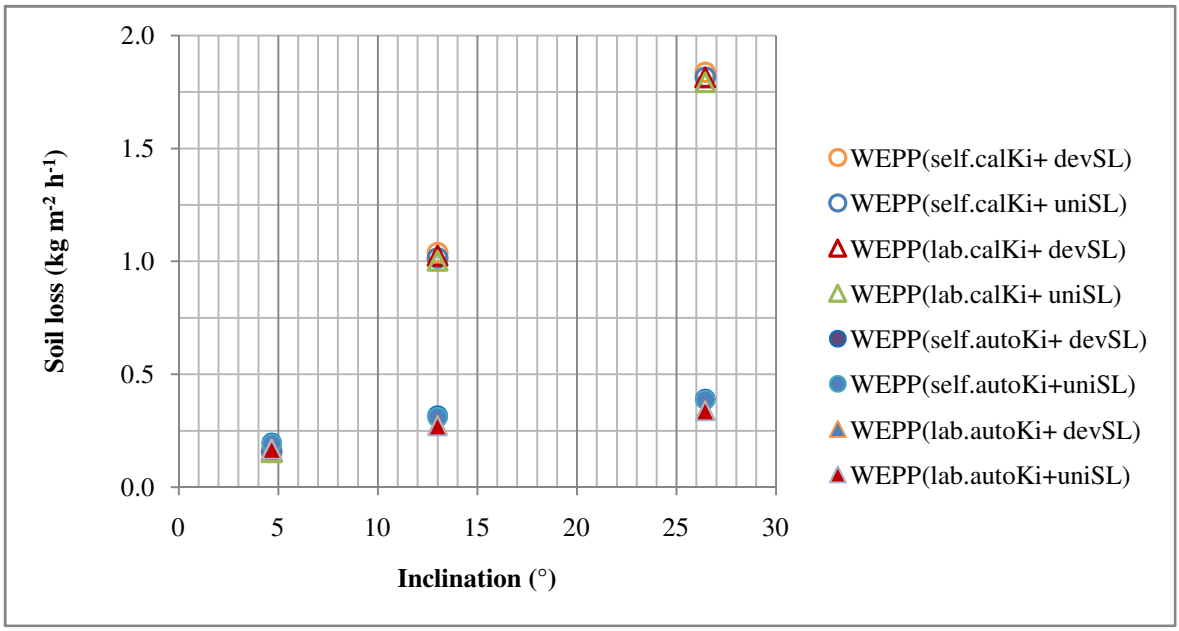

Figure 13. Modeled soil loss values resulting from experimental Ki and model auto-calculated Ki values depending on slope from Caton Material.

The first modeling attempt shows that the difference between the uniform and segmented slope file are small. The segmented profile evokes a higher soil loss of maximum 3.2 percent and therefore this differentiation is not further considered in the following comparisons. Only the uniform slope is taken into account. The next noticeable remark is that the different grain size distributions have not much influence on the interrill soil loss. The abbreviation “lab” uses the soil characterized by the Hill Laboratory and “self” is formed by using the soil properties from Caton Bay dertermined with a PSA. A maximum difference of 2.3 percent is recorded for the experimentally derived interrill erodibility parameter (calKi). The difference of the values for the soil loss obtained from the WEPP auto-calculated Ki (autoKi) can augments to a maximum of 15 percent. This higher deviation can origin from the small soil loss values which are obtained from using the autoKi value, but also from the way of calculation. The influencing factors of the autoKi calculations is only the clay fraction. A clear mismatch can be recognized by comparing the soil loss resulting from autoKi values with experiments results (calKi) at higher inclination. This shows that with increasing inclination the difference between the model-calculated Ki values and the experimental Ki values increments.

The values for the different soil losses are shown in Table 8:

Table 8. Values for first modeling attempt of Caton Bay material. At 100 % initial saturation, Intensity= 18.49; kf_{eff}=0.61 m h^{-1}.

Caton	d=1h; I=18.49mm	Exper (Ave)	self.calKi +devSL	self.calKi +uniSL	lab.calKi +devSL	lab.calKi +uniSL	self.autoKi +devSL	self.autoKi +uniSL	lab.autoKi +devSL	lab.autoKi +uniSL
Slope	4.67									
100%sat	Soil loss (kg m^{-2})	0.187	0.161	0.156	0.158	0.154	0.197	0.192	0.172	0.167
	Q (mm)	14.27	14.45	14.41	14.26	14.22	14.45	14.41	14.26	14.22
Slope	13									
100%sat	Soil loss (kg m^{-2})	1.230	1.038	1.015	1.024	1.002	0.316	0.309	0.276	0.27
	Q (mm)	16.93	14.500	14.5	14.31	14.31	14.5	14.5	14.45	14.31
Slope	26.44									
100%sat	Soil loss (kg m^{-2})	2.233	1.837	1.815	1.813	1.792	0.390	0.386	0.341	0.337
	Q (mm)	15.06	14.500	14.5	14.31	14.31	14.5	14.5	14.31	14.31

Comparison of the modeled and experimental values

The next comparison is made by introducing the soil loss values of the experiment with the WEPP modeled values. Both soil types (lab and self) are used as input file with “autoKi” and “calKi” value, but only with one uniform slope. The range of the experimental soil loss value is caluculated with the averages resulting from the three parallel observed containers. The values are listed in Table 9 and illustrated in Figure 14.

Table 9. Average soil loss values and Discharge values for Caton Bay Material

kf=0.61(0.65)mm h^{-1}	Soil loss values (kg m^{-2} h^{-1})			Difference Exp. - auto	Difference Exp. - cal
slope	auto.Ki	cal.Ki	Experiment	(%)	(%)
4.67	0.1795	0.155	0.187	96.0	82.9
Q(mm)=	14.315	14.315	13.06		
13	0.290	1.009	1.23	23.5	82.0
Q(mm)=	14.405	14.405	15.77		
26.44	0.362	1.804	2.233	16.2	80.8
Q(mm)=	14.405	14.405	14.41		

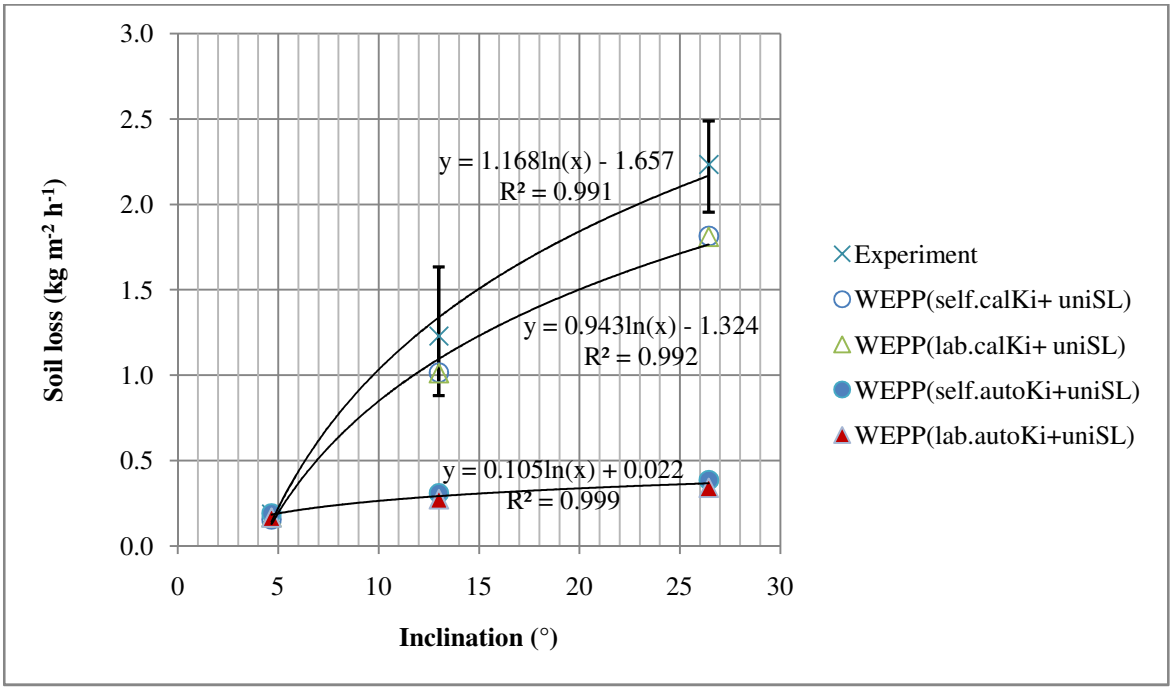

Figure 14: Comparison of the obtained soil loss values depending on slope, Caton Bay material.

Figure 14 shows that the soil loss at an inclination around 5 degrees is approximately the same for all attempts. The experimental value for the soil loss is augmenting the soil loss values obtained from the WEPP model using calKi. It can be recognized that the experimental values change logarithmically with increasing slope as well as the modeled K_i values, but those with a lower inclination. The experimental soil loss is more than 4 times bigger than the auto-calculated for the middle slope and more than 6 times above for the steepest slope. By using the experimental $K_i$values (calKi) as model input parameter, the soil loss at middle slope lies within the experimental range of the experimental values whereas at steeper slope it does not.

By comparing the discharge results of the experiment with the model values, a higher discharge is observed for the experiments at higher inclination. As the initial water content is already set to complete saturation, it is tried to adjust the values by modifying the hydraulic conductivity. It is lowered from 0.61 mm h^{-1} and 0.65 mm h^{-1} to 0.4 mm h^{-1}. Although the modeled discharge increases the experimental discharge, the soil loss could only be augmented to a maximum of 5.3 percent which does not significantly change the former results. The illustrated results are shown in Figure 15.

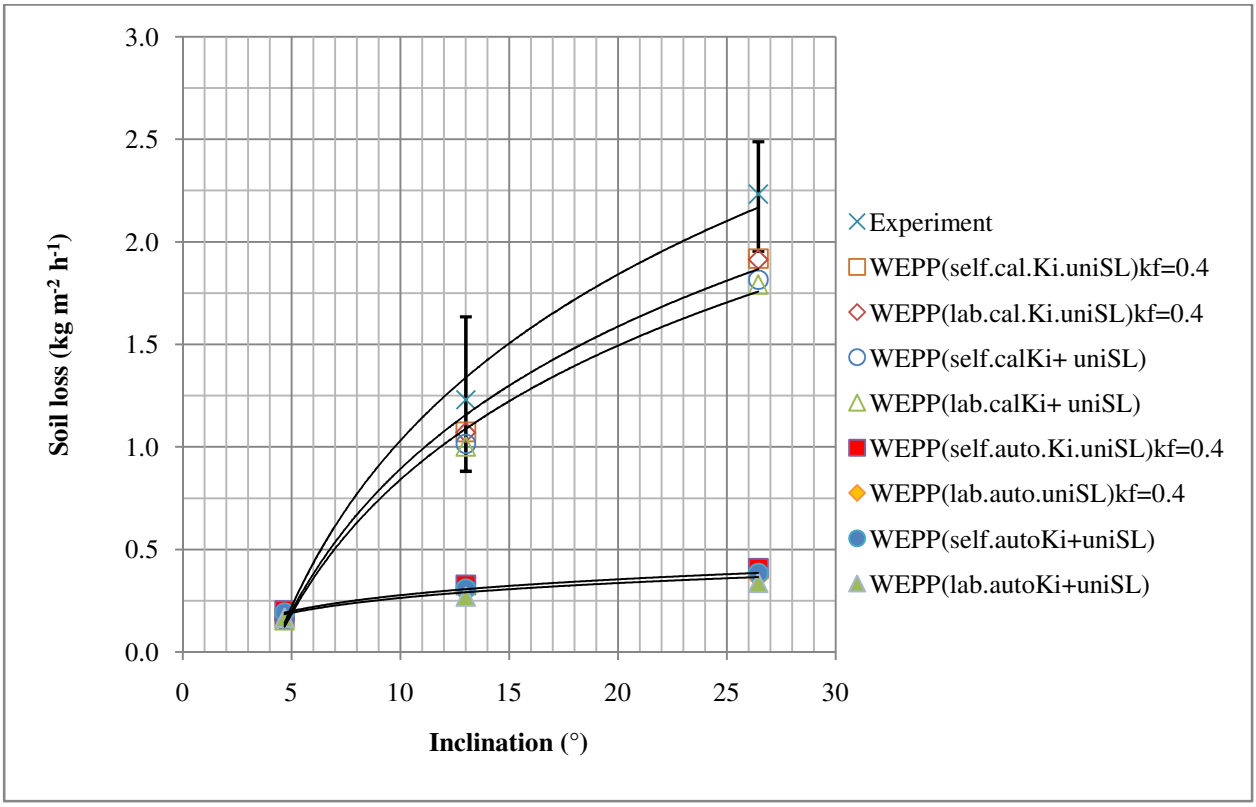

Figure 15. Showing the influence of changing the hydraulic conductivity. Comparison of soil loss values depending on slope with a different hydraulic conductivity, Caton Bay material

The values for a hydraulic conductivity of 0.4 m $h^{-1}$are listed in Table 10.

Table 10. Soil loss and discharge resulting from lower hydraulic conductivity for Caton Bay material

kf=0.4mm h^{-1}	Soil loss values (kg m^{-2} h^{-1})			Difference Exp. - auto	Difference Exp. - cal	Difference kf 0.6 - 0.4
slope	auto.Ki	cal.Ki	Experiment	(%)	(%)	(%)
4.67	0.191	0.165	0.187	102.1	88.2	5.3
Q(mm)=	15.21	15.210	13.06			
13	0.308	1.072	1.23	25.0	87.1	5.1
Q(mm)=	15.300	15.300	15.77			
26.44	0.384	1.916	2.233	17.2	85.8	5.0
Q(mm)=	15.300	15.300	14.41			

4.2.2 Okana Material

Interrill Experiment:

The same methods and procedures as they are used to define the soil loss and interrill erodibiltity parameter for the material of Caton Bay are applied to the material from the Okana valley. The progression of the runoff (Q) and the inherent detachment rate (D_i) values as well as the course of the interrill erodibility values (K_i) for the Okana Material can be seen in the Appendix A. The slope values needed for the calculation are shown in Table 11, the intensity is taken from the Rainfall Simulator calibration.

Table 11. Averages of the different slopes measured for Okana material

	1st Experiment	2nd Experiment	3rd Experiment
Average(°)	4.72	14.00	26.17
Upper(°)	4.00	13.50	26.00
Middle(°)	6.00	15.00	27.00
Lower(°)	5.00	12.50	26.50

The ranges of the interrill erodibility parameters are resulting from the last six detachment rate values of each experiment and are shown in Figure 16:

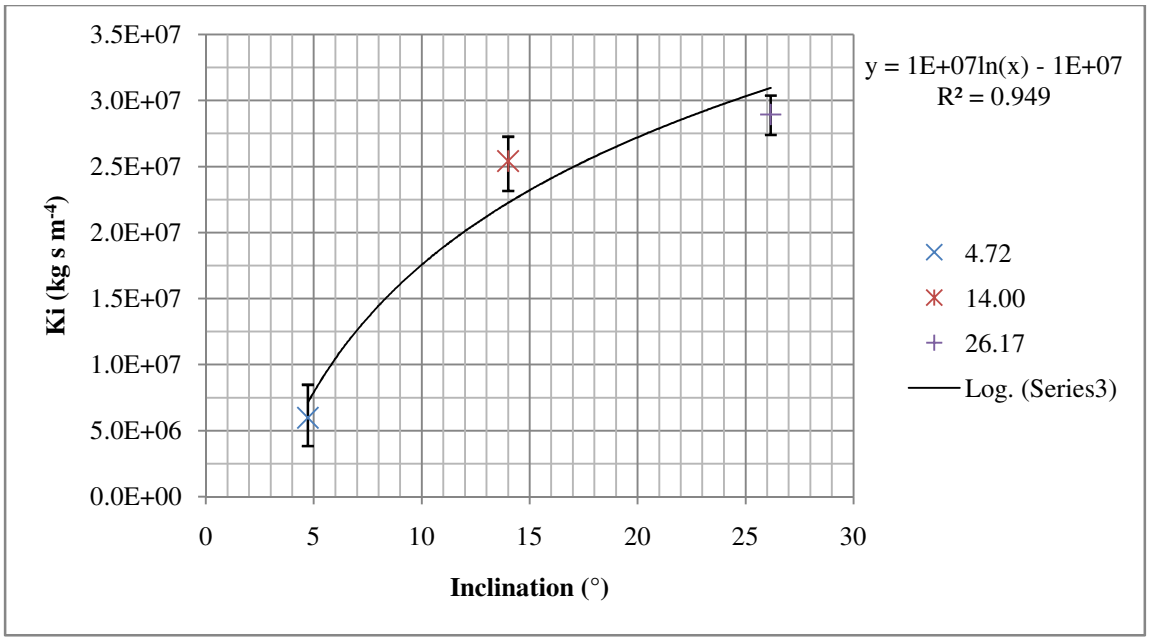

Figure 16. Average interrill erodibility (K_i) values for material collected at Okana Valley.

The average K_i values measured form each soil container are shown in Table12.

Table 12: Average interrill erodibility for Okana material calculated with experimental data.

Okana	calculated Ki (kg s m^{-4})		
Slope	Min	Average	Max
4.72	4.16E+06	5.96E+06	8.81E+06
14.00	2.27E+07	2.54E+07	2.68E+07
26.17	2.73E+07	2.89E+07	3.02E+07

Interrill Modeling

The same approach as for the Caton material is made. The four different soil input files construe from different soil texture results and different interrill erodibility parameters. Considering those at two different slopes, a uniform and a segmented slope, for the lower, middle and upper inclination lead to finally 8 modeling values for each slope step. The results are illustrated in Figure 17 and the values can be found in Table 13.

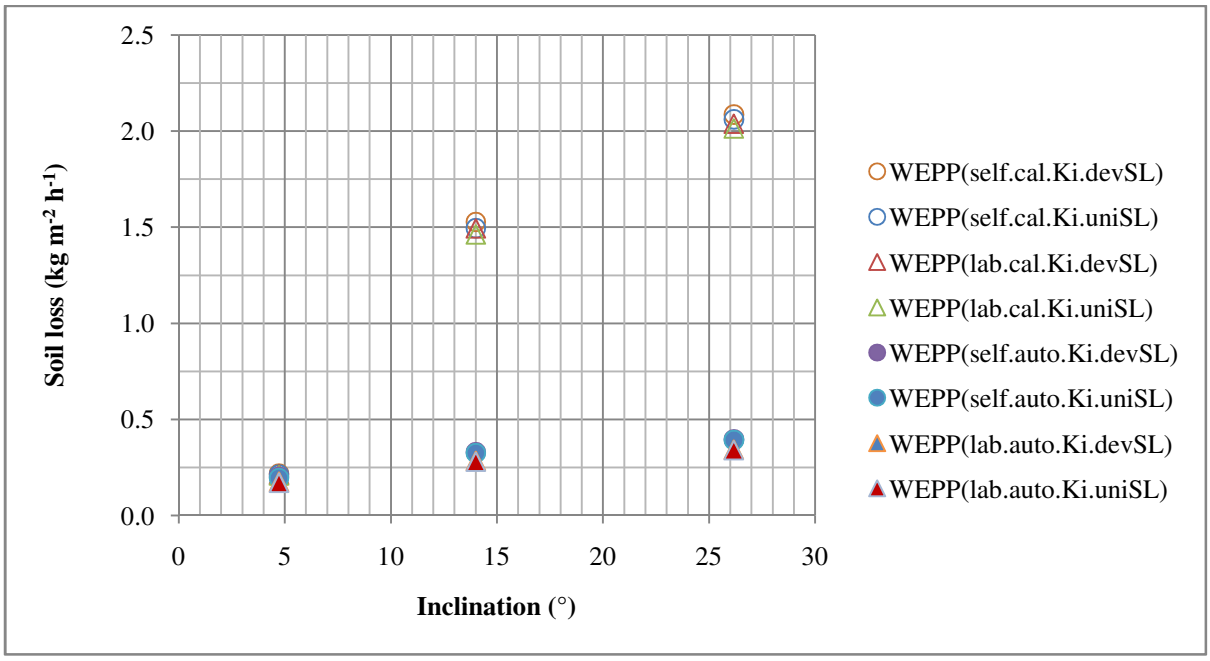

Figure 17. Modeled soil loss values resulting from experimental Ki and model auto-calculated Ki values from Okana Material depending on slope

Table 13. Values for first modeling attempt of the material from the Okana Valley. At 100 % initial saturation, Intensity= 18.49; kf=0.69 m h^{-1}, soil loss in kg m^{-2} h^{-1} and Q in mm

Okana	d=1h; I=18.49mm	Exper (Ave)	self.calKi +devSL	self.calKi + uniSL	lab.calKi +devSL	lab.calKi +uniSL	self.autoKi +devSL	self.autoKi +uniSL	lab.autoKi + devSL	lab.autoKi +uniSL
Slope	4.72									
100%sat	Soil loss (kg m^{-2})	0.255	0.215	0.209	0.206	0.206	0.198	0.196	0.175	0.17
	Q (mm)	17.76	14.48	14.45	14.26	14.23	14.45	14.42	14.41	14.37
Slope	14									
100%sat	Soil loss (kg m^{-2})	1.742	1.501	1.468	1.479	1.447	0.328	0.322	0.284	0.278
	Q (mm)	17.92	14.530	14.53	14.31	14.31	14.66	14.66	14.31	14.31
Slope	26.17									
100%sat	Soil loss (kg m^{-2})	2.491	2.049	2.024	2.018	1.994	0.394	0.39	0.34	0.336
	Q (mm)	15.97	14.53	14.53	14.31	14.31	14.66	14.66	14.31	14.31

As it is already recognized for the material of Caton Bay, the difference between segmented and uniform slope is negligible. A maximum of 3 percent divergence is present for the Okana material. For further comparisons only the uniform slope is applied. Comparing the values from "General"(lab) soil file with the "Okana"(self) the differences are minor. A maximum deviation from 1.5 percent for the soil losses calculated with calKi (upper values in the graph) and 15 percent for the soil loss derived from the soil losses calculated with autoKi (lower values in the graph) is calculated. The main misalignment of the result for one inclination is caused by the use of different K_i values. Although all the soil loss values fit together for the lowest slope, a clear difference is developing between the soil loss obtained from WEPP auto-calculated interrill erodibility and the soil loss calculated with experimental derived interrill erodibility with increasing slope.

Comparison of the modeled and experimental values

Same comparison as explained for Caton Material is made with the Okana material. Showing the difference between experimental soil loss, soil loss obtained from the WEPP model using the experimental K_i value (calKi) and using the WEPP auto-calculated value (autoKi). To emphasis it is illustrated in Figure 18:

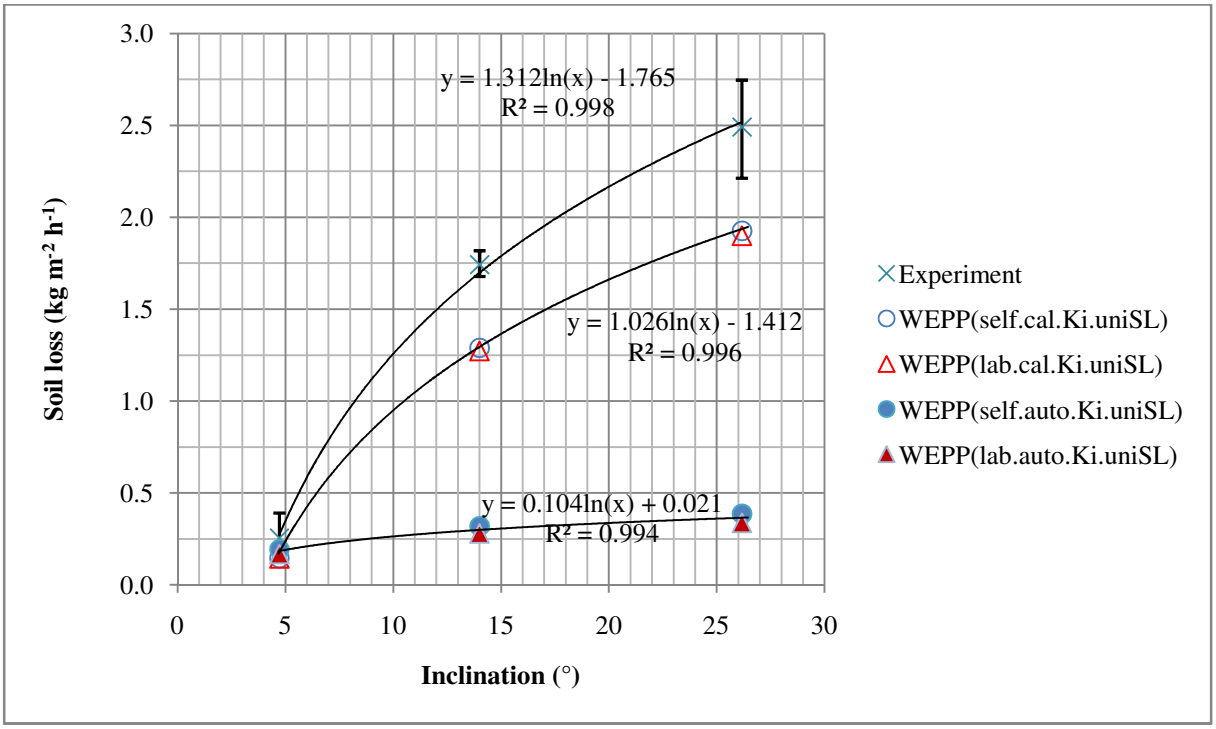

Figure 18: Comparison of the obtained soil loss values

The application of the material collected at the Okana valley represents that the soil loss obtained from the experiments exceeds both simulated values. Although the simulated soil loss derived with the experimental K_i value (calKi) is rather approaching the experimental value than the value obtained from the WEPP auto-calculated (autoKi) soil loss, it is not within the range of the experimental average soil loss values. The detachment rate simulated with calKi is approximately 80 percent of the experimental values whereas the detachment rates derived with autoKi show less than 20 percent for the middle and steeper slope of the experimental value. At the lowest inclination it reaches 71 percent. The values are shown in Table 14:

Table 14. Average soil loss values and discharge values for the Okana Material

kf=0.69(0.65)mm h^{-1}	Soil loss values (kg m^{-2} h^{-1})			Difference Exp. - auto	Difference Exp. - cal
slope	auto.Ki	cal.Ki	Experiment	(%)	(%)
4.67	0.181	0.208	0.255	71.0	81.4
Q(mm)=	14.395	14.340	17.760		
13	0.300	1.458	1.742	17.2	83.7
Q(mm)=	14.485	14.420	17.920		
26.44	0.363	2.009	2.491	14.6	80.7
Q(mm)=	14.485	14.420	15.970		

As the obtained runoff values from the model are lower than the experimental, the hydraulic conductivity is lowered from 0.69 and 0.65 mm h^{-1} to 0.4 mm h^{-1}. The graphic result is shown in Graph 19 and the inherent values in Table 15.

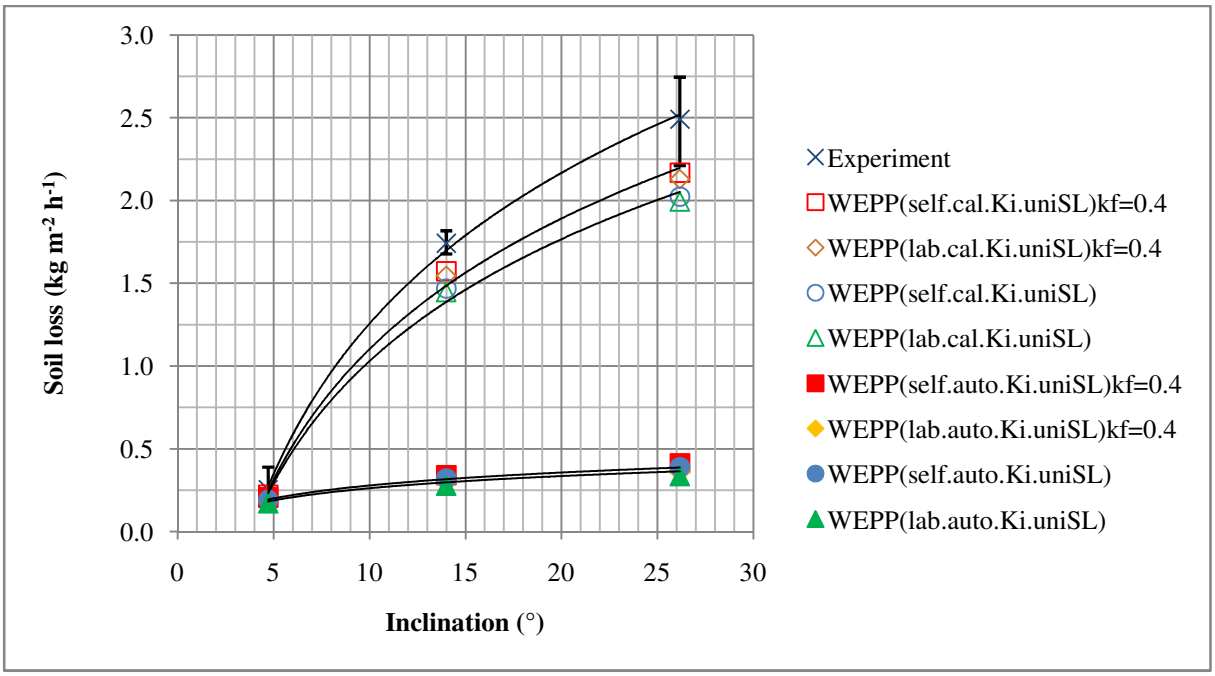

Figure 19: Comparison of obtained soil loss values depending on slope. Showing the influence of changing the hydraulic conductivity of Okana Material

Although the modified simulated discharges induce a higher detachment, it is not possible to eliminate the differences between the experimental and the simulated soil loss values for slopes with a higher inclination than 5 degree. With the increased runoff almost 90 percent of the experimental soil loss is achieved with the self calculated interrill erodibility parameter (self.cal.Ki).

Table 15: Results of soil loss and discharge resulting from lower hydraulic conductivity for Okana

kf=0.4mm h^{-1}	Soil loss values (kg m^{-2} h^{-1})			Difference Exp. - auto	Difference Exp. - cal	Difference kf 0.7 - 0.4
slope	auto.Ki	cal.Ki	Experiment	(%)	(%)	(%)
4.72	0.1935	0.222	0.255	75.9	87.1	5.7
Q(mm)=	15.335	15.335	17.760			
14	0.319	1.560	1.742	18.3	89.5	5.9
Q(mm)=	15.420	15.420	17.920			
26.17	0.386	2.149	2.491	15.5	86.3	5.6
Q(mm)=	15.420	15.420	15.970			

4.3 Rill Erosion

The results of the rill erodibility are divided to represent the values obtained for the Caton and Okana material separately. Within one material further distinction are made to exemplify the experimental and simulated outcomes and their comparison.

4.3.1 Caton Bay

In the following paragraphs firstly the experimental procedure, secondly the modeled attempt and thirdly the comparison of both are described. The two different grain size distributions do not influence the results of the rill experiments but have to be considered for the rill modeling.

Rill Experiment

The parameter obtained from collecting and analyzing the discharge from the rill experiments is the net rill detachment capacity (D_c). It is the maximum rill detachment rate (D_f) that is assumed to occur when there is no sediment in the water. This assumption is taken for the following calculations into account. The progression of the Rill Detachment capacity (D_c) shows that the values are depending on the initial conditions. It is necessary to introduce the discharge long enough so that an equilibrium can be evolved. Figure 20 and Figure 22 show that this is achieved after approximately 4 minutes.

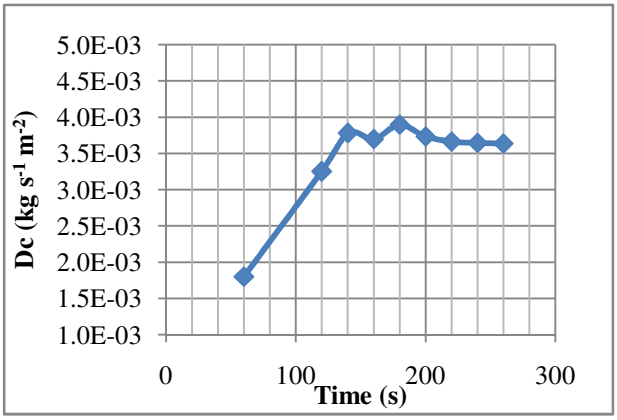

Figure 20. Shows the Rill Detachment Rate of the Caton material at a slope of 16.3°.

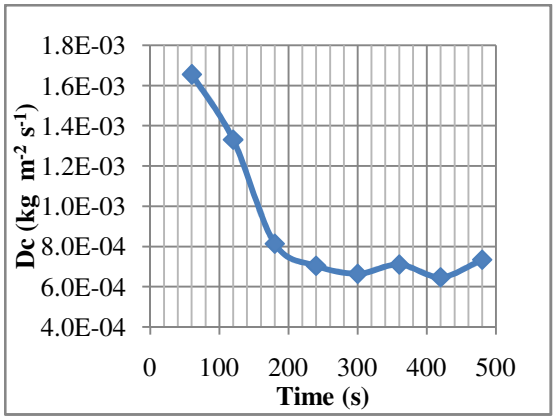

Figure 21. Shows the Rill Detachment Rate of the Caton material at a slope of 6.3°..

For each experiment one rill detachment rate is formed by using the average of the last three observed values. Two hydraulic shear stresses are calculated with Equation 3-15 . The values are listed in Table 17. One is resulting from the discharge recorded with a measuring device ($\tau_1(Q)$) and the other resulting from the measured flow depth ($\tau(h)$). So all experimental rill detachment capacity values (D_c) obtained for the Caton material arise with two inherent shear stress values, illustrated in Figure 22. The abbreviations are explained in Table 16.

Table 16. Explanation of the abbreviations in Graph 14

Exp_t(h)	Values obtained from calculating τ with h
Exp_t1(Q)	Values obtained from calculating τ with Q

Table 17. Rill detachment capacity and inherent critical shear stresses for Caton material

Trial	Dr (kg m^{-2} s^{-1})	Exp_t(h) (Pa)	Exp_t1(Q) (Pa)
1	3.12E-04	1.71	0.70
2	3.04E-04	1.83	0.91
3	6.97E-04	2.65	0.93
4	3.20E-03	5.40	2.06
5	4.08E-03	4.65	1.50
6	3.65E-03	5.21	1.85
7	3.66E-03	4.54	2.69

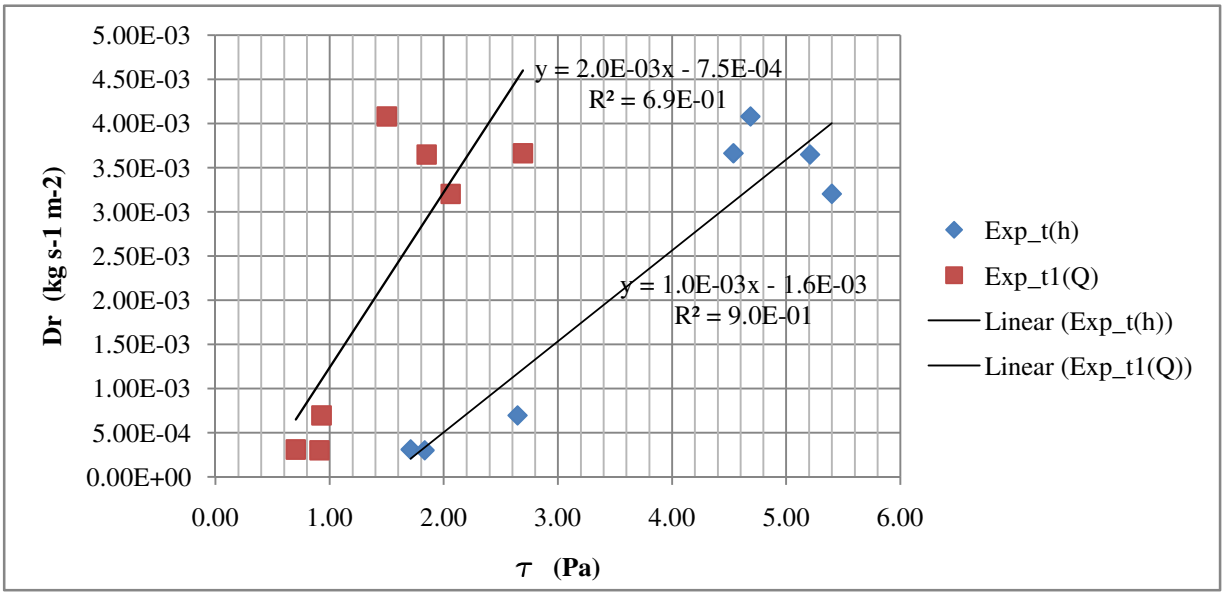

Figure 22. Linear regression Dc(τ) for Caton material. Rill detachment rate (D_c) depending on shear stress (τ).

The main influencing factor causing the linear regression within the values of one calculation method can either results from the different gradient of the soil surfaces and or the

implemented discharges. As the discharge ranges between 37.4 and 40.3 ml s^{-1} the different point clouds are obtained by changing the inclination. Contrary to expectations the results from the different calculation methods show a clear difference. That can originate from the difficulty of measuring a flow depth of only a few millimeters manually and or from uneven soil surface. The results obtained by using the captured discharge (Exp_t1(Q)) are considered as more convenient and are therefore taken for further comparisons. The slope of each regression delivers the rill erodibility factor (Kr) and the intersection with the horizontal axes is the critical shear stress (τ_c) of the soil. The derived values are shown in Table 18:

Table 18. Experimental evolved Critical Shear Stress and rill erodibility for Caton Material.

	Exp_t(h)	**Exp_t(Q)**
tc (Pa)	1.6	**0.4**
Kr (s m^{-1})	1.0E-03	**2.0E-03**

4.3.1.1 Rill Modeling

For Rill Modeling the WEPP program is not used. As the rill erodibility depends on the critical shear stress of the soil both input parameter would have needed adjustment in the model. With two varying parameter the process becomes less clear. WEPP auto-calculates values for the critical shear stress (τ_c) and the rill erodibility for Cropland and Rangeland with the equations shown in Chapter 3.1. For the equations which take the soil texture into account, two different results are obtained for the Caton Bay material. One is derived from the Soil Texture determined with the PSA (self) and one from the results of Hill Laboratories (lab). Table 19 shows the different WEPP-autocalculated rill erodibility (Kr) and shear stress (τ_c):

Table 19. Shear stress and Rill erodibility values for Rangeland and Cropland for two different grain sizes distribution from Caton Bay

Caton	Cropland (self)	Croplandl(lab)	Rangeland(self)	Rangeland(lab)
tc (Pa)	3.50	3.50	3.68	3.54
Kr (s m^{-1})	2.60E-02	8.72E-03	2.03E-04	4.85E-04

The different calculated critical shear stresses of the soil show minor divergences, whereas the rill erodibilities display clear differences. The main difference results from using the equation for Cropland and Rangeland. Both Cropland rill erodibility exceeds the Rangeland erodibility. The alteration within the Cropland results are influences by the different clay content as these are the only varying input parameter for the equation. The rangeland equation considers the bulk density, the organic matter and the water content. The rill erodibility calculated with the PSA(self) results in 41.9 percent of the Rangeland interrill of the soil properties derived at the

Hill Laboratories(lab). For the Cropland the (lab) material is only 33.6 percent of the erodibility parameter for the PSA defined soil (self).

Comparison of the modeled and experimental values

To illustrate the obtained experimental and simulation values, shear stress values are calculated for different rill detachment rate values. This was done by using the linear regression $y = k * x + d$. Where $\tau_c = \frac{-d}{k}$. The description of the abbreviations is presented in Table 20 and the different results are shown in Figure 23:

Table 20. Explanation of abbreviation in Figure 23.

Exp_t1(Q)	Experimental values obtained from discharge
Mod.Crl(self)	Cropland Value for soil texture from PSA
Mod.Crl(lab)	Cropland Value for soil texture from Hydrometer
Mod.Ral(self)	Rangeland Value for soil texture from PSA
Mod.Ral(lab)	Rangeland Value for soil texture from Hydrometer

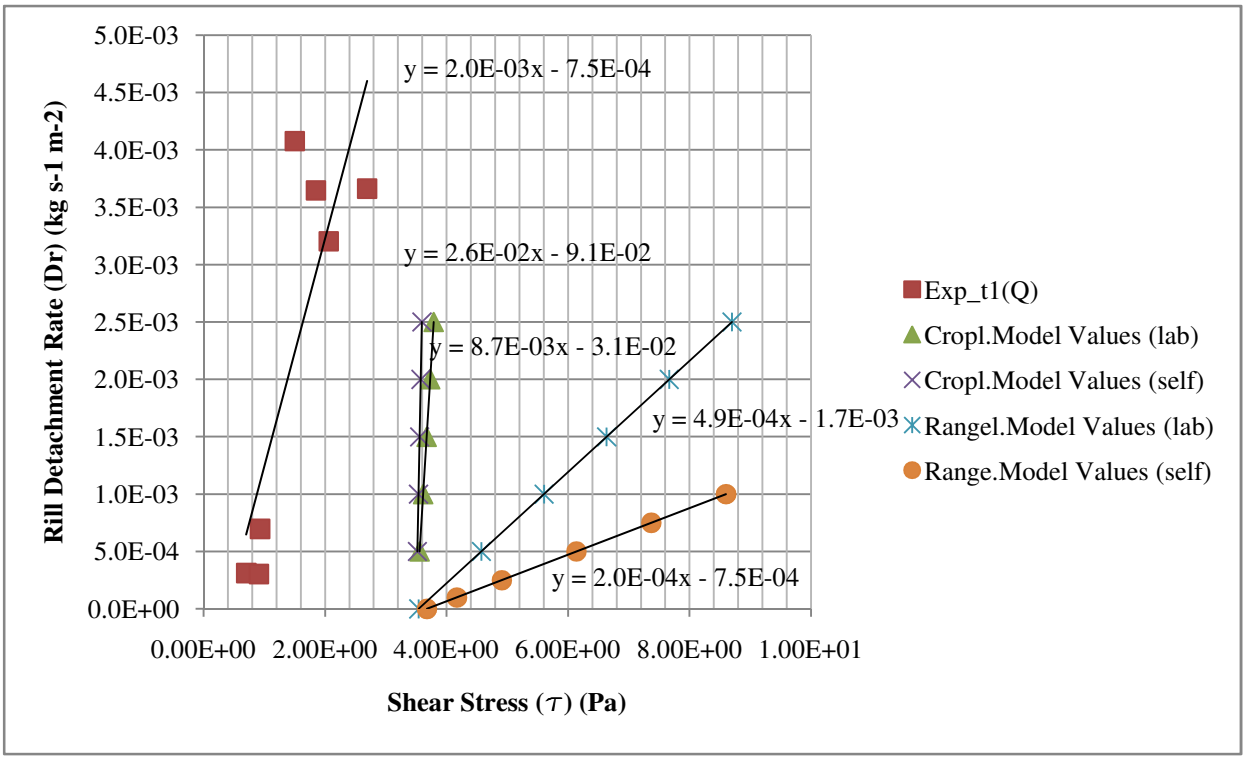

Figure 23. Comparison of rill erodibility (K_r) and critical shear strength (τ_c) of Caton Material. The rill detachment rate (Dc) is plotted over the hydraulic shear stress (τ).

The comparison shows a clear mismatch between the critical shear stresses. The experimental value is 7 times inferior than the simulated one. The experimental achieved rill erodibility (Kr) lies in between the Rangeland and Cropland WEPP suggested rill erodibility. The erodibility

calculated for Cropland exceeds and the erodibility derived from the Rangeland equations deceeds the experimental erodibility by one decimal power.

4.3.2 Okana Valley

The results obtained for the Okana material are presented in three different chapters. Beginning with the experimental derived, then the model calculated and finally the comparison of both. The same attempt has been applied for the previously described Caton Material.

Rill Experiment

The detachment rate of each experiment is calculated out of the three last captured values. The appertaining progress and values can be found in the Appendix B. In difference to the Caton Bay material, the results derived from an inclination of 5 and 17 degrees, did not lead to a coherent linear regression. That is the reason why the experiments with the material from the Okana Valley are run at an additional inclination of 30 degrees. The high gradient leads to a higher detachment rates which cause the larger scale in Figure 24 compared to the Caton material.

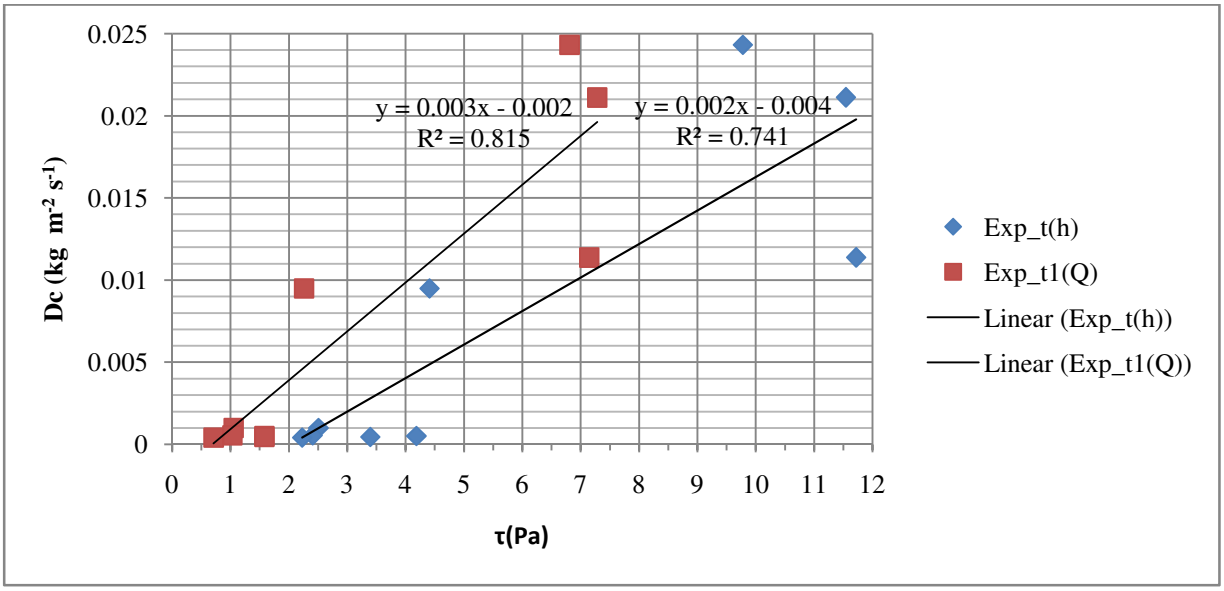

Figure 24. Detachment capacity (Dc) depending on shear stress (τ). Linear Regression Dc (τ) derived from Okana Material.

The two different linear regressions result from different calculations of the hydraulic shear stress. The lower curve is obtained by utilizing the measured height of the flowing water (Exp_t(h)) and the steeper results from measurements considering the recorded discharge

(Exp_t(Q)). The second attempt is regarded as more convenient and used for further comparisons. The measured average inflows of the trials range between 37.1 and 42.9 ml s^{-1}. These values and the three different slopes lead to two critical shear stresses (τ_c) and two rill erodiblity parameters (K_r) for the Okana rill experiment, which is shown in Table 21.

Table 21. Experimental evolved critical shear stress and rill erodibility for Okana material.

	Exp_t(h)	Exp_t1(Q)
tc (pa)	2.1	**0.7**
Kr (s m^{-1})	2.0E-03	**3.0E-03**

Rill Modeling

The model was is not utilized directly, but its calculation equations are contemplated. The WEPP employed equations to calculate the critical shear stress and the rill erodibility deliver different results for the grain size distribution of the PSA (self) and the Hydrometer (lab). Although the results for Cropland and Rangeland for the Laboratory analyzed material for Caton and Okana are the same, the values are shown in Table 22 again to facilitate the comparisons for the Okana material.

Table 22. Shear stress and rill erodibility values for Rangeland and Cropland for two different grain size distribution for the Okana material.

	Cropland(self)	Cropland(lab)	Rangeland(self)	Rangeland(lab)
tc (Pa)	3.50	3.50	3.34	3.69
Kr (s m^{-1})	4.82E-02	8.72E-03	8.36E-05	4.58E-04

Only small differences between all the WEPP calculated critical shear stress (τ_c) are recognized. In contrasts, the results of the rill erodibility (Kr) show clear divergences. The Cropland equation reveals a hundredfold larger Kr compared to the Rangeland. The higher clay content in the hydrometer determined soil texture (lab) evokes only 18.1 percent of the of the Cropland rill erodibility calculated with the PSA material (self). Whereas the lower clay content in the Rangeland equation results in a Ki determined with the PSA (self) of only 18.2 percent of the Ki defined by the Hill Laboratories (lab).

Comparison of the modeled and experimental values

To show how the model calculated rill erodibility pramameter correspond with the experimental results, the shear strength of some detachment rates is calculated according to Equation 3-15 and plotted in Figure 25:

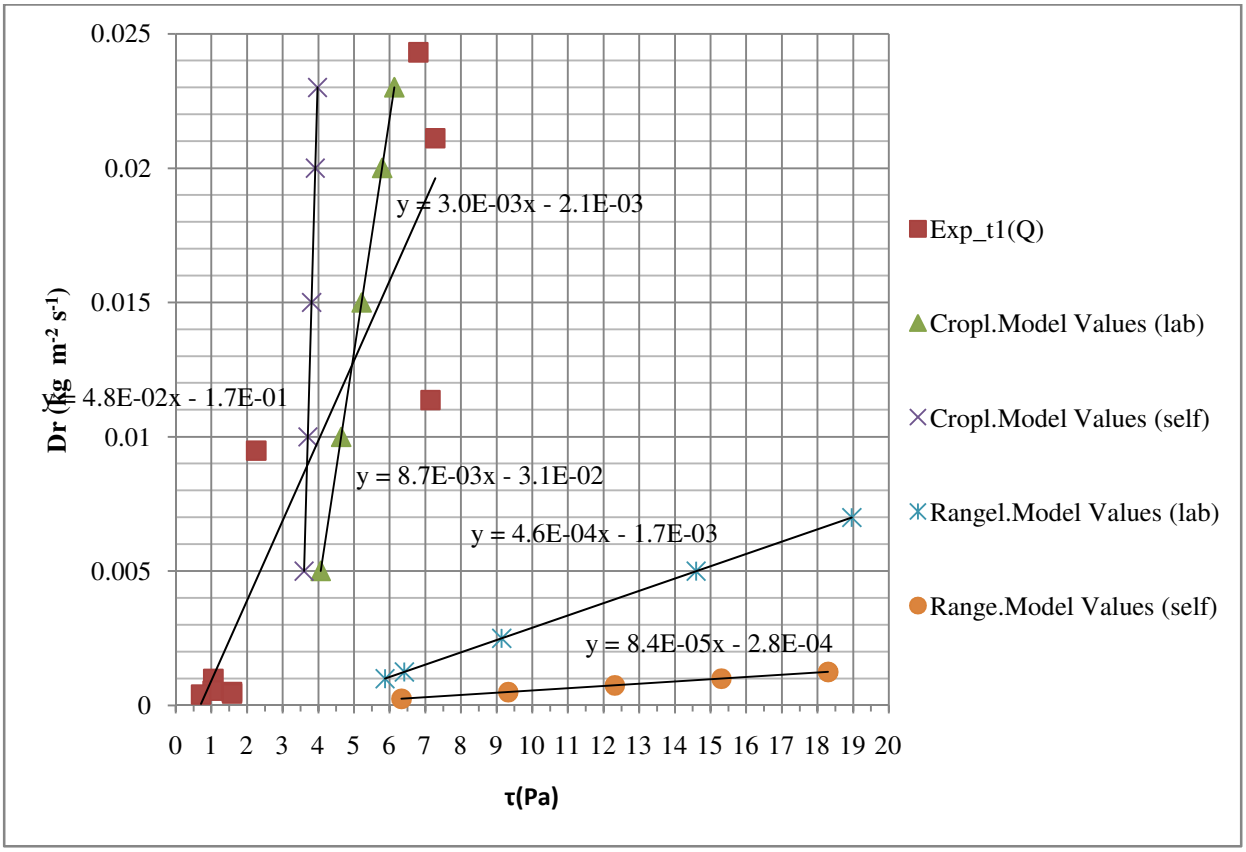

Figure 25. Comparison of the rill erodibility (K_r) and the critical shear stress (τ_c) of the Okana material. The rill detachment rate (D_c) is plotted over the hydraulic shear stress (τ)

The experimental rill erodibility lies in between the model calculated Cropland and Rangeland rill erodibility. The comparison of model and experimental value lead to a maximum deviation of one decimal power for the Cropland equation and a maximum divergence of two decimal power for the Rangeland assumption. The critical shear strength of the experiment is only one fifth of the τ_c are derived from the model suggested equations.

5 DISCUSSION

Separate attempts are considered for the interrill and rill modeling and experiments.

5.1 Interrill erodibility:

To amplify the slope input parameter for the WEPP model, the distinction between segmented and uniform slope for the low, middle and steep slope was done. Which results show that in a small scale the variations need not to be described separately.

To define the WEPP sensitivity to the different soil textures of one material, all derived grain size distributions are considered. The results deduced from the varying soil texture of both materials, show that the present difference between the single soil classes can be neglected for the interrill erodibility. An average value for the soil texture with a certain range of each fraction is derived for the material from Okana valley and Caton Bay, listed in Table 23 and Table 24.

Table 23. Soil characteristic for the material from Caton Bay.

Caton _average		Caton_range	
Clay	15.63 %	9.75 - 21.50	%
Silt	73.57 %	66.50 - 80.65	%
Sand	10.80 %	9.60 - 12.00	%

Table 24. Soil characteristic for the material from the Okana valley.

Okana_average		Okana_range	
Clay	13.69 %	5.89 - 21.50	%
Silt	71.23 %	66.50 - 75.95	%
Sand	15.08 %	12.00 - 18.16	%

Although the materials show high similarity, there is one major difference which can be seen in correlating the interrill erodibility of Figure 12 and Figure 16. It is the regression of the soil loss simulated with the experimental derived interrill erodibilitv value (cal.Ki). An exponential increase of the soil loss is derived from both materials, but the visible larger range of the experimental soil loss at the middle slope of the Caton material can be recognized. This could lead to the assumption that a high interaction between detachment, entrainment, transport and deposition is present, causing different detachment rates. There might be a treshold up to a certain inclination before the critical shear strength is overcome. The slope of the middle

inclined Caton experiment was 29 percent (13 degrees) whereas the inclination for the Okana material was set up at 31 percent (14 degrees) and a more constant but higher interrill erodibility is recognized. But this presumption would need further experiments to be proven.

The independent comparison of the experimental and simulated results of the Okana and Caton material shows, that the use of the WEPP auto-calculated K_i value should not be utilized for loess deposits at steeper slopes. A clear discordance is recognized for a slope larger than 13 degrees (29%). In case of a soil with high silt content (between 67 and 81 percent) the following K_i values for different inclined slopes in New Zealand are suggested:

Table 25. Interrill erodibility for Caton and Okana material

	low slope	middle slope	steep slope
Caton Ki (kg s m^{-4})	4.04E+06 - 4.75E+06	1.56E+07 - 2.30E+07	2.43E+07 - 2.72E+07
Okana Ki (kg s m^{-4})	4.16E+06 - 8.81E+06	2.27E+07 - 2.68E+07	2.73E+07 - 3.02E+07

Although the WEPP model still underestimates the total soil loss of bare soil an approximation from the WEPP Model to the experiments can be derived by using those suggested values. That leads to the conclusion that WEPP can be applied for further simulations also in steeper terrain if the interrill erodibility (K_i) of the soil is known.

To achieve a slope independent interrill erodibility another approach is needed. A new equation which includes slope length and runoff is defined (F.-B. Zhang, Wang, & Yang, 2014). In this study the Sf factor, which Zhang et. al. and the WEPP use to calculate the detachment, is modified with a power exponent. It leads to the following equation:

$$D_i = K_i * R * I^{0.22} * {S_f}^{3.349} * L^{-0,25} \qquad 5\text{-}1$$

K_i = 26815 kg s m^{-4}

R ... Runoff (m^3 s^{-1})

I... Intensity (m s^{-1})

S_f ... Slopefactor (-)

L ... Length (m)

This equation is tested for slopes with an inclination between 4 and 30 degrees with a soil texture which lies within the range of the Caton or Okana soil characteristics listed in Table 27. The comparison between the calculated and the measured(experimental) values shows a linear relationship, illustrated in Figure 26:

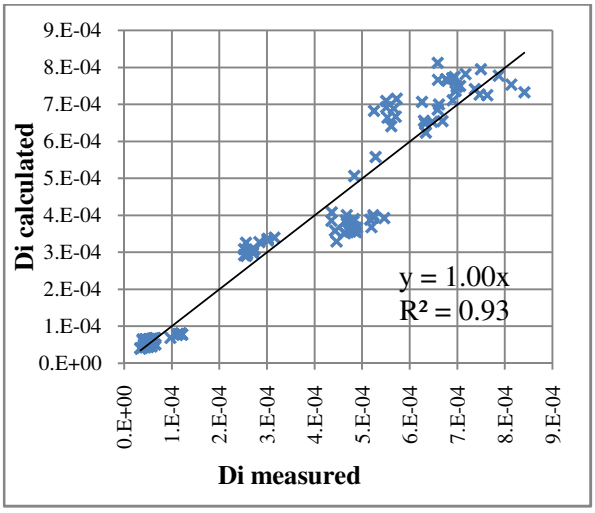

Figure 26. Linear regression between measured detachment rate and detachment rate calculated with 5-1.

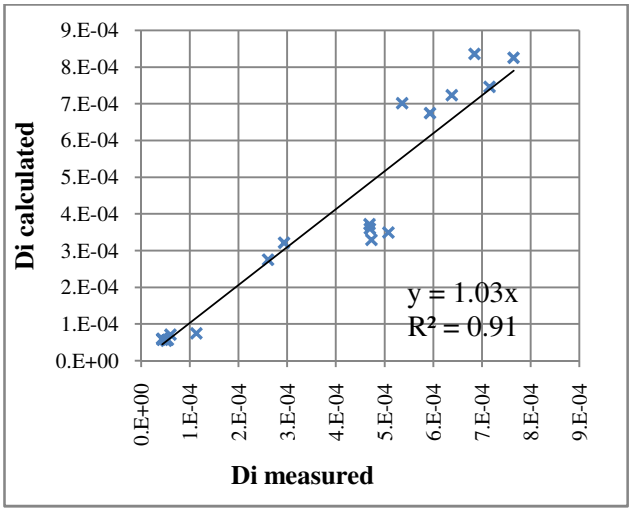

Figure 27. Linear regression between measured detachment rate and detachment rate calculated with 3-9.

To compare the new defined equation from Zhang et al. 2014 with the equation used previously, the same attempt was fulfilled with Equation 3-9 which lead to the following modification of the Sf factor:

$$D_i = K_i * I^2 * {S_f}^{3.423} \qquad 5\text{-}2$$

K_i = 4.00E+07 kg s m^{-4}

I... Intensity (m s^{-1})

S_f ... Slopefactor (-)

The potted values compared with the average measured can be seen in Figure 27. Although Equation 5-1 leads to a higher correlation, it is suggested to use Equation 5-2 since this interrill erodibility parameter also lies within the range of the previously defined slope depending interrill erodibility. Furthermore runoff and slope length are not required, but the results show an acceptable approximation.

5.2 Rill Erodibility

No different rill erodibility values are derived for changing the implemented inclination, but the hydraulic shear stresses and inherent rill detachment rates are strongly influenced by the slopes. The variations in the different experiments lead to a final rill erodibilty parameter for each material. For the modeled rill erodibility and critical shear stress the slope did not influence the results. As their calculations are based on empirical equations which consider exclusively the organic matter, bulk density and clay content. The application of different grain size distributions for one material shows how sensitve the the rill erodibility equation reacts. Since the clay content is the only input parameter a highly accurate soil texture analysis is required. Whereas the values for the critical shear strength of both soils show a maximal deviation of 5 percent.

When comparing the independent executed experiments for the Okana and Caton material with the inherent model used equations, their results show high similarities. Both experimental derived Kr values lie under the Cropland and above the Rangeland calculated value. According to this thesis the application of the Cropland equation provides a better approximation to the experimental rill erodibility value. However the thesis does not give any suggestions according to the model proposed critical shear values. Both of them are significant different from the experimental derived. The use of the WEPP auto calculated rill erodibility and critical shear strength for soils with a high silt content is not recommended, especially when bare soil is modeled. The critical shear stress and the suggested rill erodibility for the soil textures listed in Table 23 and Table 24, are represented in Table 26:

Table 26. Rill erodibility and critical shear stress values

	Okana	Caton
tc (pa)	0.7	0.4
Kr (s m^{-1})	0.003	0.002

The similarity of those two values and the related soil texture of both materials results in a proposal for a new rill erodibility equation which combines these results:

$$Kr = a\,(silt) + b(clay) \qquad 5\text{-}3$$

$$Kr = 0.000195(silt) - 0.0008(clay) \qquad 5\text{-}4$$

The ranges of the soil classes, where this equation can be applied to calculate the rill erodibility are listed in Table 27. These values are resulting from the grain size distribution for the Caton and Okana material.

Table 27. Range of soil classes for application of the rill erodibility calculation with 5-4.

Range			
Clay (%)	5.89	-	21.50
Silt (%)	66.50	-	80.65
Sand (%)	9.60	-	18.16

The linear regression is calculated with the averages result from Table 23 and Table 24 and suggests a determination possibility for the rill erodibility. The equation can be applied for soils around the Bank Peninsula in New Zealand which grain size distribution is covered by the range of Table 27. Although other previous studies have shown that the lower erodibility is resulting from soils with higher clay content (Romero et al., 2007) which is also the case for this equation does not readily deliver the rill erodibility for all soils within the range from Table 27. Significant differences in the organic matter content or the bulk density might cause invalidity.

6 SUMMARY

To obtain experimental parameter to validate the WEPP output, separate attempts are fullfilled to measure the rill and interrill soil loss. Both experiments show that the inclination of the soil surface is a crucial parameter. For the interrill erosion, different slopes are used to represent their influence on the interrill erodibility. The rill erodibility is derived from different rill detachment rates depending on the different slopes and runoff. The reason for the different grain size distribution could either originate from the different methods or from the difficulty of collection and analysis of representative soil samples. The possible variations of the different results could be taken into account by defining a whole range of the different soil classes. It shows that more than one analysis should be executed to describe one material.

Firstly this thesis should provide information to facilitate small scale interrill and rill erodibility calculations and can be a support for further WEPP interrill and rill erodibility calibrations. Secondly the supply/allocation of the interrill erodibility, rill erodibility and critical shear stress values for the study area, its surroundings and similar settings. Different interrill erodibility paramerters are derived, depending and not depending on the slope for a defined soil texture. For the rill erodibility parameter, only one value is suggested. Their applicability has already been tested with WEPP watershed calculation of the Caton valley and lead to satisfying results. (Hamader, 2014)

LIST OF REFERENCES

Black, C. A. (1965). *Methods of Soil Analysis* (Vol. 1). Madison: American Society of Agrnonomy.

Bryan, R. B. (1968). The development, use and efficiency of indices of soil erodibility. *Geoderma*, *2*(1), 5–26.

Carsel, R. F., & Parrish, R. S. (1988). Developing joint probability distributions of soil water retention characteristics. *Water Resources Research*, *24*(5), 755–769.

Cochrane, T. A. (1995). *Detachment and Deposition in a Simulated Rill*. Purdue University.

Dane, J. H. (2002). *Methods of Soil Analysis* (Vol. 4). Madison: Soil Science Society of America.

Decagon Devices, I. (2007). Mini Disk Infiltrometer, *Version 9*.

Decagon Devices, I. (2013). *EC - 5 Soil Moisture Sensor - Overview*. USA.

Delleur, J. W. (2007). *The handbook of groundwater engineering*. Boca Raton: CRC press.

Dissmeyer, G. E., & Foster, G. R. (1980). *A guide for predicting sheet and rill erosion on forest land*. Atlanta, Ga. (1720 Peachtree Road, N.W., Atlanta, Ga. 30367): USDA-Forest Service, Southeastern Area. Retrieved from http://catalog.hathitrust.org/Record/002063984

Dohrmann, R. (2006). Cation exchange capacity methodology I: An efficient model for the detection of incorrect cation exchange capacity and exchangeable cation results. *Applied Clay Science*, *34*(1), 31–37.

Elliott, W. J., Liebenow, A. M., Laflen, J. M., & Kohl, K. D. (1989). A compendium of soil erodibility data from wepp cropland soil field erodibility experiments 1987 & 1988. *Lafayette, Indiana, Ohio State University and USDA Agricultural Research Service National Soil Erosion Research Laboratory Report*, (3).

Flanagan, D. C., Frankenberger, J. C., & Ascough, J. C. (2012). WEPP: Model Use, Calibration, and Validation. *Transactions of the ASABE*, *55*(4). http://doi.org/10.13031/2013.42254

Flanagan, D. C., & Livingston, S. J. (1995). USDA- Water Erosion Prediction Project: WEPP User Summary. *NSERL Rep*, *11*.

Flanagan, D. C., Nearing, M. A., Lane, L. J., Risse, L. M., & Finkner, S. C. (1995). USDA-Water Erosion Prediction Project: Hillslope Profile and Watershed Model Documentation. *NSERL Report*, *10*.

Foster, G. R., Meyer, L. D., & Onstad, C. A. (1977). An erosion equation derived from basic erosion principles. *Transactions of the ASAE [American Society of Agricultural Engineers](USA)*.

Hairsine, P. B., & Rose, C. W. (1992a). Modeling water erosion due to overland flow using physical principles: 1. Sheet flow. *Water Resources Research*, *28*(1), 237–243. http://doi.org/10.1029/91WR02380

Hairsine, P. B., & Rose, C. W. (1992b). Modeling water erosion due to overland flow using physical principles: 2. Rill flow. *Water Resources Research*, *28*(1), 245–250. http://doi.org/10.1029/91WR02381

Hamader, K. (2014, May 29). *Estimation of Soil Loss in steep Terrain - New Zealand*. University of Natural Resources and Life Sciences, Vienna. Retrieved from file:///C:/Users/Hanna/Downloads/fulltext_12436.pdf

Laflen, J. M., Elliot, W. J., Simanton, J. R., Holzhey, C. S., & Kohl, K. D. (1991). WEPP: Soil erodibility experiments for rangeland and cropland soils. *Journal of Soil and Water Conservation*, *46*(1), 39–44.

Léonard, J., & Richard, G. (2004). Estimation of runoff critical shear stress for soil erosion from soil shear strength. *Catena*, *57*(3), 233–249.

Metzinger, J. (n.d.). *Norton Rainfall Simulator Specification*.

Morgan, R. P. C., & Nearing, M. A. (2011). *Handbook of erosion modelling*. Wiley Online Library.

Moss, A. J., Walker, P. H., & Hutka, J. (1979). Raindrop-stimulated transportation in shallow water flows: an experimental study. *Sedimentary Geology*, *22*(3), 165–184.

Musy, A., & Higy, C. (2011). *Hydrology: A Science of Nature, English Edn*. CRC Press, Science Publishers, Boca Raton, FL, Enfield, NH.

Nearing, M. A., Foster, G. R., Lane, L. J., & Finker, S. C. (1989). A process-based soil erosion model for USDA-water erosion prediction project technology. *Transactions of the ASAE*, *32*(5), 1587–1593.

Reed, A. H., & Reed, A. W. (1960). *Soil Erosion and Conservation in New Zealand* (Vol. Herald Resource Book 2). Wellington.

Renard, K. G., Foster, G. R., Weesies, G. A., McCool, D. K., & Yoder, D. C. (1997). Predicting soil erosion by water: a guide to conservation planning with the revised universal soil loss equation (RUSLE). *Agriculture Handbook (Washington)*, (703).

Romero, C. C., Stroosnijder, L., & Baigorria, G. A. (2007). Interrill and rill erodibility in the northern Andean Highlands. *Catena*, *70*(2), 105–113.

Rose, C. W. . (2004). *An Introduction to the Environmental Physics of Soil, Water and Watersheds*. Cambridge University Press. Retrieved from http://dx.doi.org/10.1017/CBO9780511801426

Schaetzl, R. J., & Anderson, S. (2005). *Soils: Genesis and geomorphology*. Cambridge University Press.

Schumacher, B. A. (2002). Methods for the Determination of Total Organic Carbon (TOC) in Soils and Sediments. Las Vegas, NV, United States Environmental Protection Agency. *Environmental Sciences Division*.

Shi, H., & Shao, M. (2000). Soil and water loss from the Loess Plateau in China. *Journal of Arid Environments*, *45*(1), 9–20. http://doi.org/10.1006/jare.1999.0618

Soil Survey Division Staff. (1993). *Soil Survey Manual* (Vol. Department of Acriculture Handbook). Lincoln, Nebraska: USDA NRCS.

Tan, K. H. (2005). *Soil Sampling, Preparation, and Analysis, Second Edition*. Boca Raton, FL: Taylor & Francis Group.

Toy, T. ., Foster, G. R., & Renard, K. G. (2002). *Soil Erosion: Processes Prediction Measurement and Control.* New York: John Wiley & Sons.

Wischmeier, W. H., & Smith, D. D. (1978). Predicting rainfall erosion losses. Agricultural Handbook 537. *Agricultural Research Service, United States Department of Agriculture*.

Yan, L. J., Yu, X. X., Lei, T. W., Zhang, Q. W., & Qu, L. Q. (2008). Effects of transport capacity and erodibility on rill erosion processes: A model study using the Finite Element method. *Geoderma*, *146*(1), 114–120.

Zhang, F.-B., Wang, Z.-L., & Yang, M.-Y. (2014). Validating and Improving Interrill Erosion Equations. *PLoS ONE*, *9*(2), e88275. http://doi.org/10.1371/journal.pone.0088275

Zhang, R. D. (1997). Determination of soil sorptivity and hydraulic conductivity from the disk infiltrometer. *Soil Science Society of America Journal*, *61*(4), 1024–1030.

APPENDICES

Appendix A: Interrill Erosion

Simulation Form No: 7

Soil Caton

Surface: 0.091 m² / 906.5 cm²
Length: 0.37 m
Width: 0.245 m

Date: 26.7.13
Start: 10:10
End: 11:40
Tot Dur: 1:30:00

Average Values:	Q(mm h^{-1}) (ml min^{-1})	Slope (°)	(%)
	14.27	4.667	10.37
	21.6698		

	Intensity (mm h^{-1})	Water Cont. (%)	slope(°)(%) (start)	(end)	S_f			TIME of change	Time Step (min)	plastic empty (g)	plastic full (g)	glass empty (g)	glass dried (g)	sediment (g)	flow (ml min^{-1})	D_i (kg m^{-2} s^{-1})	K_i (kg s m^{-4})	Runoff (mm)	Q(mm h^{-1}) (ml min^{-1})	D_i (kg m^{-2} h^{-1})	Item	Values Di	Values all Di	Ki	Item	Values Ki	Values all Ki
Soil Container No.: 2	19.31	10.9	5	11	0.43	1	10	09:50	10.00	53.4	55.14	197.74	197.85	0.11	0.17	2.02E-06	158672	0.018	16.676	0.23	q1	0.21	0.01	5.00E+06	q1	4.59E+06	4.14E+06
		12.3	4	9		2	20	19:50	10.00	53.39	195.8	199.5	204.11	4.61	13.95	8.48E-05	6648545	1.52	25.32	0.24	Min	0.19	0.12	5.15E+06	Min	4.14E+06	3.21E+06
		11.5	4	9	0.47	3	30	29:50	10.00	53.39	290.58	189.38	195.01	5.63	23.37	1.04E-04	8119590	2.554		0.23	Med	0.22	0.19	4.93E+06	Med	4.85E+06	4.62E+06
		36.8	7	16		4	40	39:50	10.00	53.38	313.4	188.46	193.24	4.78	25.70	8.79E-05	6893719	2.816		0.19	Max	0.24	0.24	4.14E+06	Max	5.15E+06	5.96E+06
		21.6	4	9	0.43	5	50	49:50	10.00	51.16	324.02	278.7	282.7	4	27.04	7.35E-05	5768803	2.966		0.22	q3	0.23	0.22	4.76E+06	q3	4.99E+06	4.99E+06
		35.8	5	11		6	70	09:50	10.00	51.19	308.11	314.23	317.7	3.47	25.48	6.38E-05	5004436	2.796		0.21	Ave	0.22	0.19	4.53E+06	Ave	4.75E+06	4.49E+06
			4.8	10.7	0.44	1.1	60	59:50	10.00	51.17	312.11	317.5	321.07	3.57	25.87	6.56E-05	5148656	2.839									
						1.2	80	19:50	10.00	51.15	306.55	141.64	145.06	3.42	25.33	6.29E-05	4932326	2.78									
						1.3	90	29:50	10.00	51.21	301.94	303.95	306.82	2.87	24.89	5.28E-05	4139116	2.734									
						1.4	100	39:50	10.00	51.15	305.14	292.36	295.66	3.3	25.19	6.07E-05	4759262	2.765									
						1.5	110	49:50	10.00	51.17	304.64	282.92	286.06	3.14	25.15	5.77E-05	4528510	2.762									
Soil Container No.: 3	17.72	6.4	6	13	0.49	7	10	10:00	10.00	51.17	54.83	188.78	188.88	0.1	0.36	1.84E-06	171630	0.039	10.8303	0.21	q1	0.13		5.39E+06	q1	3.30E+06	
		20.2	6	13		8	20	20:00	10.00	53.55	168.5	187.22	190.6	3.38	11.28	6.21E-05	5801103	1.231	16.45	0.18	Min	0.12		4.74E+06	Min	3.21E+06	
		20.1	4	9	0.43	9	30	30:00	10.00	51.18	198.66	198.38	201.12	2.74	14.58	5.04E-05	4702669	1.597		0.16	Med	0.15		4.15E+06	Med	3.84E+06	
		35.7	5	11		10	40	40:00	10.00	53.2	287.82	187.47	190.41	2.94	23.28	5.41E-05	5045930	2.556		0.14	Max	0.21		3.54E+06	Max	5.39E+06	
		30.3	4	9	0.41	11	50	50:00	10.00	53.57	231.49	279.7	282.84	3.14	17.60	5.77E-05	5389190	1.928		0.12	q3	0.18		3.23E+06	q3	4.59E+06	
		34.0	4	9		12	60	00:00	10.00	51.22	223.28	153.82	156.58	2.76	17.03	5.07E-05	4736995	1.868		0.12	Ave	0.16		3.21E+06	Ave	4.04E+06	
			4.8	10.7	0.44	7.1	70	10:00	10.00	51.18	218.28	251.02	253.44	2.42	16.56	4.45E-05	4153452	1.817									
						7.2	80	20:00	10.00	51.2	212.47	136.4	138.46	2.06	16.00	3.79E-05	3535583	1.756									
						7.3	90	30:00	10.00	51.19	210.18	267.46	269.34	1.88	15.78	3.46E-05	3226649	1.733									
						7.4	100	40:00	10.00	51.2	209.76	252.02	253.89	1.87	15.74	3.44E-05	3209486	1.729									
						7.5	110	50:00	10.00	51.18	280.73	303.75	306.59	2.84	22.78	5.22E-05	4874299	2.501									
Soil Container No.: 4	18.43	8.7	4	9	0.41	13.0	40	40:10	10.00	53.35	61.85	190.39	190.88	0.49	0.82	9.01E-06	815734	0.088	15.3111	0.24	q1	0.17		5.96E+06	q1	4.18E+06	
		23.3	4	9		14.0	20	20:10	10.00	53.76	111.79	188.15	191.75	3.6	5.58	6.62E-05	5993148	0.6	23.24	0.21	Min	0.15		5.29E+06	Min	3.78E+06	
		28.7	5	11	0.45	15.0	30	30:10	10.00	53.7	279.38	253.42	260.15	6.73	22.15	1.24E-04	1.1E+07	2.415		0.19	Med	0.18		4.71E+06	Med	4.45E+06	
		21.5	5	11		16.0	10	10:10	10.00	51.2	263.59	275.06	279.27	4.21	20.98	7.74E-05	7008653	2.297		0.17	Max	0.24		4.20E+06	Max	5.96E+06	
		23.5	5	11	0.41	13.1	50	50:10	10.00	51.18	283.15	300.19	304.12	3.93	22.95	7.23E-05	6542520	2.516		0.17	q3	0.20		4.18E+06	q3	5.15E+06	
		30.6	3	7		13.2	60	00:10	10.00	51.17	285.02	280.38	283.96	3.58	23.16	6.58E-05	5959852	2.54		0.15	Ave	0.19		3.78E+06	Ave	4.69E+06	
			4.3	9.6	0.42	17.0	70	10:10	10.00	51.16	285.63	307.13	310.31	3.18	23.25	5.85E-05	5293947	2.551									
						18.0	80	20:10	10.00	53.3	284.39	248.29	251.12	2.83	22.93	5.20E-05	4711280	2.518									
						13.3	90	30:10	10.00	51.2	277.38	261.36	263.88	2.52	22.46	4.63E-05	4195203	2.467									
						13.4	100	40:10	10.00	51.17	294.54	252.67	255.18	2.51	24.18	4.61E-05	4178556	2.657									
						13.5	110	50:10	10.00	51.21	287.09	267.37	269.64	2.27	23.45	4.17E-05	3779013	2.577									

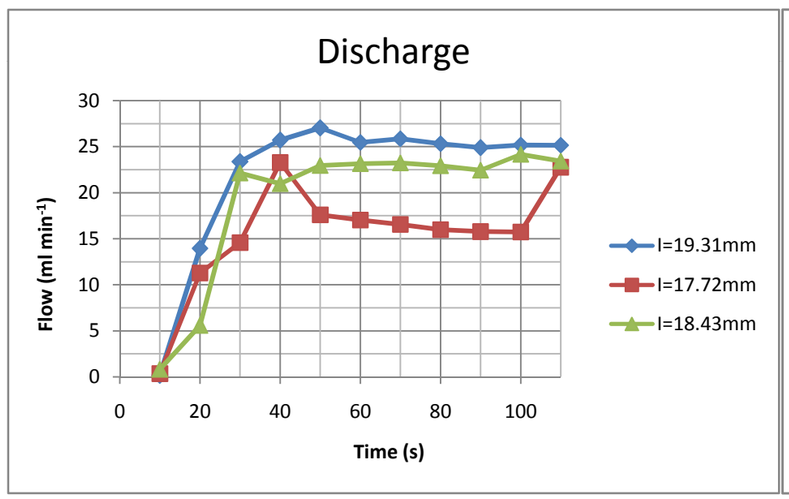

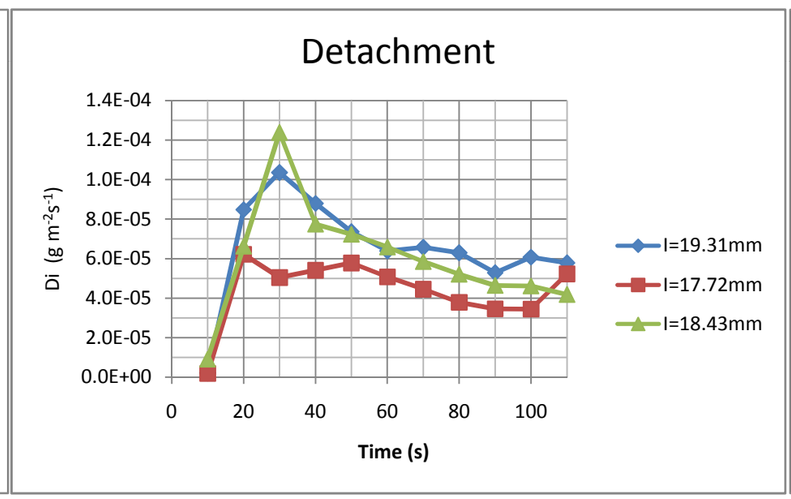

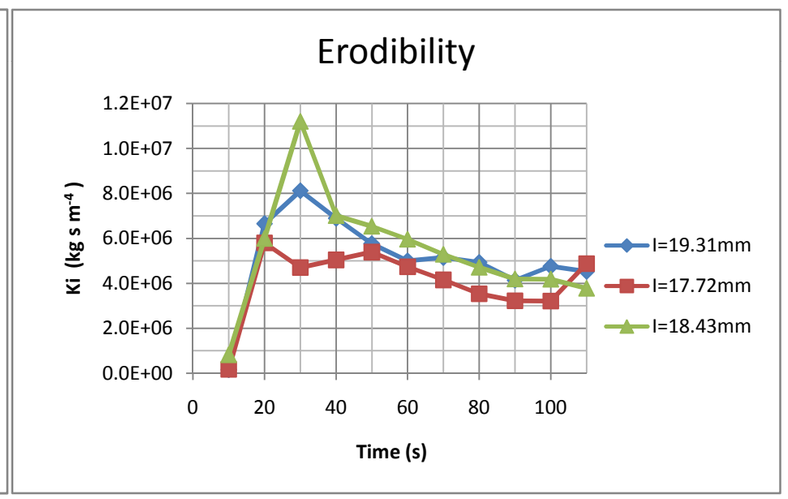

Simulation Form No: 6

Soil Caton

Surface: 0.091 m² / 906.5 cm²
Length: 0.35 m
Width: 0.245 m

Date: 24.7.13
Start: 10:03
End: 11:43
Tot Dur: 1:40:00

Average Values:	Q(mm h^{-1}) (ml min^{-1})	Slope (°)	%
	16.93	13.00	28.89
	26.28		

	Intensity (mm)	Water Cont. (%)	slope(°)(%) (start)	(end)	S_f			TIME of change	Time Step (min)	plastic empty (g)	plastic full (g)	glass empty (g)	glass dried (g)	sediment (g)	flow (ml min^{-1})	D_i (kg m^{-2} s^{-1})	K_i (kg s m^{-4})	Runoff (mm)	Q(mm h^{-1}) (ml min^{-1})	D_i (kg m^{-2} h^{-1})	Item	Values Di	Values all Di	K_i (kg s m^{-4})	Item	Values Ki	Values all Ki
Soil Container No.: 2	19.31	1.7	15	33	0.72	1	10	09:50	10.00	53.41	109.08	197.73	200	2.27	5.43	4.17E-05	2.04E+06	0.59	17.30	1.67	q1	1.67	0.09	2.26E+07	q1	2.3E+07	1.5E+07
		10.0	12	27		2	20	19:50	10.00	53.41	309.94	199.5	213.34	13.84	24.79	2.54E-04	1.24E+07	2.68	27.10	1.61	Min	1.61	0.91	2.18E+07	Min	2.2E+07	1.4E+07
		7.5	13	29	0.73	3	30	29:50	10.00	53.37	337.73	189.37	211.16	21.79	27.08	4.01E-04	1.96E+07	2.90		1.71	Med	1.69	1.09	2.32E+07	Med	2.3E+07	1.6E+07
		13.6	15	33		4	40	39:50	10.00	53.26	350.15	188.46	214.04	25.58	28.10	4.70E-04	2.30E+07	2.99		1.67	Max	1.75	1.75	2.27E+07	Max	2.4E+07	2.4E+07
		4.1	15	33	0.69	5	50	49:50	10.00	53.39	341.76	278.7	303.87	25.17	27.27	4.63E-04	2.26E+07	2.90		1.75	q3	1.73	1.65	2.38E+07	q3	2.4E+07	2.2E+07
		14.9	10	22		6	70	09:50	10.00	51.16	320.98	153.79	178.08	24.29	25.47	4.47E-04	2.18E+07	2.71		1.74	Ave	1.69	1.23	2.36E+07	Ave	2.3E+07	1.8E+07
			13.3	29.6	0.71	1.1	60	59:50	10.00	51.15	342.78	317.5	343.36	25.86	27.55	4.75E-04	2.32E+07	2.93									
						1.2	80	19:50	10.00	51.16	339.02	327.33	352.6	25.27	27.21	4.65E-04	2.27E+07	2.90									
						1.3	90	29:50	10.00	51.21	341.91	303.95	330.46	26.51	27.42	4.87E-04	2.38E+07	2.91									
						1.4	100	39:50	10.00	51.2	344.56	292.36	318.66	26.3	27.70	4.84E-04	2.36E+07	2.95									
Soil Container No.: 3	17.72	6.1	15	33	0.72	7	10	10:00	10.00	51.23	109.07	188.78	190.6	1.82	5.67	3.35E-05	2.00E+06	0.62	16.57	0.91	q1	0.91		1.50E+07	q1	1.5E+07	
		15.0	12	27		8	20	20:00	10.00	53.57	282.47	187.21	195.87	8.66	22.35	1.59E-04	9.50E+06	2.43	25.57	0.91	Min	0.91		1.51E+07	Min	1.5E+07	
		7.2	13	29	0.68	9	30	30:00	10.00	51.2	313.84	198.36	210.14	11.78	25.53	2.17E-04	1.29E+07	2.77		0.93	Med	0.93		1.55E+07	Med	1.5E+07	
		10.1	11	24		10	40	40:00	10.00	53.29	330.6	187.47	201.64	14.17	26.85	2.61E-04	1.55E+07	2.90		0.92	Max	0.99		1.53E+07	Max	1.6E+07	
		5.8	14	31	0.68	11	50	50:00	10.00	53.6	325.76	279.7	293.4	13.7	26.36	2.52E-04	1.50E+07	2.85		0.97	q3	0.96		1.62E+07	q3	1.6E+07	
		8.3	10	22		12	60	00:00	10.00	51.22	309.87	141.63	155.35	13.72	25.01	2.52E-04	1.51E+07	2.70		0.99	Ave	0.94		1.64E+07	Ave	1.6E+07	
			12.5	27.8	0.69	7.1	70	10:00	10.00	51.19	313.58	251.02	265.11	14.09	25.36	2.59E-04	1.55E+07	2.74									
						7.2	80	20:00	10.00	51.21	308.41	278.53	292.5	13.97	24.85	2.57E-04	1.53E+07	2.68									
						7.3	90	30:00	10.00	51.2	315.63	267.46	282.19	14.73	25.53	2.71E-04	1.62E+07	2.75									
						7.4	100	40:00	10.00	51.2	323.83	252.02	266.94	14.92	26.33	2.74E-04	1.64E+07	2.84									
Soil Container No.: 4	18.43	5.7	14	31	0.70	13.0	40	40:10	10.00	53.42	63.43	190.39	190.7	0.31	0.98	5.70E-06	3.07E+05	0.11	16.91	0.92	q1	1.04		1.38E+07	q1	1.6E+07	
		14.4	12	27		14.0	20	20:10	10.00	53.76	262.35	188.14	193.67	5.53	20.51	1.02E-04	5.48E+06	2.24	26.15	1.09	Min	0.92		1.63E+07	Min	1.4E+07	
		5.1	15	33	0.73	15.0	30	30:10	10.00	53.76	304.36	253.42	260.44	7.02	24.62	1.29E-04	6.96E+06	2.69		1.09	Med	1.09		1.63E+07	Med	1.6E+07	
		12.0	13	29		16.0	10	10:10	10.00	51.22	310.43	275.06	285.26	10.2	25.29	1.88E-04	1.01E+07	2.75		1.02	Max	1.14		1.53E+07	Max	1.7E+07	
		7.3	15	33	0.69	13.1	50	50:10	10.00	51.19	315.26	307.11	321.03	13.92	25.54	2.56E-04	1.38E+07	2.76		1.09	q3	1.09		1.63E+07	q3	1.6E+07	
		23.8	10	22		13.2	60	00:10	10.00	53.34	324.47	248.29	264.72	16.43	26.09	3.02E-04	1.63E+07	2.81		1.14	Ave	1.06		1.70E+07	Ave	1.6E+07	
			13.2	29.3	0.71	17.0	70	10:10	10.00	51.2	324.75	300.15	316.57	16.42	26.33	3.02E-04	1.63E+07	2.84									
						18.0	80	20:10	10.00	51.2	318.35	316.35	331.83	15.48	25.75	2.85E-04	1.53E+07	2.78									
						13.3	90	30:10	10.00	51.2	325.97	261.36	277.77	16.41	26.46	3.02E-04	1.63E+07	2.85									
						13.4	100	40:10	10.00	51.2	329.2	252.64	269.82	17.18	26.73	3.16E-04	1.70E+07	2.88									

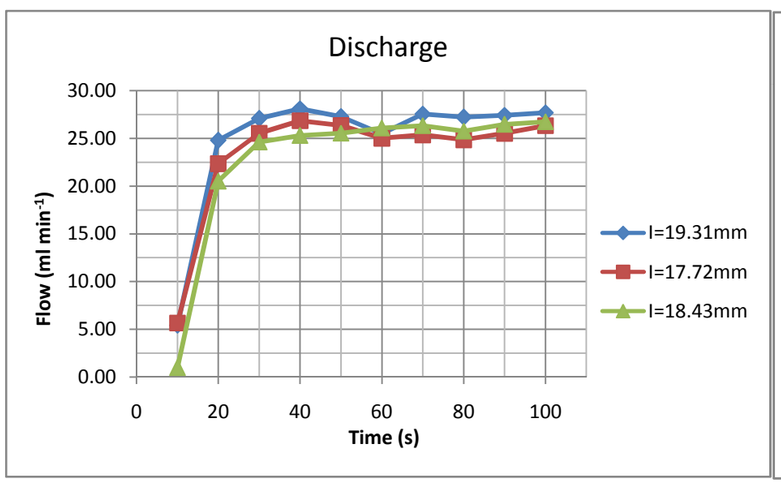

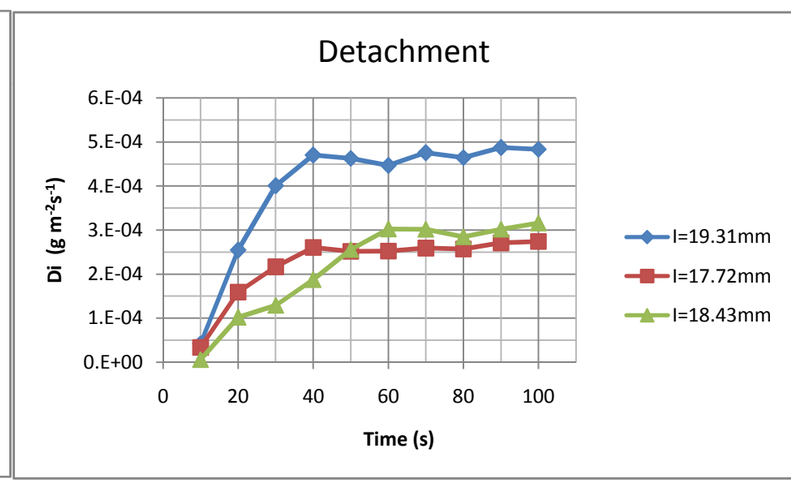

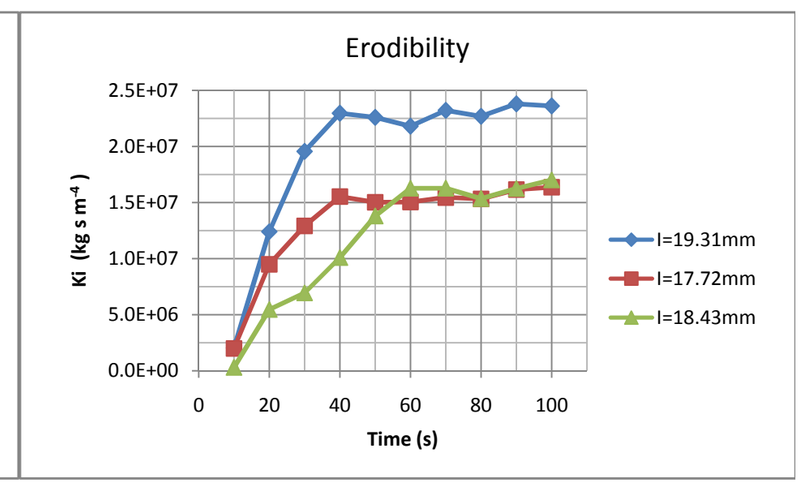

Simulation Form No: 8

Soil Caton

Surface: 0.091 m² = 906.5 cm²
Length: 0.35 m
Width: 0.245 m

Date: 30.7.13
Start: 10:10
End: 11:40
Tot Dur: 1:30:00

Average Values:	Q(mm h^{-1}) (ml min^{-1})	Slope (°)	(%)
	15.06	26.44	58.77
	24.01996		

	Inten-sity (mm)	Water Cont. (%)	slope(°)(%) (start)	(end)	S_f			TIME of change	Time Step (min)	plastic empty (g)	plastic full (g)	glass empty (g)	glass dried (g)	sediment (g)	flow (ml min^{-1})	D_i (kg m^{-2} s^{-1})	K_i (kg s m^{-4})	Runoff (mm)	Q(mm h^{-1}) (ml min^{-1})	D_i (kg m^{-2} h^{-1})	Item	Values Di	Values all Di	K_i (kg s m^{-4})	Item	Values Ki	Values all Ki
Soil Container No.: 2	19.31	16.2	28	62	0.91	1	10	09:50	10.00	53.54	95.53	197.73	205.68	7.95	3.70	1.46E-04	5583770	0.38	16.22	2.49	q1	2.40	2.03	2.64E+07	q1	2.55E+07	2.51E+07
		17.4	25	56		2	20	19:50	10.00	53.34	205.27	199.53	224.43	24.9	13.64	4.58E-04	1.7E+07	1.40	25.92	2.51	Min	2.37	1.74	2.66E+07	Min	2.52E+07	2.19E+07
		16.4	30	67	0.93	3	30	29:50	10.00	53.36	273.54	189.47	223.53	34.06	19.90	6.26E-04	2.4E+07	2.05		2.58	Med	2.48	2.35	2.74E+07	Med	2.64E+07	2.61E+07
		28.5	29	64		4	40	39:50	10.00	53.4	275.86	188.51	222.3	33.79	20.14	6.21E-04	2.4E+07	2.08		2.48	Max	2.58	2.58	2.63E+07	Max	2.74E+07	2.85E+07
		24.6	26	58	0.89	5	50	49:50	10.00	51.12	317.11	278.69	316.25	37.56	24.26	6.91E-04	2.6E+07	2.52		2.37	q3	2.50	2.40	2.52E+07	q3	2.65E+07	2.72E+07
		38.6	24	53		6	70	09:50	10.00	51.19	325.58	314.21	352.07	37.86	25.08	6.96E-04	2.7E+07	2.61		2.37	Ave	2.47	2.23	2.52E+07	Ave	2.62E+07	2.59E+07
			27.0	60.0	0.91	1.1	60	59:50	10.00	51	341.08	317.53	356.52	38.99	26.58	7.17E-04	2.7E+07	2.77									
						1.2	80	19:50	10.00	51.2	336.29	282.9	320.38	37.48	26.18	6.89E-04	2.6E+07	2.73									
						1.3	90	29:50	10.00	51.15	333.27	303.95	339.83	35.88	25.98	6.60E-04	2.5E+07	2.72									
						1.4	100	39:50	10.00	51.12	347.82	267.39	303.22	35.83	27.44	6.59E-04	2.5E+07	2.88									
Soil Container No.: 3	17.72	20.1	29	64	0.91	7	10	10:00	10.00	51.11	114	188.78	195.74	6.96	5.86	1.28E-04	5800851	0.62	13.45	1.74	q1	1.89		2.19E+07	q1	2.38E+07	
		22.1	25	56		8	20	20:00	10.00	53.51	172.66	187.22	201.58	14.36	11.02	2.64E-04	1.2E+07	1.16	21.43	1.90	Min	1.74		2.39E+07	Min	2.19E+07	
		23.1	29	64	0.92	9	30	30:00	10.00	51.15	231.4	198.38	222.73	24.35	16.51	4.48E-04	2E+07	1.72		2.02	Med	1.95		2.54E+07	Med	2.45E+07	
		28.5	26	58		10	40	40:00	10.00	53.26	244.98	187.47	215.33	27.86	17.44	5.12E-04	2.3E+07	1.81		2.05	Max	2.05		2.59E+07	Max	2.59E+07	
		25.0	27	60	0.90	11	50	50:00	10.00	53.56	245.98	279.7	306	26.3	17.60	4.84E-04	2.2E+07	1.83		1.99	q3	2.01		2.51E+07	q3	2.53E+07	
		34.3	25	56		12	60	00:00	10.00	51.12	262.78	153.8	182.53	28.73	19.38	5.28E-04	2.4E+07	2.02		1.89	Ave	1.93		2.38E+07	Ave	2.43E+07	
			26.8	59.6	0.91	7.1	70	10:00	10.00	51.16	291.98	253.42	283.94	30.52	22.18	5.61E-04	2.5E+07	2.32									
						7.2	80	20:00	10.00	51.18	300.79	303.74	334.78	31.04	23.03	5.71E-04	2.6E+07	2.41									
						7.3	90	30:00	10.00	51.13	298.93	267.44	297.52	30.08	22.91	5.53E-04	2.5E+07	2.40									
						7.4	100	40:00	10.00	51.19	303.53	252.01	280.55	28.54	23.46	5.25E-04	2.4E+07	2.47									
Soil Container No.: 4	18.43	15.0	26	58	0.89	13.0	40	40:10	10.00	53.29	124.17	190.39	198.9	8.51	6.56	1.56E-04	6666299	0.69	15.49	2.41	q1	2.27		2.85E+07	q1	2.69E+07	
		21.6	24	53		14.0	20	20:10	10.00	53.73	179.63	188.15	203.67	15.52	11.62	2.85E-04	1.2E+07	1.22	24.71	2.33	Min	2.06		2.76E+07	Min	2.44E+07	
		22.1	29	64	0.92	15.0	30	30:10	10.00	53.68	250.34	141.63	169.55	27.92	17.93	5.13E-04	2.2E+07	1.86		2.37	Med	2.35		2.81E+07	Med	2.78E+07	
		29.9	26	58		16.0	10	10:10	10.00	51.15	312.12	253.73	289.53	35.8	23.87	6.58E-04	2.8E+07	2.48		2.38	Max	2.41		2.82E+07	Max	2.85E+07	
		26.0	25	56	0.88	17.0	50	50:10	10.00	51.13	310.97	307.09	343.47	36.38	23.72	6.69E-04	2.8E+07	2.47		2.25	q3	2.38		2.67E+07	q3	2.81E+07	
		35.6	23	51		18.0	60	00:10	10.00	53.26	311.25	248.29	283.48	35.19	23.61	6.47E-04	2.8E+07	2.46		2.06	Ave	2.30		2.44E+07	Ave	2.72E+07	
			25.5	56.7	0.90	13.1	70	10:10	10.00	51.16	320.97	300.13	335.95	35.82	24.75	6.59E-04	2.8E+07	2.58									
						13.2	80	20:10	10.00	51.14	325.88	280.35	316.31	35.96	25.23	6.61E-04	2.8E+07	2.63									
						13.3	90	30:10	10.00	51.14	326.36	261.35	295.38	34.03	25.40	6.26E-04	2.7E+07	2.66									
						13.4	100	40:10	10.00	51.2	326.31	252.67	283.79	31.12	25.57	5.72E-04	2.4E+07	2.69									

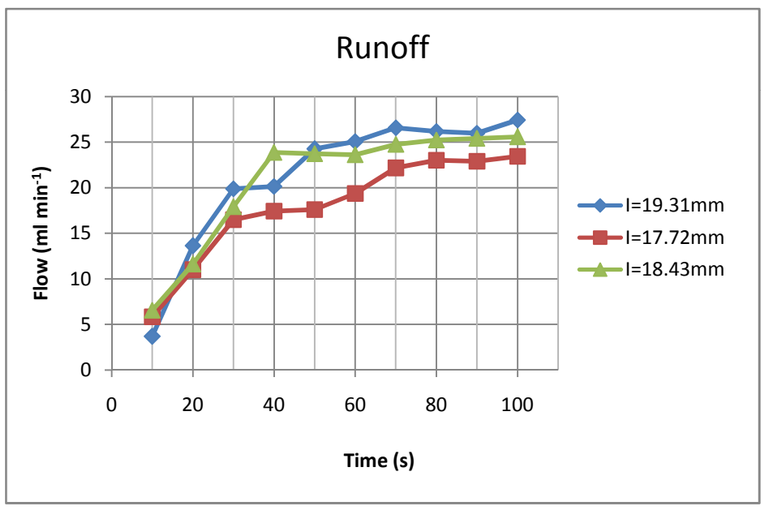

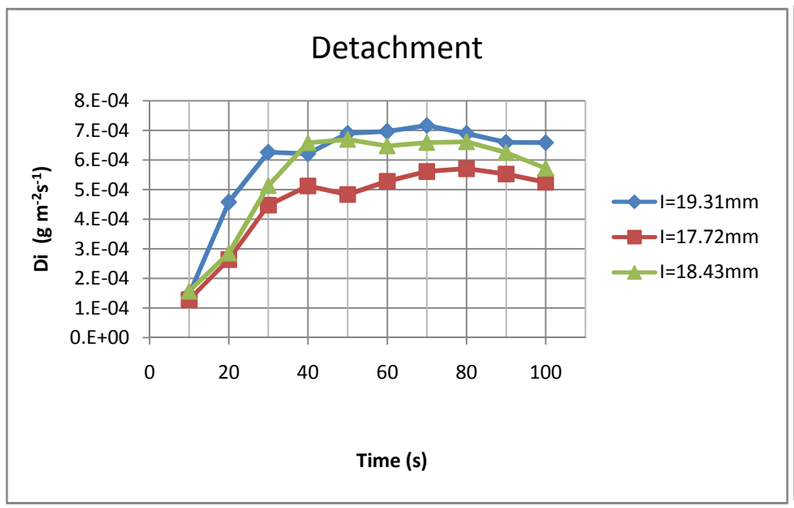

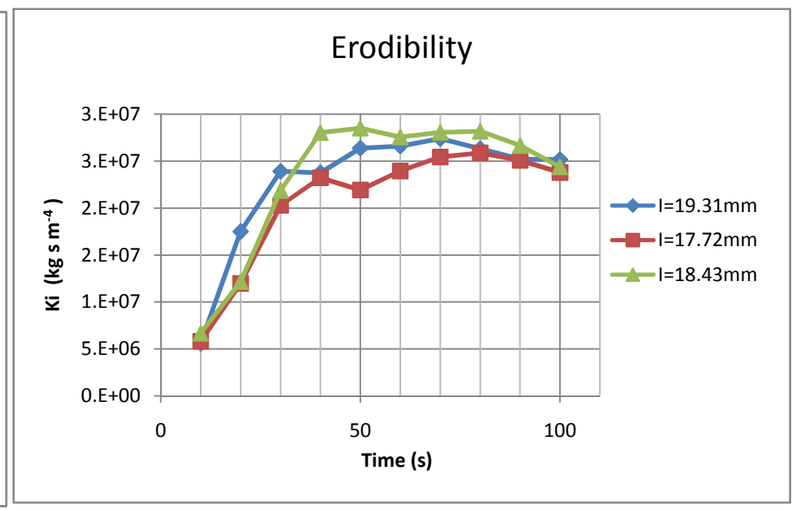

Simulation Form

No: 3

Soil Okana

Surface: 0.0907 m²
906.5 cm²
Length: 0.35 m
Width: 0.245 m

Date:	12.07.13
Start:	14:58
End:	16:48
Tot Dur:	1:50:00

Average Values:	Q(mm h^{-1}) (ml min^{-1})	Slope (°)	(%)
	17.76	4.72	10.49
	16.19		

	Inten-sity (mm)	Water Cont. (%)	slope(°)(%) (start)	(end)	S_f			TIME of change	Time Step (min)	plastic empty (g)	plastic full (g)	glass empty (g)	glass dried (g)	sediment (g)	flow (ml min^{-1})	D_i (kg m^{-2} s^{-1})	K_i (kg s m^{-4})	Runoff (mm)	Q(mm h^{-1}) (ml min^{-1})	D_i (kg m^{-2} h^{-1})	Item	Values Di	Values all Di	K_i (kg s m^{-4})	Item	Values Ki	Values all Ki
Soil Container No.: 2	19.31	16.1	4 4	9 9	0.41	1	10	09:50	10.00	53.43	166.4	303.74	306.48	2.74	11.13	0.05	3894477	1.22	18.31	0.35	q1	0.40	0.02	7.53E+06	q1	8.65E+06	4.20E+06
						2	20	19:50	10.00	53.44	227.7	279.3	283.25	3.95	17.18	0.07	5614300	1.88	16.7354	0.44	Min	0.35	0.14	9.45E+06	Min	7.53E+06	3.59E+06
		23.0	6 6	13 13	0.49	3	30	29:50	10.00	53.44	223.9	283.86	287.81	3.95	16.80	0.07	5614300	1.84		0.43	Med	0.42	0.20	9.31E+06	Med	8.98E+06	5.13E+06
						4	40	39:50	10.00	53.42	242.8	253.46	257.48	4.02	18.68	0.07	5713794	2.04		0.40	Max	0.44	0.44	8.61E+06	Max	9.45E+06	9.45E+06
		28.7	5 5	11 11	0.45	5	50	49:50	10.00	51.18	275.1	317.51	322.17	4.66	22.10	0.09	6623453	2.42		0.41	q3	0.43	0.39	8.77E+06	q3	9.28E+06	8.34E+06
						1.1	70	09:50	10.00	51.18	302.5	250.12	255.42	5.3	24.80	0.10	7533112	2.71		0.43	Ave	0.41	0.26	9.20E+06	Ave	8.81E+06	5.96E+06
			5.0	11.1	0.45	6	60	59:50	10.00	51.2	335.3	281.65	288.3	6.65	28.00	0.12	9451923	3.06									
						1.2	80	19:50	10.00	51.16	343.7	291.55	298.1	6.55	28.84	0.12	9309789	3.15									
						1.3	90	29:50	10.00	51.18	333	278.7	284.76	6.06	27.80	0.11	8613332	3.04									
						1.4	100	39:50	10.00	51.2	341	307.11	313.28	6.17	28.60	0.11	8769679	3.13									
						1.5	110	49:50	10.00	51.17	348.3	252.04	258.51	6.47	29.31	0.12	9196082	3.21									
Soil Container No.: 3	17.72	18.5	4 5	9 11	0.43	7	10	10:00	10.00	51.21	175.5	292.35	294.51	2.16	12.29	0.04	3761080	1.35	16.90	0.16	q1	0.15		4.14E+06	q1	3.92E+06	
						8	20	20:00	10.00	53.61	238.2	248.29	250.79	2.5	18.30	0.05	4353102	2.01	15.3706	0.18	Min	0.14		4.84E+06	Min	3.73E+06	
		22.7	5 5	11 11	0.45	9	30	30:00	10.00	51.22	271.3	275.04	277.67	2.63	21.84	0.05	4579463	2.40		0.16	Med	0.16		4.25E+06	Med	4.16E+06	
						10	40	40:00	10.00	51.31	266.9	249.83	251.99	2.16	21.42	0.04	3761080	2.35		0.15	Max	0.18		3.85E+06	Max	4.84E+06	
		29.5	4 5	9 11	0.43	11	50	50:00	10.00	53.6	264.9	280.73	282.73	2	21.00	0.04	3482481	2.31		0.16	q3	0.16		4.18E+06	q3	4.23E+06	
						12	60	00:00	10.00	51.2	286.3	267.45	269.83	2.38	23.36	0.04	4144153	2.57		0.14	Ave	0.16		3.73E+06	Ave	4.16E+06	
			4.7	10.4	0.44	7.1	70	10:00	10.00	51.23	314.9	303.95	306.73	2.78	26.20	0.05	4840649	2.88									
						7.2	80	20:00	10.00	51.18	315.4	303.09	305.53	2.44	26.27	0.04	4248627	2.89									
						7.3	90	30:00	10.00	51.19	305.9	316.36	318.57	2.21	25.34	0.04	3848142	2.79									
						7.4	100	40:00	10.00	51.21	315.4	279	281.4	2.4	26.27	0.04	4178978	2.89									
						7.5	110	50:00	10.00	51.19	315.2	251.01	253.15	2.14	26.27	0.04	3726255	2.89									
Soil Container No.: 4	18.43	19.8	7 6	16 13	0.51	16.0	40	40:10	10.00	51.23	183.6	280.36	282.22	1.86	13.12	0.03	3059816	1.44	18.08	0.22	q1	0.19		5.41E+06	q1	4.69E+06	
						14.0	20	20:10	10.00	53.81	235.1	188.78	191.46	2.68	17.96	0.05	4408768	1.97	16.453	0.22	Min	0.14		5.53E+06	Min	3.59E+06	
		29.3	4 4	9 9	0.41	15.0	30	30:10	10.00	53.76	293.1	187.46	190.98	3.52	23.71	0.06	5790620	2.60		0.22	Med	0.20		5.53E+06	Med	5.06E+06	
						13.0	10	10:10	10.00	53.39	235	189.38	192.24	2.86	17.98	0.05	4704879	1.97		0.19	Max	0.22		4.70E+06	Max	5.53E+06	
		31.3	4 2	9 4	0.36	17.0	50	50:10	10.00	51.2	322.4	253.44	257.19	3.75	26.89	0.07	6168984	2.95		0.19	q3	0.22		4.69E+06	q3	5.50E+06	
						18.0	60	00:10	10.00	53.31	318.3	327.35	330.64	3.29	26.30	0.06	5412256	2.89		0.14	Ave	0.20		3.59E+06	Ave	4.91E+06	
			4.5	10.0	0.43	13.1	70	10:10	10.00	51.21	332.3	199.49	202.85	3.36	27.90	0.06	5527410	3.06									
						13.2	80	20:10	10.00	51.19	334.5	282.91	286.27	3.36	28.12	0.06	5527410	3.09									
						13.3	90	30:10	10.00	51.19	328.1	190.39	193.25	2.86	27.51	0.05	4704879	3.02									
						13.4	100	40:10	10.00	51.19	330.8	198.35	201.2	2.85	27.79	0.05	4688428	3.05									
						13.5	110	50:10	10.00	51.19	321.6	188.14	190.32	2.18	26.91	0.04	3586236	2.96									

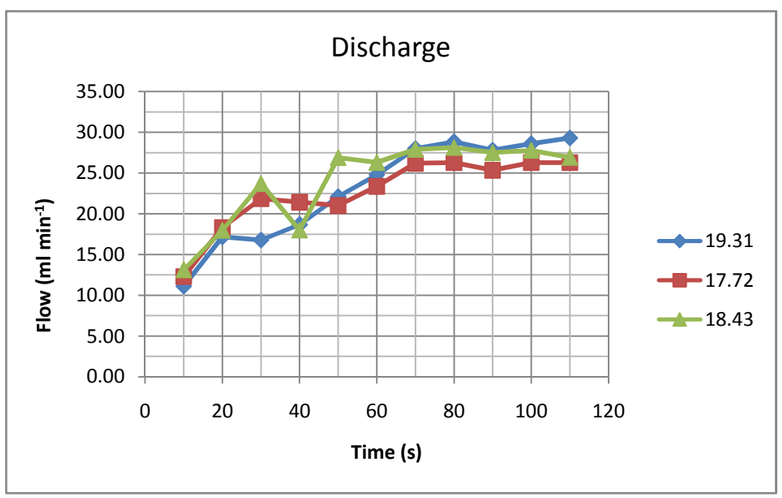

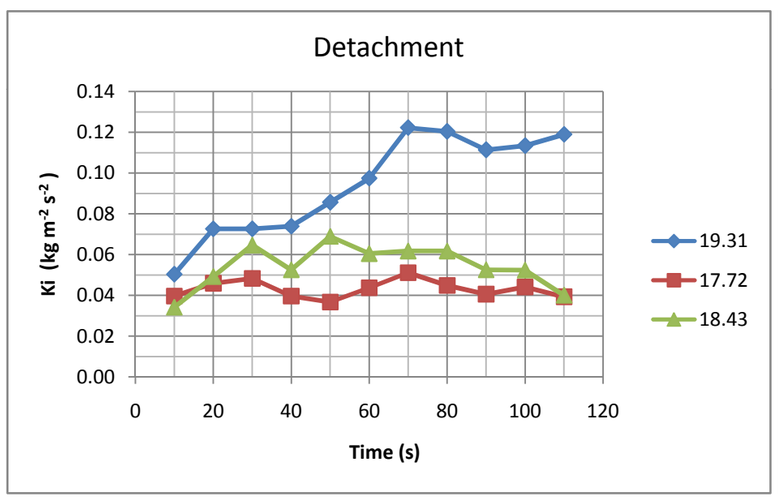

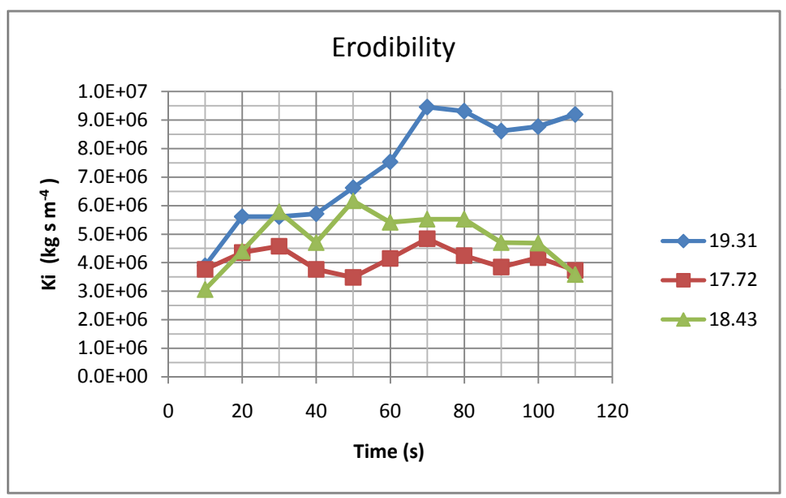

Simulation Form | No: 5

Date:	18.07.13
Start:	11:20
End:	12:50
Tot Dur:	1:30:00

Average Values:	Q(mm h^{-1}) (ml min^{-1})	Slope (°)	(%)
	17.92	14.00	31.11
	16.84		

Soil Okana

Surface: 0.091 m²
906.5 cm²
Length: 0.35 m
Width: 0.245 m

	Inten-sity (mm)	Water Cont. (%)	slope(°)(%) (start)	(end)	S_f			TIME of change	Time Step (min)	plastic empty (g)	plastic full (g)	glass empty (g)	glass dried (g)	sediment (g)	flow (ml min^{-1})	D_i (kg m^{-2} s^{-1})	K_i (kg s m^{-4})	Runoff (mm)	Q(mm h^{-1}) (ml min^{-1})	D_i (kg m^{-2} h^{-1})	Item	Values Di	Values all Di	K_i (kg s m^{-4})	Item	Values Ki	Values all Ki
Soil Container No.: 2	19.31	26.0	14	31	0.72	1	10	09:50	10.00	53.42	116.9	187.22	188.68	1.46	6.26	0.03	1297156	0.68	17.92	1.71	q1	1.68	0.09	2.29E+07	q1	2.26E+07	2.33E+07
		27.7	13	29		2	20	19:50	10.00	53.42	324.4	300.13	312.37	12.24	26.33	0.23	1.1E+07	2.85	16.83	1.74	Min	1.60	1.57	2.33E+07	Min	2.14E+07	2.14E+07
		29.8	15	33	0.75	3	30	29:50	10.00	43.41	349.2	278.51	298.84	20.33	29.32	0.37	1.8E+07	3.15		1.74	Med	1.70	1.73	2.33E+07	Med	2.28E+07	2.48E+07
		34.7	15	33		4	40	39:50	10.00	53.42	349.5	251.01	276.84	25.83	28.00	0.47	2.3E+07	2.98		1.68	Max	1.74	1.97	2.25E+07	Max	2.33E+07	2.94E+07
		30.1	13	29	0.69	5	50	49:50	10.00	51.16	354	307.09	333.32	26.23	28.65	0.48	2.3E+07	3.05		1.69	q3	1.73	1.84	2.27E+07	q3	2.32E+07	2.75E+07
			12	27		6	70	09:50	10.00	51.22	358.3	314.2	340.42	26.22	29.08	0.48	2.3E+07	3.10		1.60	Ave	1.69	1.74	2.14E+07	Ave	2.27E+07	2.54E+07
			13.7	30.4	0.72	1.1	60	59:50	10.00	51.17	355.3	278.69	304.01	25.32	28.84	0.47	2.2E+07	3.08									
						1.2	80	19:50	10.00	51.18	336.5	278.68	304.26	25.58	26.94	0.47	2.3E+07	2.87									
						1.3	90	29:50	10.00	51.22	333.8	316.35	340.46	24.11	26.76	0.44	2.1E+07	2.85									
Soil Container No.: 3	17.72	27.3	16	36	0.76	7	10	10:00	10.00	51.25	66.99	188.76	189.24	0.48	1.54	0.01	499431	0.17	17.45	1.72	q1	1.61		2.71E+07	q1	2.53E+07	0.00E+00
		32.9	15	33		8	20	20:00	10.00	53.58	239.8	303.94	312.19	8.25	18.11	0.15	8583967	1.96	16.40	1.74	Min	1.57		2.74E+07	Min	2.46E+07	0.00E+00
		25.8	14	31	0.74	9	30	30:00	10.00	51.2	346.2	253.41	275.83	22.42	28.10	0.41	2.3E+07	3.01		1.87	Med	1.73		2.94E+07	Med	2.72E+07	0.00E+00
		34.1	15	33		10	40	40:00	10.00	53.29	335.6	327.34	353.38	26.04	26.61	0.48	2.7E+07	2.83		1.76	Max	1.87		2.77E+07	Max	2.94E+07	0.00E+00
		27.2	15	33	0.69	11	50	50:00	10.00	53.6	337.4	317.52	343.84	26.32	26.74	0.48	2.7E+07	2.84		1.57	q3	1.76		2.46E+07	q3	2.76E+07	0.00E+00
		37..8	10	22		12	60	00:00	10.00	51.22	336.7	292.33	320.58	28.25	26.79	0.52	2.9E+07	2.84		1.57	Ave	1.71		2.47E+07	Ave	2.68E+07	0.00E+00
			14.2	31	0.73	7.1	70	10:00	10.00	51.19	334.1	252.01	278.61	26.6	26.63	0.49	2.8E+07	2.83									
						7.2	80	20:00	10.00	51.18	344.1	267.44	291.13	23.69	27.82	0.44	2.5E+07	2.97									
						7.3	90	30:00	10.00	51.21	360.2	268.92	292.63	23.71	29.43	0.44	2.5E+07	3.15									
Soil Container No.: 4	18.43	25.0	17	38	0.77	13.0	40	40:10	10.00	53.39	118.4	199.5	202.12	2.62	6.34	0.05	2530137	0.69	18.39	1.70	q1	1.74		2.48E+07	q1	2.54E+07	0.00E+00
		33.3	15	33		14.0	20	20:10	10.00	53.78	289.1	248.33	259.55	11.22	22.83	0.21	1.1E+07	2.47	17.30	1.89	Min	1.68		2.75E+07	Min	2.46E+07	0.00E+00
		28.3	17	38	0.77	15.0	30	30:10	10.00	53.73	353.2	267.36	288.86	21.5	28.61	0.40	2.1E+07	3.07		1.97	Med	1.87		2.87E+07	Med	2.73E+07	0.00E+00
		34.4	15	33		16.0	10	10:10	10.00	51.21	347.8	279.7	305.43	25.73	28.05	0.47	2.5E+07	2.99		1.89	Max	1.97		2.75E+07	Max	2.87E+07	0.00E+00
		25.0	12	27	0.64	13.1	50	50:10	10.00	51.2	358.2	261.36	289.86	28.5	28.92	0.52	2.8E+07	3.07		1.86	q3	1.89		2.72E+07	q3	2.75E+07	0.00E+00
		33.0	9	20		13.2	60	00:10	10.00	53.31	360.7	275.03	304.74	29.71	28.89	0.55	2.9E+07	3.06		1.68	Ave	1.83		2.46E+07	Ave	2.67E+07	0.00E+00
			14.2	31.5	0.73	17.0	70	10:10	10.00	51.22	362.8	252.65	281.13	28.48	29.39	0.52	2.8E+07	3.12									
						18.0	80	20:10	10.00	51.18	353.6	282.89	311.01	28.12	28.49	0.52	2.7E+07	3.03									
						13.3	90	30:10	10.00	51.22	359.3	303.75	329.18	25.43	29.23	0.47	2.5E+07	3.12									

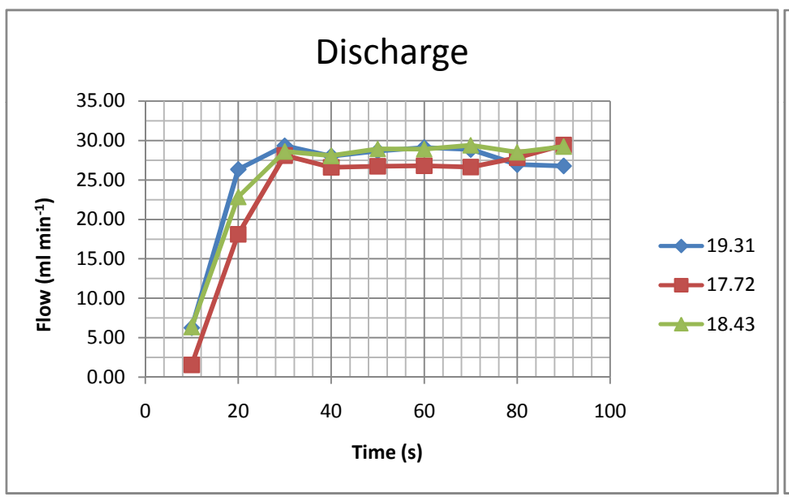

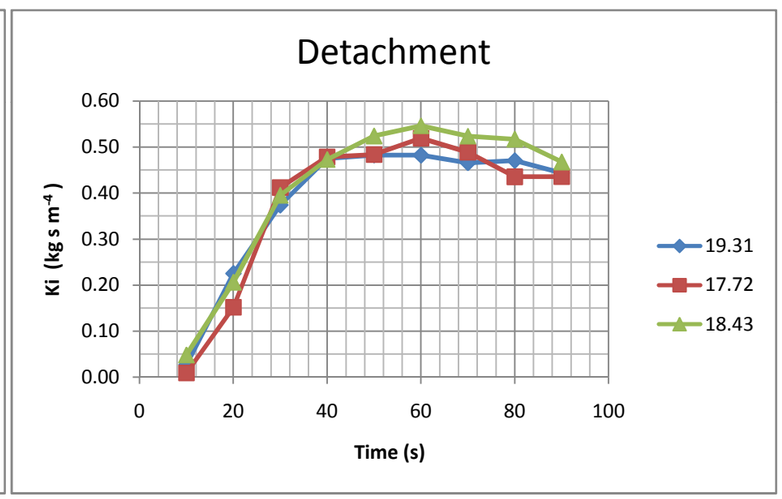

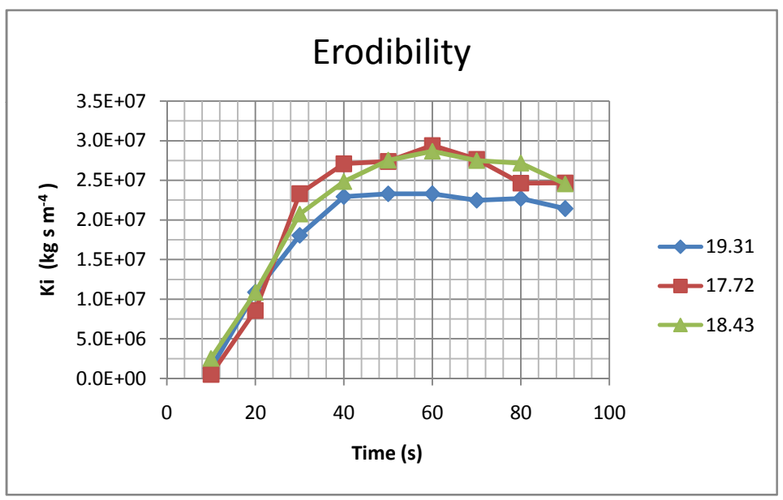

Simulation Form No: 4

Soil Okana

Surface: 0.091 m² / 906.5 cm²
Length: 0.35 m
Width: 0.245 m

Date: 30.7.13
Start: 10:10
End: 11:40
Tot Dur: 1:30:00

Average Values:	Q(mm h^{-1}) (ml min^{-1})	Slope (°)	(%)
	15.9688	26.17	58.15
	15.3278		

	Inten-sity (mm)	Water Cont. (%)	slope(°)(%) (start)	(end)	S_f			TIME of change	Time Step (min)	plastic empty (g)	plastic full (g)	glass empty (g)	glass dried (g)	sediment (g)	flow (ml min^{-1})	D_i (kg m^{-2} s^{-1})	K_i (kg s m^{-4})	Runoff (mm)	Q(mm h^{-1}) (ml min^{-1})	D_i (kg m^{-2} h^{-1})	Item	Values Di	Values all Di	K_i (kg s m^{-4})	Item	Values Ki	Values all Ki
Soil Container No.: 2	19.31	21.2	27	60	0.90	1	10	09:50	10.00	53.4	194.4	303.74	322.58	18.84	12.92	0.35	1.3E+07	1.35	16.14	3.03	q1	2.66	0.17	3.22E+07	q1	2.83E+07	2.83E+07
		24.9	25	56		2	20	19:50	10.00	53.4	308.5	279.27	317.38	38.11	23.13	0.70	2.7E+07	2.39	15.5757	2.93	Min	2.54	1.98	3.11E+07	Min	2.70E+07	2.53E+07
		31.9	27	60	0.91	3	30	29:50	10.00	53.41	337.4	283.86	329.58	45.72	25.56	0.84	3.2E+07	2.63		2.69	Med	2.69	2.51	2.86E+07	Med	2.86E+07	2.88E+07
		31.6	27	60		4	40	39:50	10.00	53.39	342.6	253.48	297.71	44.23	26.17	0.81	3.1E+07	2.70		2.65	Max	3.03	3.03	2.82E+07	Max	3.22E+07	3.32E+07
		32.3	27	60	0.91	5	50	49:50	10.00	51.15	328	317.54	358.14	40.6	25.16	0.75	2.9E+07	2.61		2.54	q3	2.87	2.70	2.70E+07	q3	3.05E+07	2.94E+07
		31.6	26	58		6	70	09:50	10.00	51.2	332.5	281.66	321.73	40.07	25.63	0.74	2.8E+07	2.66		2.70	Ave	2.76	2.49	2.87E+07	Ave	2.93E+07	2.89E+07
			26.5	58.9	0.91	1.1	60	59:50	10.00	51.18	333.5	250.07	288.44	38.37	25.84	0.71	2.7E+07	2.69									
						1.2	80	19:50	10.00	51.16	350.5	291.57	332.33	40.76	27.40	0.75	2.9E+07	2.85									
Soil Container No.: 3	17.72	19.8	27	60	0.91	7	10	10:00	10.00	51.19	230.8	292.33	323.78	31.45	16.00	0.58	2.7E+07	1.63	15.13	2.28	q1	2.00		2.91E+07	q1	2.55E+07	
		23.1	26	58		8	20	20:00	10.00	53.58	274.9	248.29	280.24	31.95	20.14	0.59	2.7E+07	2.09	14.4426	2.27	Min	1.98		2.89E+07	Min	2.53E+07	
		25.9	25	56	0.90	9	30	30:00	10.00	53.18	300.6	275.04	309.52	34.48	22.60	0.63	2.9E+07	2.35		2.28	Med	2.15		2.90E+07	Med	2.75E+07	
		30.5	26	58		10	40	40:00	10.00	53.28	311.4	249.82	284.07	34.25	23.68	0.63	2.9E+07	2.47		2.04	Max	2.28		2.60E+07	Max	2.91E+07	
		30	25	56	0.89	11	50	50:00	10.00	53.6	309.1	286.73	321.13	34.4	23.41	0.63	2.9E+07	2.44		1.98	q3	2.27		2.53E+07	q3	2.90E+07	
		31.5	25	56		12	60	00:00	10.00	51.2	317	267.46	298.29	30.83	24.66	0.57	2.6E+07	2.59		1.98	Ave	2.14		2.53E+07	Ave	2.73E+07	
			25.67	57.04	0.90	7.1	70	10:00	10.00	51.19	317.3	303.96	333.9	29.94	24.74	0.55	2.5E+07	2.60									
						7.2	80	20:00	10.00	51.2	323.3	303.09	333.02	29.93	25.34	0.55	2.5E+07	2.67									
Soil Container No.: 4	18.43	20.8	28	62	0.92	13.0	40	40:10	10.00	53.37	252.4	189.38	223.7	34.32	17.77	0.63	2.7E+07	1.82	16.64	2.75	q1	2.46		3.22E+07	q1	2.88E+07	
		28.5	28	62		14.0	20	20:10	10.00	53.79	290.6	188.77	224.19	35.42	21.47	0.65	2.7E+07	2.22	15.965	2.83	Min	2.43		3.32E+07	Min	2.85E+07	
		26.7	27	60	0.90	15.0	30	30:10	10.00	53.74	335.1	187.46	228.95	41.49	25.56	0.76	3.2E+07	2.65		2.51	Med	2.51		2.95E+07	Med	2.94E+07	
		33.7	25	56		16.0	10	10:10	10.00	51.21	351.3	280.37	323.17	42.8	27.35	0.79	3.3E+07	2.84		2.50	Max	2.83		2.93E+07	Max	3.32E+07	
		28.6	26	58	0.89	17.0	50	50:10	10.00	53.33	338.9	253.43	291.42	37.99	26.19	0.70	2.9E+07	2.73		2.43	q3	2.69		2.85E+07	q3	3.15E+07	
		36.3	24	53		18.0	60	00:10	10.00	51.2	345.3	327.36	365.13	37.77	27.06	0.69	2.9E+07	2.83		2.45	Ave	2.58		2.87E+07	Ave	3.02E+07	
			26.33	59	0.91	13.1	70	10:10	10.00	51.2	342.2	199.5	236.28	36.78	26.81	0.68	2.9E+07	2.80									
						13.2	80	20:10	10.00	51.2	341.1	282.91	319.88	36.97	26.69	0.68	2.9E+07	2.79									

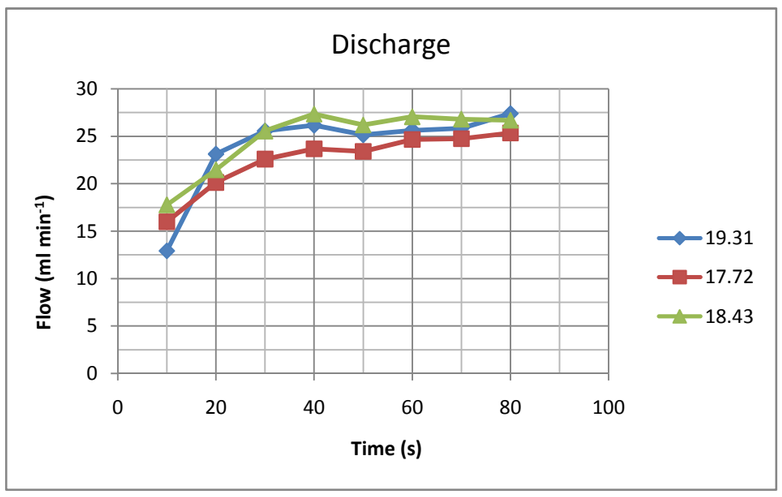

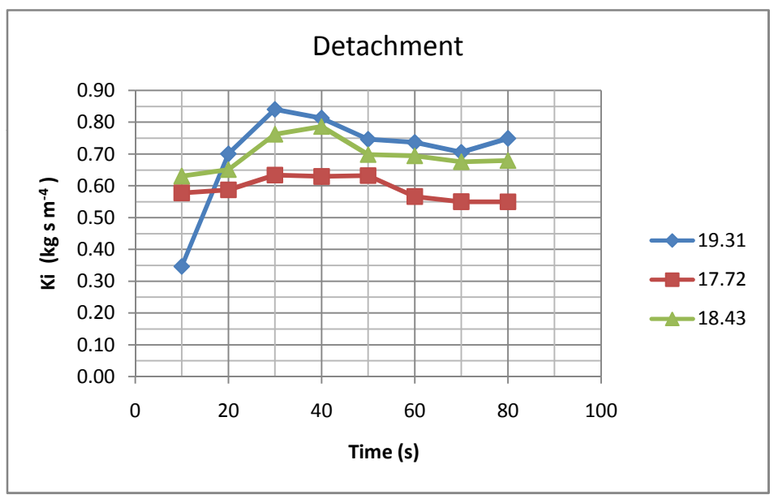

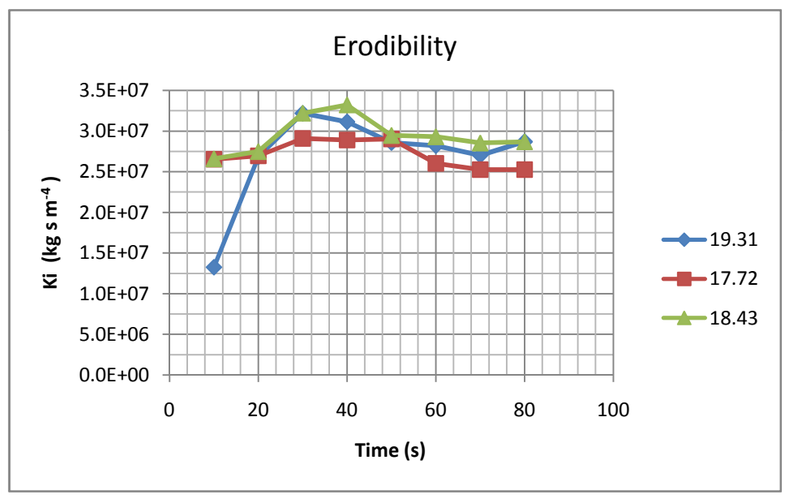

Appendix B. Rill Erosion

Simulation No.:												
			Soil	Caton						Date		2.8.13
Width (mm)		80										
Depth (Q) (mm)		0.97										
Depth (h) (mm)		2	2	2	1.5	3	2.5	1	2	2	2	2
Channel L (mm)		1410										
Inclination (°) start		5.2	4	6	6	5	5	5	6	5	5	5
Inclination (°) end		6	6	7	7	6	5	6	6	5	7	5
Gradient (-) start		0.091										
Gradient (-) end		0.105										
In-/Outflow (ml s^{-1})		39.94	40.72									
Hydr. R (Q) (mm)		0.947										
Hydr. R (h) (mm)		1.905										
Surface (mm^2)		1E+05										
Time	(sec)	2.74	3.4	2.69	2.59	2.54	2.62	2.6				
Velocity (mm s-1)		514.6										
Intensity (mm/h)		1300										
Hydr. Shear (Q) (Pa)		0.911										
Hydr. Shear (h) (Pa)		1.832	start	1.7005	end	1.9639						
Dr (kg s^{-1} m^2)		3E-04										

Container #	Inflow (ml s^{-1})	Time Change	Time Step (s)	emp plast (g)	full plast (g)	dried plastic (g)	Dr (kg s^{-1} m^{-2})	Water amount (ml)	Outflow (ml s^{-1})	Intensity (mm min^{-1})	Concentration (g/l)
1	40.2	60	60	167.12	2294.73	169.90	4.11E-04	2190	36.5	19.4	1.3
2	40.4	120	60	163.82	2451.37	165.37	2.29E-04	2570	42.8	22.8	0.6
3	40.1	180	60	166.70	2395.51	167.88	1.74E-04	2510	41.8	22.3	0.5
4	40.8	240	60	163.97	2515.24	165.52	2.29E-04	2365	39.4	21.0	0.7
5	40.7	300	62	167.78	2593.67	169.06	1.83E-04	2470	39.8	21.2	0.5
6	39.2	360	58	163.15	2453.23	164.49	2.05E-04	2470	42.6	22.7	0.5
7	39.6	420	60	167.85	2599.32	169.57	2.54E-04	2475	41.3	21.9	0.7
8	39.7	480	60	157.49	2373.24	159.09	2.36E-04	2400	40.0	21.3	0.7
9	39.3	540	60	163.89	2490.62	165.74	2.73E-04	2455	40.9	21.8	0.8
10	39.6	600	60	163.46	2488.06	165.69	3.29E-04	2465	41.1	21.9	0.9
11	39.7	660	60	167.58	2568.39	169.67	3.09E-04	2500	41.7	22.2	0.8

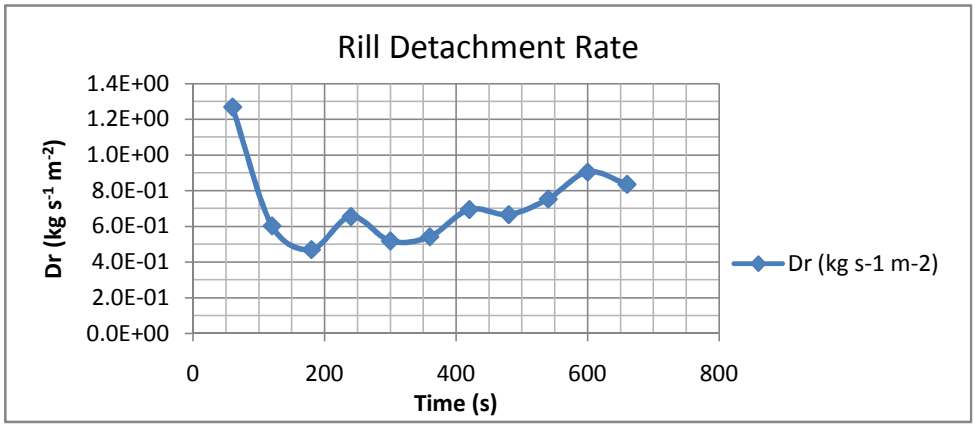

Simulation No.:		18										
		Soil	Caton							Date		14.8.13
Width (mm)	90											
Depth (Q) (mm)	0.8753											
Depth (h) (mm)	2.5833	1.5	2.5	3	2.5	3	1.5	3				
Channel L (mm)	1400											
Inclination (°) start	5.9	6	7	5	6	3	5	7	6	9	5	
Inclination (°) end	6.7	6	7	7	4	7	7	7	8	5	9	
Gradient (-) start	0.1033											
Gradient (-) end	0.1175											
In-/Outflow (ml s^{-1})	38.9	39.23										
Hydr. R (Q) (mm)	0.8586											
Hydr. R (h) (mm)	2.4431											
Surface (mm^2)	126000											
Time (sec)	3.15	3.15										
Velocity (mm s-1)	444.44											
Intensity (mm/h)	1121											
Hydr. Shear (Q) (Pa)	0.9299											
Hydr. Shear (h) (Pa)	2.6461	start	2.4767	end	2.8154							
Dr (kg s^{-1} m^2)	0.0007											

Container #	Inflow (ml s^{-1})	Time Change	Time Step (s)	emp plast (g)	full plast (g)	dried plastic (g)	Dr (kg s^{-1} m^{-2})	Water amount (ml)	Outflow (ml s^{-1})	Intensity (mm min^{-1})	Concentration (g/l)
1	39	60	60	163.33	2102.84	175.84	1.65E-03	2000	33.3	15.9	6.3
2	39.4	120	60	163.20	2529.18	173.26	1.33E-03	2470	41.2	19.6	4.1
3	38.9	180	60	163.46	2433.76	169.61	8.13E-04	2335	38.9	18.5	2.6
4	38.7	240	60	167.83	2464.48	173.15	7.04E-04	2395	39.9	19.0	2.2
5	39.4	300	62	167.29	2501.51	172.48	6.64E-04	2480	40.0	19.0	2.1
6	38.7	360	58	167.33	2471.58	172.52	7.10E-04	2390	41.2	19.6	2.2
7	38.4	420	60	167.52	2452.21	172.41	6.47E-04	2360	39.3	18.7	2.1
8	38.7	480	60	157.45	244.35	163.00	7.34E-04	2400	40.0	19.0	2.3

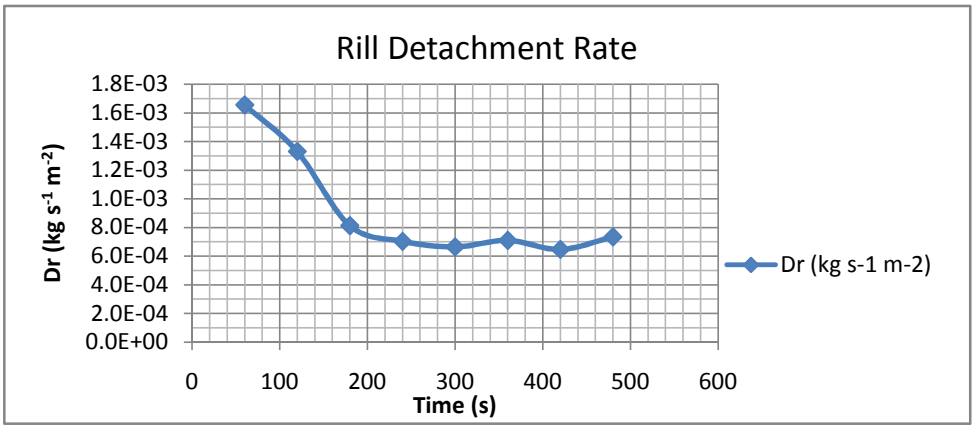

Simulation No.:		20									
		Soil	Caton						Date		14.8.13
Width (mm)	90										
Depth (Q) (mm)	0.744										
Depth (h) (mm)	1.85	2	1	1	3	1	1.5	1	3	2	2
Channel L (mm)	1405										
Inclination (°) start	5.2	4	6	6	5	5	5	6	5	5	5
Inclination (°) end	6	6	7	7	6	5	6	6	5	7	5
Gradient (-) start	0.091										
Gradient (-) end	0.105										
In-/Outflow (ml s^{-1})	38.16	37.4									
Hydr. R (Q) (mm)	0.732										
Hydr. R (h) (mm)	1.777										
Surface (mm^2)	1E+05										
Time (sec)	2.74	3.4	2.69	2.59	2.54	2.62	2.6				
Velocity (mm s-1)	512.8										
Intensity (mm/h)	354.6										
Hydr. Shear (Q) (Pa)	0.704										
Hydr. Shear (h) (Pa)	1.709	start	1.5864	end	1.8322						
Dr (kg s^{-1} m^2)	3E-04										

Container #	Inflow (ml s^{-1})	Time Change	Time Step (s)	emp plast (g)	full plast (g)	dried plastic (g)	Dr (kg s^{-1} m^{-2})	Water amount (ml)	Outflow (ml s^{-1})	Intensity (mm min^{-1})	Concentration (g/l)
1	38	20	20	267.39	804.54	268.64	4.94E-04	570	28.5	4.5	2.2
2	38.4	40	20	291.59	1032.06	292.47	3.48E-04	750	37.5	5.9	1.2
3	37.9	60	20	275.06	994.98	275.77	2.81E-04	730	36.5	5.8	1.0
4	38.2	80	20	279.29	1033.61	280.02	2.89E-04	780	39.0	6.2	0.9
5	38.3	100	20	282.93	1026.31	283.66	2.89E-04	780	39.0	6.2	0.9
6	38.2	120	20	249.84	999.87	250.53	2.73E-04	780	39.0	6.2	0.9
7	38.5	140	20	250.13	1002.56	250.86	2.89E-04	780	39.0	6.2	0.9
8	37.7	160	20	280.38	1020.18	281.09	2.81E-04	750	37.5	5.9	0.9
9	38.1	180	20	253.49	1001.56	254.29	3.16E-04	750	37.5	5.9	1.1
10	38.2	200	20	290.91	1036.64	291.66	2.97E-04	760	38.0	6.0	1.0
11	38.3	220	20	280.74	1053.05	281.56	3.24E-04	790	39.5	6.2	1.0

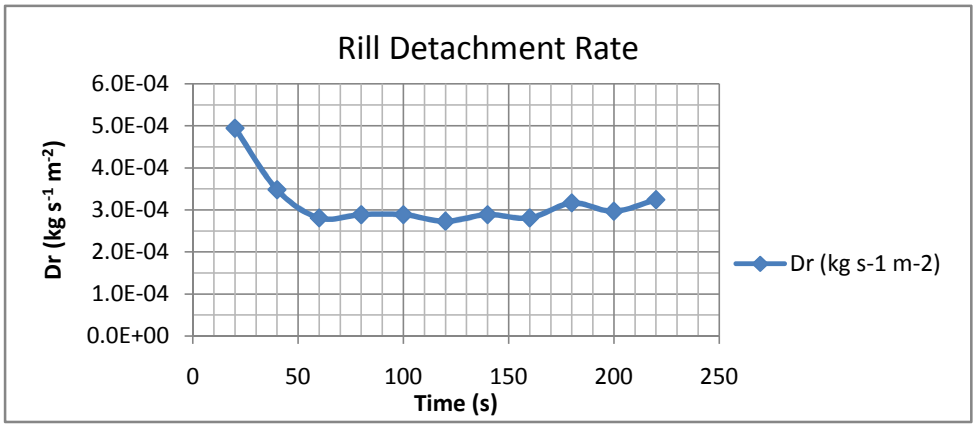

Simulation No.:												
			Soil	Caton							Date	20.8.13
Width (mm)		90										
Depth (Q) (mm)		0.691										
Depth (h) (mm)		1.857	1.5	3	3	2	2	1	1	1		
Channel L (mm)		1405										
Inclination (°) start		16.8	15	17	20	15	17	16	16	20	15	17
Inclination (°) end		17.5	16	18	20	16	18	16	16	19	18	18
Gradient (-) start		0.302										
Gradient (-) end		0.315										
In-/Outflow (ml s^{-1})		37.36	13.31									
Hydr. R (Q) (mm)		0.681										
Hydr. R (h) (mm)		1.784										
Surface (mm2)		1E+05										
Time	(sec)	2.598	2.5	2.4	2.44	2.9	2.85	2.5				
Velocity (mm s-1)		540.7										
Intensity (mm/h)		379										
Hydr. Shear (Q) (Pa)		2.06										
Hydr. Shear (h) (Pa)		5.4	start	5.2825	end	5.5166						
Dr (kg s^{-1} m^{2})		0.003										

Container #	Inflow (ml s^{-1})	Time Change	Time Step (s)	emp plast (g)	full plast (g)	dried plastic (g)	Dr (kg s^{-1} m^{-2})	Water amount (ml)	Outflow (ml s^{-1})	Intensity (mm min^{-1})	Concentration (g/l)
1	37.5	60	60	167.69	2236.55	225.35	7.60E-03	810	13.5	6.406	71.2
2	37	120	60	163.6	2413.84	207.92	5.84E-03	780	13	6.168	56.8
3	37.5	180	60	167.64	2385.26	203.82	4.77E-03	790	13.17	6.248	45.8
4	38.1	240	60	162.89	2444.78	195.71	4.33E-03	800	13.33	6.327	41
5	38	300	60	167.32	2459.69	197.58	3.99E-03	790	13.17	6.248	38.3
6	37.2	360	60	166.64	2324.95	191.86	3.32E-03	790	13.17	6.248	31.9
7	37.2	420	60	167.62	2415.44	192.5	3.28E-03	830	13.83	6.564	30
8	36.4	480	60	162.86	2314.07	185.66	3.01E-03	800	13.33	6.327	28.5

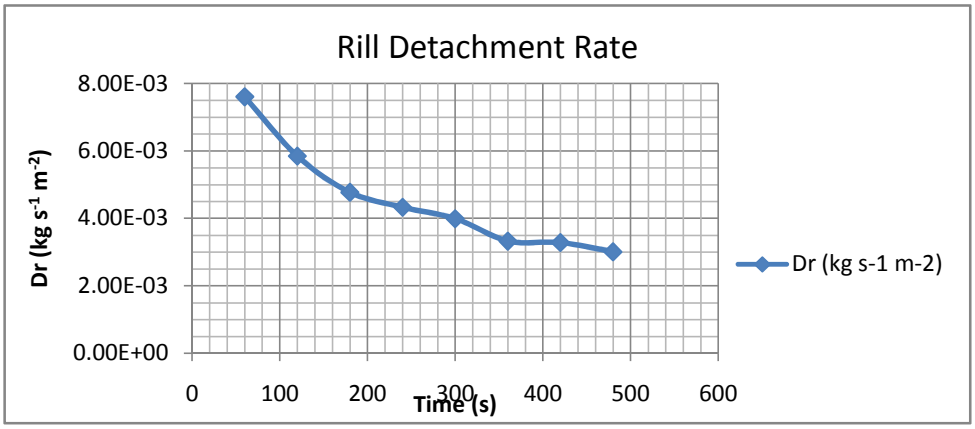

Simulation No.:		24										
		Soil	Caton								Date	20.8.13
Width (mm)	100											
Depth (Q) (mm)	0.522											
Depth (h) (mm)	1.667	1	2	2	2	1	2	1				
Channel L (mm)	1425											
Inclination (°) start	16.38	16	17	16	15	17	18	15	17			
Inclination (°) end	16.63	16	17	16	17	18	16	16	17			
Gradient (-) start	0.294											
Gradient (-) end	0.299											
In-/Outflow (ml s^{-1})	38.49	40.02										
Hydr. R (Q) (mm)	0.517											
Hydr. R (h) (mm)	1.613											
Surface (mm2)	1E+05											
Time (sec)	1.933	1.88	1.72	1.91	2.22							
Velocity (mm s-1)	737.4											
Intensity (mm/h)	1011											
Hydr. Shear (Q) (Pa)	1.501											
Hydr. Shear (h) (Pa)	4.687	start	4.6493	end	4.7244							
Dr (kg s^{-1} m^{2})	0.004											

Container #	Inflow (ml s^{-1})	Time Change	Time Step (s)	emp plast (g)	full plast (g)	dried plastic (g)	Dr (kg s^{-1} m^{-2})	Water amount (ml)	Outflow (ml s^{-1})	Intensity (mm min^{-1})	Concentration (g/l)
3	39.9	70	70	166.36	2939.43	177.40	1.11E-03	2770	39.6	16.7	4.0
10	40	130	60	167.63	1977.72	179.80	1.42E-03	1850	30.8	13.0	6.6
1	38.5	150	20	283.81	1036.16	290.26	2.26E-03	770	38.5	16.2	8.4
2	38.2	170	20	280.28	1067.48	287.59	2.56E-03	800	40.0	16.8	9.1
3	38.3	190	20	278.66	975.70	285.46	2.39E-03	720	36.0	15.2	9.4
4	39.9	220	30	281.61	820.36	292.25	2.49E-03	1100	36.7	15.4	9.7
5	39.7	240	20	290.64	1105.64	300.15	3.34E-03	840	42.0	17.7	11.3
6	39.8	260	20	250.08	1040.93	259.61	3.34E-03	800	40.0	16.8	11.9
7	39.9	280	20	314.14	1149.76	324.68	3.70E-03	900	45.0	18.9	11.7
8	29.8	300	20	303.90	1065.93	314.02	3.55E-03	800	40.0	16.8	12.7
9	39.8	320	20	253.38	1044.80	264.03	3.74E-03	790	39.5	16.6	13.5
10	39.7	340	20	261.33	1060.32	272.74	4.00E-03	820	41.0	17.3	13.9
11	39.8	360	20	317.50	1116.98	328.96	4.02E-03	830	41.5	17.5	13.8
12	39.5	380	20	282.88	1086.77	294.87	4.21E-03	830	41.5	17.5	14.4

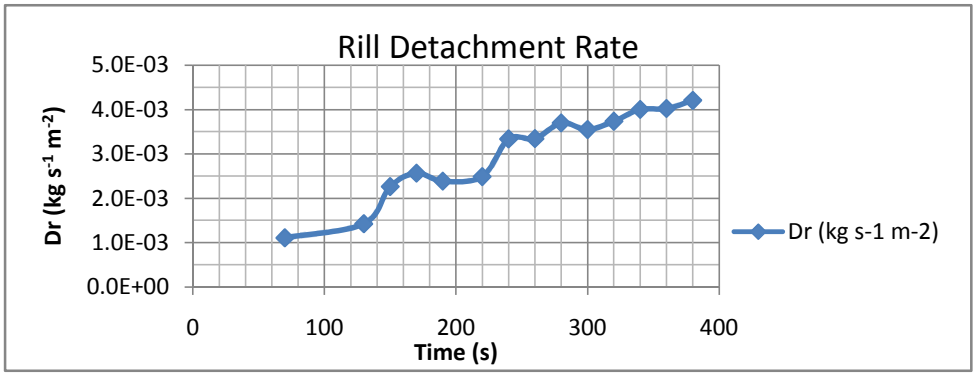

Simulation No.:												
			Soil	Caton							Date	22.8.13
Width (mm)		100										
Depth (Q) (mm)		0.651										
Depth (h) (mm)		1.875	1.5	1.5	2	2	2					
Channel L (mm)		1330										
Inclination (°) start		16.2	17	18	15	16	14	18	17	15	17	15
Inclination (°) end		16.55	18	17	15	16	16	14	17	18	16	18
Gradient (-) start		0.291										
Gradient (-) end		0.297										
In-/Outflow (ml s^{-1})		38.8	39									
Hydr. R (Q) (mm)		0.642										
Hydr. R (h) (mm)		1.807										
Surface (mm^2)		1E+05										
Time	(sec)	2.23	2.34	2.35	2							
Velocity (mm s-1)		596.4										
Intensity (mm/h)		3911										
Hydr. Shear (Q) (Pa)		1.851										
Hydr. Shear (h) (Pa)		5.209	start	5.1507	end	5.2668						
Dr (kg s^{-1} m^{-2})		0.004										

Container #	Inflow (ml s^{-1})	Time Change	Time Step (s)	emp plast (g)	full plast (g)	dried plastic (g)	Dr (kg s^{-1} m^{-2})	Water amount (ml)	Outflow (ml s^{-1})	Intensity (mm min^{-1})	Concentration (g/l)
9	39.4	60	60	163.54	2312.13	177.90	1.80E-03	2080	34.7	15.6	6.9
2	39.3	120	60	166.53	2464.01	192.45	3.25E-03	2290	38.2	17.2	11.3
1	39	140	20	307.07	1070.55	317.12	3.78E-03	800	40.0	18.0	12.6
2	38.9	160	20	250.99	998.74	260.82	3.70E-03	780	39.0	17.6	12.6
3	38.8	180	20	541.86	1315.16	552.22	3.89E-03	800	776.0	350.1	13.0
4	38.6	200	20	541.94	1290.68	551.87	3.73E-03	780	39.0	17.6	12.7
5	38.8	220	20	538.78	1287.64	548.52	3.66E-03	770	38.5	17.4	12.6
6	38.8	240	20	537.46	1299.32	547.15	3.64E-03	780	39.0	17.6	12.4
7	38.6	260	20	537.57	1313.02	547.24	3.64E-03	800	40.0	18.0	12.1

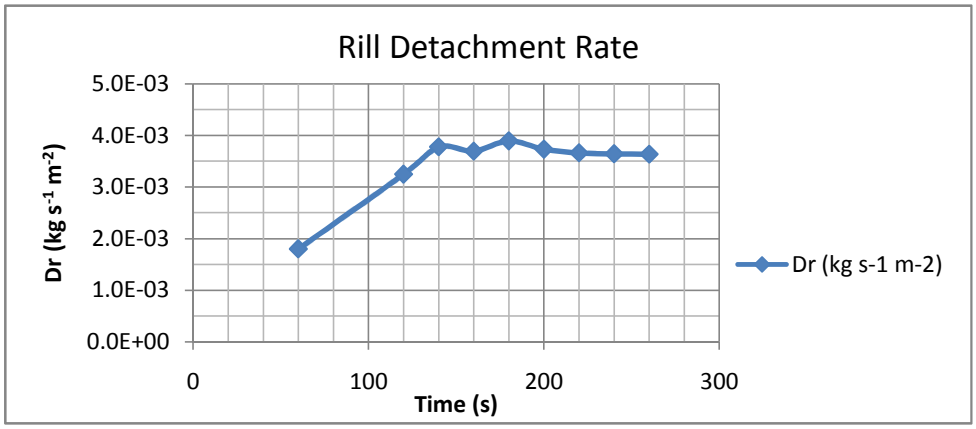

Simulation No.:												
			Soil	Caton							Date	22.8.13
Width (mm)		80										
Depth (Q) (mm)		0.949										
Depth (h) (mm)		1.625	1.5	1.5	2	1.5	1.5					
Channel L (mm)		1330										
Inclination (°) start		16.22	16	17	15	17	17	15	16	16	17	
Inclination (°) end		16.78	18	17	16	16	17	17	17	16	17	
Gradient (-) start		0.291										
Gradient (-) end		0.301										
In-/Outflow (ml s^{-1})		40.3	40									
Hydr. R (Q) (mm)		0.927										
Hydr. R (h) (mm)		1.562										
Surface (mm^2)		1E+05										
Time	(sec)	3.132	2.88	2.28	2.54	5.43	2.53					
Velocity (mm s-1)		424.6										
Intensity (mm/h)		1375										
Hydr. Shear (Q) (Pa)		2.694										
Hydr. Shear (h) (Pa)		4.538	start	4.457	end	4.6186						
Dr (kg s^{-1} m^2)		0.004										

Container #	Inflow (ml s^{-1})	Time Change	Time Step (s)	emp plast (g)	full plast (g)	dried plastic (g)	Dr (kg s^{-1} m^{-2})	Water amount (ml)	Outflow (ml s^{-1})	Intensity (mm min^{-1})	Concentration (g/l)
8	38.8	60	60	167.33	2368.36	190.88	3.69E-03	2230	37.2	21.0	10.6
6	40	120	60	157.17	2467.17	180.13	3.60E-03	2310	38.5	21.7	9.9
3.1	40.2	140	20	538.97	1359.31	546.48	3.53E-03	850	42.5	24.0	8.8
3.2	40.5	160	20	547.74	1290.93	555.30	3.55E-03	790	39.5	22.3	9.6
3.3	40.2	180	20	541.45	1293.17	549.36	3.72E-03	860	43.0	24.2	9.2
3.4	40.3	200	20	538.44	1314.63	546.49	3.78E-03	800	40.0	22.6	10.1
3.5	40.3	220	20	541.42	1305.79	549.15	3.63E-03	780	39.0	22.0	9.9
3.6	40.5	240	20	550.03	1329.37	557.90	3.70E-03	800	40.0	22.6	9.8
3.7	40.3	260	20	544.06	1319.38	551.84	3.66E-03	810	40.5	22.8	9.6

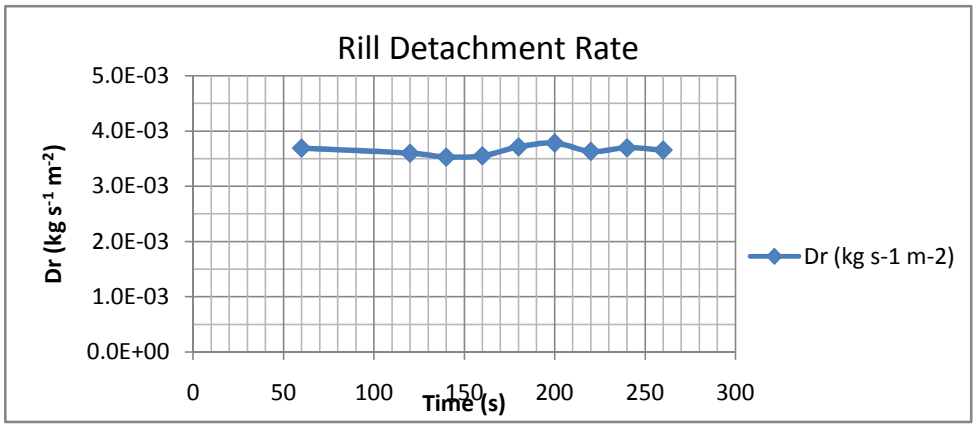

Simulation No.:		13									
		Soil	Okana						Date	2.8.13	
Width (mm)	100										
Depth (Q) (mm)	0.705										
Depth (h) (mm)	2.278	3	2	2	2	2.5	2.5	2	3	2	2.5
Channel L (mm)	1410										
Inclination (°) start	5.7	6	5	6	6	7	6	5	6	5	5
Inclination (°) end	6.2	7	7	6	6	7	6	6	6	6	5
Gradient (-) start	0.1										
Gradient (-) end	0.109										
In-/Outflow (ml s^{-1})	40.66										
Hydr. R (Q) (mm)	0.696										
Hydr. R (h) (mm)	2.179										
Surface (mm^2)	1E+05										
Time (sec)	2.446	3.37	3.46	3.4	1	1					
Velocity (mm s-1)	576.5										
Intensity (mm/h)	1039										
Hydr. Shear (Q) (Pa)	0.711										
Hydr. Shear (h) (Pa)	2.227	start	2.133	end	2.3217						
Dr (kg s^{-1} m^2)	4E-04										

Container #	Inflow (ml s^{-1})	Time Change	Time Step (s)	emp plast (g)	full plast (g)	dried plastic (g)	Dr (kg s^{-1} m^{-2})	Water amount (ml)	Outflow (ml s^{-1})	Intensity (mm min^{-1})	Concentration (g/l)
1	40	60	60	163.27	2249.24	170.89	9.01E-04	2190	36.5	15.5	3.5
2	40.4	120	60	166.61	2459.54	171.77	6.10E-04	2570	42.8	18.2	2.0
3	41.2	180	60	167.74	2503.63	173.07	6.30E-04	2510	41.8	17.8	2.1
4	41.1	240	60	163.31	2468.55	166.73	4.04E-04	2365	39.4	16.8	1.4
5	40.2	300	62	166.56	2564.14	170.51	4.52E-04	2470	39.8	17.5	1.6
6	40.9	360	58	157.30	2486.61	160.40	3.79E-04	2470	42.6	17.5	1.3
7	40.9	420	60	167.62	2538.28	171.00	4.00E-04	2475	41.3	17.6	1.4
8	40.9	480	60	163.07	2659.23	166.05	3.52E-04	2400	40.0	17.0	1.2
9	40.4	540	60	167.41	2453.14	171.12	4.39E-04	2455	40.9	17.4	1.5
10	40.7	600	60	167.48	2525.11	171.90	5.22E-04	2465	41.1	17.5	1.8
11	40.6	660	60	163.09	2544.09	166.73	4.30E-04	2500	41.7	17.7	1.5

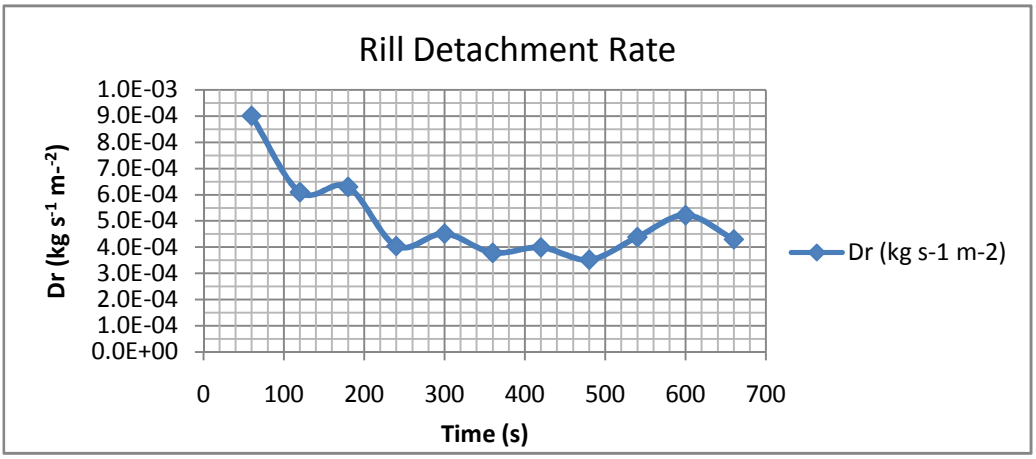

Simulation No.:		17										
		Soil	Okana							Date		9.8.13
Width (mm)	100											
Depth (Q) (mm)	0.87178											
Depth (h) (mm)	2.125	2	2	1.5	2.5	2.5						
Channel L (mm)	1400											
Inclination (°) start	6.8	7	8	6	7	6	6	7	7	7	7	
Inclination (°) end	7.5	7	8	8	9	6	8	9	7	6	7	
Gradient (-) start	0.11924											
Gradient (-) end	0.13165											
In-/Outflow (ml s^{-1})	39.7125	40.14										
Hydr. R (Q) (mm)	0.85684											
Hydr. R (h) (mm)	2.03837											
Surface (mm^2)	1.E+05											
Time (sec)	3.07333	3.19	2.94	3.09								
Velocity (mm s-1)	455.531											
Intensity (mm/h)	1032.04											
Hydr. Shear (Q) (Pa)	1.05447											
Hydr. Shear (h) (Pa)	2.5085	start	2.3844	end	2.633							
Dr (kg s^{-1} m^2)	0.00099											

Container #	Inflow (ml s^{-1})	Time Change	Time Step (s)	emp plast (g)	full plast (g)	dried plastic (g)	Dr (kg s^{-1} m^{-2})	Water amount (ml)	Outflow (ml s^{-1})	Intensity (mm min^{-1})	Concentration (g/l)
1	39.3	60	60	167.76	2143.99	190.57	2.72E-03	2190	36.5	15.6	10.4
2	39.3	120	60	163.59	2476.10	176.34	1.52E-03	2570	42.8	18.4	5.0
3	39.9	180	60	167.62	2514.33	178.57	1.30E-03	2310	38.5	16.5	4.7
4	39.4	240	60	162.97	2474.84	172.15	1.09E-03	2395	39.9	17.1	3.8
5	39.8	300	62	167.38	2537.48	175.73	9.62E-04	2470	39.8	17.1	3.4
6	39.7	360	58	166.68	2612.52	175.73	1.11E-03	2450	42.2	18.1	3.7
7	40.3	420	60	167.47	2620.69	175.94	1.01E-03	2475	41.3	17.7	3.4
8	40.0	480	60	162.83	2401.84	170.06	8.61E-04	2400	40.0	17.1	3.0

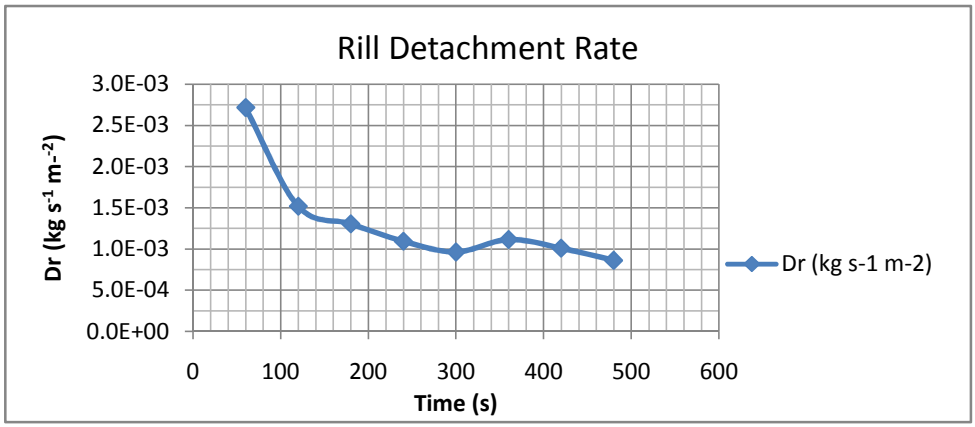

Simulation No.:		19									
		Soil	Okana						Date		9.8.13
Width (mm)	100										
Depth (Q) (mm)	1.081										
Depth (h) (mm)	2.6	4	2	4	2	2	3	3	3	2	2
Channel L (mm)	1405										
Inclination (°) start	5.6	6	6	5	6	5	6	5	5	7	5
Inclination (°) end	5.75	5	6	5	6	5	6	6	6	7.5	5
Gradient (-) start	0.098										
Gradient (-) end	0.101										
In-/Outflow (ml s^{-1})	38.81	37.4									
Hydr. R (Q) (mm)	1.058										
Hydr. R (h) (mm)	2.471										
Surface (mm^2)	1E+05										
Time (sec)	3.913	3.87	3.87	4							
Velocity (mm s-1)	359										
Intensity (mm/h)	957.4										
Hydr. Shear (Q) (Pa)	1.031										
Hydr. Shear (h) (Pa)	2.409	start	2.3773	end	2.4414						
Dr (kg s^{-1} m^2)	6E-04										

Container #	Inflow (ml s^{-1})	Time Change	Time Step (s)	emp plast (g)	full plast (g)	dried plastic (g)	Dr (kg s^{-1} m^{-2})	Water amount (ml)	Outflow (ml s^{-1})	Intensity (mm min^{-1})	Concentration (g/l)
1	38.9	20	20	253.43	769.9	254.9	5.23E-04	490	24.5	10.5	3.0
2	39	40	20	248.29	985.16	249.64	4.80E-04	700	35.0	14.9	1.9
3	38.4	60	20	283.87	1031.99	285.26	4.95E-04	770	38.5	16.4	1.8
4	39	80	20	261.35	1012.69	262.58	4.38E-04	760	38.0	16.2	1.6
5	38.4	100	20	278.73	1041.09	279.96	4.38E-04	760	38.0	16.2	1.6
6	38.9	120	20	317.55	1094.27	318.83	4.56E-04	770	38.5	16.4	1.7
7	38.7	140	20	281.68	1039.51	282.78	3.91E-04	790	39.5	16.9	1.4
8	38.8	160	20	303.76	1057.26	305.07	4.66E-04	780	39.0	16.7	1.7
9	39.1	180	20	314.24	1090.02	315.88	5.84E-04	790	39.5	16.9	2.1
10	38.7	200	20	279.73	1057.02	281.2	5.23E-04	810	40.5	17.3	1.8
11	39	220	20	303.97	1069.64	305.53	5.55E-04	800	40.0	17.1	1.9

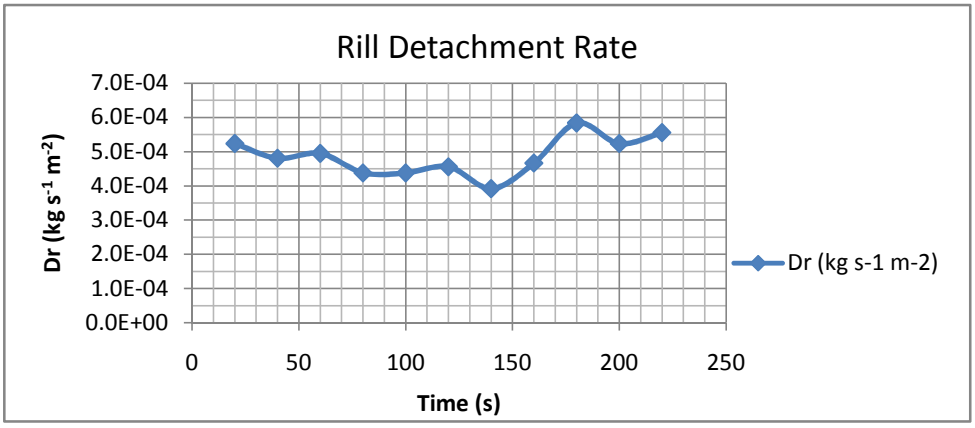

Simulation No.:											
		Soil	Okana						Date		14.8.13
Width (mm)	100										
Depth (Q) (mm)	0.841										
Depth (h) (mm)	1.667	1	2	1	2	1	2	2			
Channel L (mm)	1350										
Inclination (°) start	15.44	14	15	14	16	16	16	16	16	16	
Inclination (°) end	15.69	14	17	16.5	16	18	15	14	15		
Gradient (-) start	0.276										
Gradient (-) end	0.281										
In-/Outflow (ml s^{-1})	39.73	40.09									
Hydr. R (Q) (mm)	0.827										
Hydr. R (h) (mm)	1.613										
Surface (mm^2)	1E+05										
Time (sec)	2.858	3.22	3.06	3.15	2						
Velocity (mm s-1)	472.4										
Intensity (mm/h)	1069										
Hydr. Shear (Q) (Pa)	2.26										
Hydr. Shear (h) (Pa)	4.408	start	4.3715	end	4.444						
Dr (kg s^{-1} m^2)	0.009										

Container #	Inflow (ml s^{-1})	Time Change	Time Step (s)	emp plast (g)	full plast (g)	dried plastic (g)	Dr (kg s^{-1} m^{-2})	Water amount (ml)	Outflow (ml s^{-1})	Intensity (mm min^{-1})	Concentration (g/l)
1	39.6	20	20	252.02	1040.08	259.81	2.89E-03	810	40.5	18.0	9.6
2	39.6	40	20	280.74	1049.66	291.05	3.82E-03	780	39.0	17.3	13.2
3	39.6	60	20	249.84	1012.30	262.57	4.71E-03	790	39.5	17.6	16.1
4	39.9	80	20	291.59	1082.78	306.21	5.41E-03	800	40.0	17.8	18.3
5	39.9	100	20	253.49	1054.91	271.40	6.63E-03	790	39.5	17.6	22.7
6	40	120	20	252.65	1028.54	271.45	6.96E-03	790	39.5	17.6	23.8
7	39.7	140	20	303.68	1094.51	324.73	7.80E-03	830	41.5	18.4	25.4
8	39.4	160	20	279.24	1089.14	301.88	8.39E-03	800	40.0	17.8	28.3
9	39.8	180	20	274.98	1079.57	299.28	9.00E-03	800	40.0	17.8	30.4
10	39.9	200	20	248.24	1050.64	273.79	9.46E-03	810	40.5	18.0	31.5
11	39.6	220	20	279.67	1092.12	306.67	1.00E-02	820	41.0	18.2	32.9

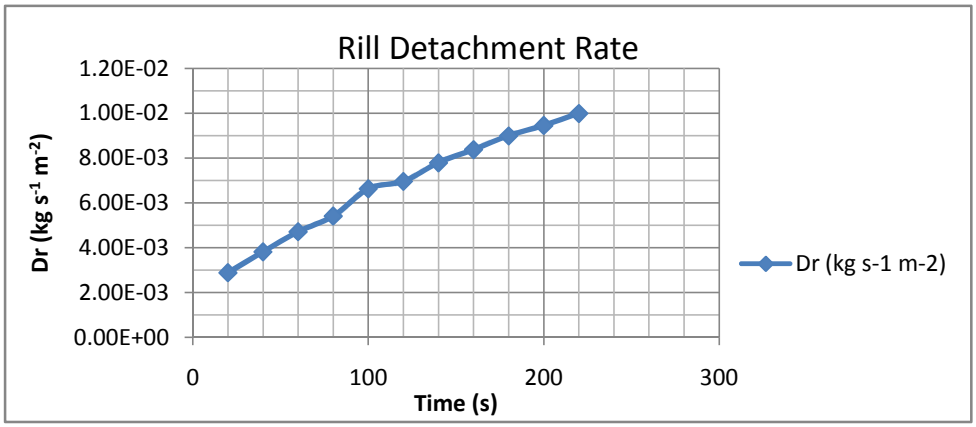

Simulation No.:												
			Soil	Okana							Date	22.8.13
Width (mm)		100										
Depth (Q) (mm)		0.591										
Depth (h) (mm)		1.6	1.5	1.5	2	2	1	1.5				
Channel L (mm)		1340										
Inclination (°) start		15.44	14	15	15	16	17	18	15	15	14	
Inclination (°) end		15.33	15	13	14	17	14	20	15	16	14	
Gradient (-) start		0.276										
Gradient (-) end		0.274										
In-/Outflow (ml s^{-1})		41.87	42.91									
Hydr. R (Q) (mm)		0.584										
Hydr. R (h) (mm)		1.55										
Surface (mm^2)		1E+05										
Time	(sec)	1.893	1.94	1.87	2.04	1.72						
Velocity (mm s-1)		708.1										
Intensity (mm/h)		1153										
Hydr. Shear (Q) (Pa)		1.578										
Hydr. Shear (h) (Pa)		4.186	start	4.202	end	4.17						
Dr (kg s^{-1} m^2)		5E-04										

Container #	Inflow (ml s^{-1})	Time Change	Time Step (s)	emp plast (g)	full plast (g)	dried plastic (g)	Dr (kg s^{-1} m^{-2})	Water amount (ml)	Outflow (ml s^{-1})	Intensity (mm min^{-1})	Concentration (g/l)
5	42	60	60	163.13	2913.60	166.70	4.44E-04	2820	47.0	21.0	1.3
7	42	120	60	167.58	3003.73	170.30	3.38E-04	2560	42.7	19.1	1.1
3	42.1	140	20	542.51	1344.95	543.24	2.72E-04	840	42.0	18.8	0.9
4	41.8	160	20	547.41	1336.32	548.23	3.06E-04	850	42.5	19.0	1.0
5	41.9	180	20	540.23	1341.66	541.58	5.04E-04	830	41.5	18.6	1.6
6	42	200	20	538.55	1329.18	539.93	5.15E-04	820	41.0	18.4	1.7
7	41.8	220	20	550.76	1360.13	552.02	4.70E-04	860	43.0	19.3	1.5
8	41.6	240	20	538.75	1636.46	540.15	5.22E-04	840	42.0	18.8	1.7
9	41.6	260	20	550.39	1385.81	551.80	5.26E-04	890	44.5	19.9	1.6

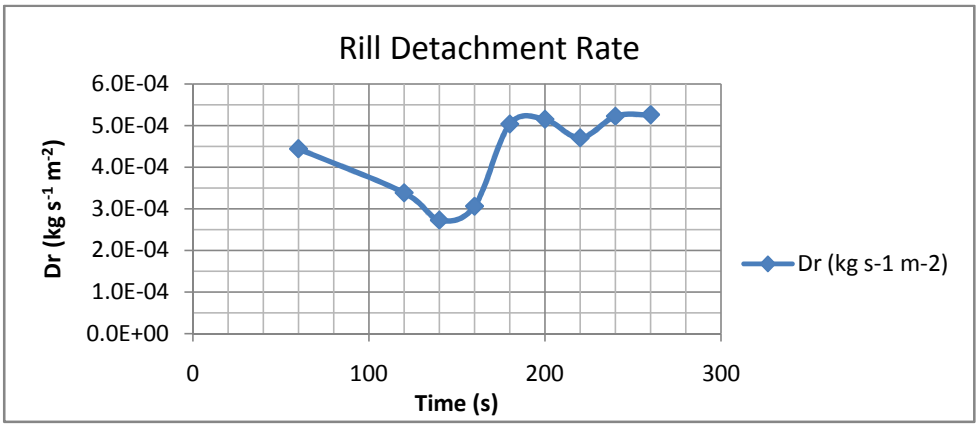

Simulation No.:												29
			Soil	Okana							Date	22.8.13
Width (mm)		100										
Depth (Q) (mm)		0.597	0.599									
Depth (h) (mm)		1.3	1	1.5	1.5	1	1	1.5				
Channel L (mm)		1325										
Inclination (°) start		15	14	13	14	17	15	15	15	17	15	
Inclination (°) end		15.56	13	14	15	16	18	18	15	16	15	
Gradient (-) start		0.268										
Gradient (-) end		0.278										
In-/Outflow (ml s^{-1})		42.14	42.28									
Hydr. R (Q) (mm)		0.59	0.592									
Hydr. R (h) (mm)		1.267										
Surface (mm^2)		1E+05										
Time	(sec)	1.876	1.75	1.75	2	1.88	2					
Velocity (mm s-1)		706.3										
Intensity (mm/h)		1149										
Hydr. Shear (Q) (Pa)		1.58	1.555									
Hydr. Shear (h) (Pa)		3.395	start	3.3306	end	3.4601						
Dr (kg s^{-1} m^2)		4E-04										

Container #	Inflow (ml s^{-1})	Time Change	Time Step (s)	emp plast (g)	full plast (g)	dried plastic (g)	Dr (kg s^{-1} m^{-2})	Water amount (ml)	Outflow (ml s^{-1})	Intensity (mm min^{-1})	Concentration (g/l)
4	43	60	60	163.60	2525.61	174.25	1.3E-03	2450	40.8	18.5	4.3
6	42.1	120	60	162.81	2665.53	166.00	4.0E-04	2470	41.2	18.6	1.3
A	42.2	140	20	327.29	1167.43	328.44	4.3E-04	870	43.5	19.7	1.3
B	42.4	160	20	268.91	1104.22	270.10	4.5E-04	870	43.5	19.7	1.4
1.1	41.9	180	20	540.56	1353.52	541.71	4.3E-04	850	42.5	19.2	1.4
1.2	42.2	200	20	540.93	1353.79	541.96	3.9E-04	840	42.0	19.0	1.2
1.3	42.1	220	20	540.25	1367.45	541.11	3.2E-04	860	43.0	19.5	1.0
1.4	42	240	20	539.96	1365.69	541.32	5.1E-04	840	42.0	19.0	1.6
1.5	41.4	260	20	541.62	1376.00	542.96	5.1E-04	840	42.0	19.0	1.6

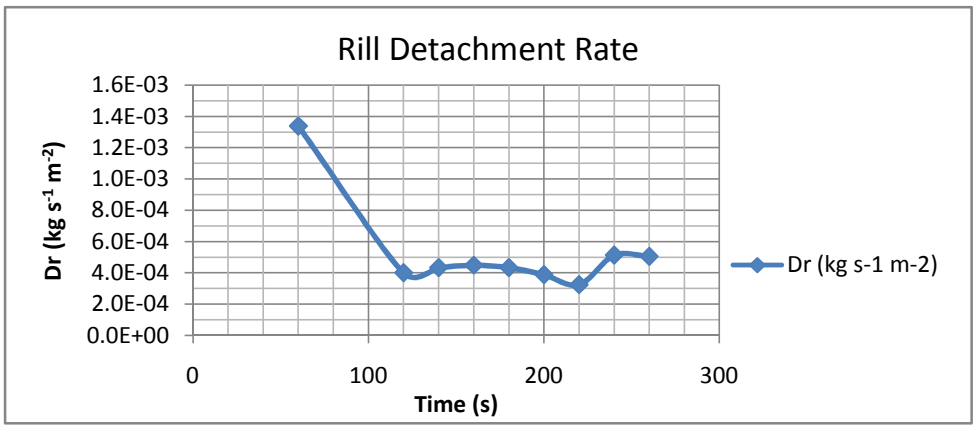

Simulation No.:	21										
	Soil	Okana						Date	14.8.13		

Width (mm)	100											
Depth (Q) (mm)	1.206											
Depth (h) (mm)	1.75	2	2	1.5								
Channel L (mm)	1325											
Inclination (°) start	29.3	29	31	29	28	29	29	30	28	32	28	
Inclination (°) end	31.7	35	32	30	32	33	30	31	32	32	30	
Gradient (-) start	0.5612											
Gradient (-) end	0.6176											
In-/Outflow (ml s^{-1})	37.075	35.71										
Hydr. R (Q) (mm)	1.1776											
Hydr. R (h) (mm)	1.6908											
Surface (mm^2)	132500											
Time (sec)	4.31	4.31										
Velocity (mm s-1)	307.42											
Intensity (mm/h)	970.19											
Hydr. Shear (Q) (Pa)	6.8087											
Hydr. Shear (h) (Pa)	9.7762	start	9.3082	end	10.244							
Dr (kg s^{-1} m^2)	0.0243											

Container #	Inflow (ml s^{-1})	Time Change	Time Step (s)	emp plast (g)	full plast (g)	dried plastic (g)	Dr (kg s^{-1} m^{-2})	Water amount (ml)	Outflow (ml s^{-1})	Intensity (mm min^{-1})	Concentration (g/l)
1	37.2	60	60	163.25	2292.28	455.87	3.68E-02	1850	30.8	14.0	158.2
2	37.7	120	60	162.89	2529.49	361.01	2.49E-02	2300	38.3	17.4	86.1
3	37	180	60	163.05	2688.67	363.29	2.52E-02	2370	39.5	17.9	84.5
4	36.4	240	60	167.63	2385.32	349.13	2.28E-02	2050	34.2	15.5	88.5

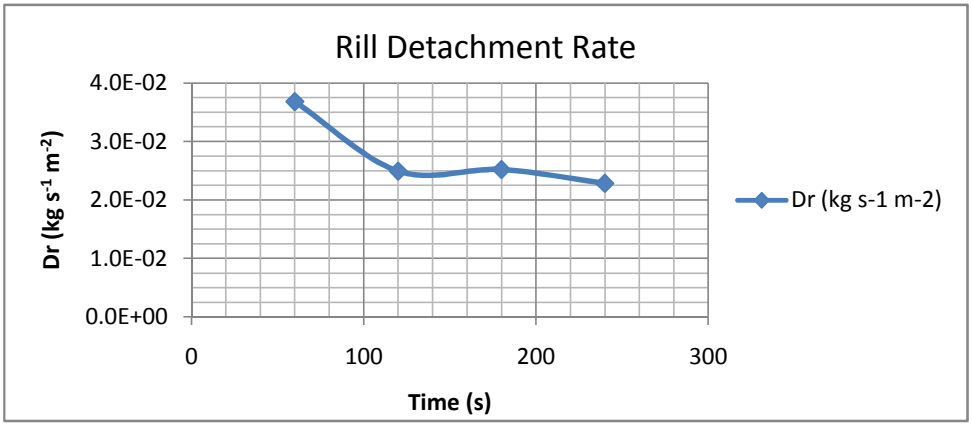

Simulation No.:											
		Soil	Okana						Date	30.8.13	
Width (mm)	80										
Depth (Q) (mm)	1.3909										
Depth (h) (mm)	2.3333	1	2	3	2						
Channel L (mm)	1330										
Inclination (°) start	28.2	29	28	28	30	30	27	28	27	28	27
Inclination (°) end	28.7	30	31	29	29	30	29	25	28	29	27
Gradient (-) start	0.5362										
Gradient (-) end	0.5475										
In-/Outflow (ml s^{-1})	42.922	28.89									
Hydr. R (Q) (mm)	1.3442										
Hydr. R (h) (mm)	2.2047										
Surface (mm^2)	106400										
Time (sec)	4.31	4.31									
Velocity (mm s-1)	308.58										
Intensity (mm/h)	977.44										
Hydr. Shear (Q) (Pa)	7.145										
Hydr. Shear (h) (Pa)	11.719	start	11.597	end	11.841						
Dr (kg s^{-1} m^2)	0.0114										

Container #	Inflow (ml s^{-1})	Time Change	Time Step (s)	emp plast (g)	full plast (g)	dried plastic (g)	Dr (kg s^{-1} m^{-2})	Water amount (ml)	Outflow (ml s^{-1})	Intensity (mm min^{-1})	Concentration (g/l)
1	43.6	60	60	167.72	2590.50	207.18	6.18E-03	0	0	0	0
2	43.2	120	60	163.62	260.53	201.68	5.96E-03	0	0	0	0
3	42.8	180	60	163.17	2712.16	216.60	8.37E-03	0	0	0	0
1	43.2	200	20	250.11	1107.45	275.69	1.20E-02	870	43.5	24.5	29.4
2	42.9	220	20	283.87	1133.18	308.65	1.16E-02	880	44.0	24.8	28.2
3	42.3	240	20	251.00	1058.44	273.21	1.04E-02	810	40.5	22.8	27.4
4	42.8	260	20	291.58	1192.04	310.68	8.98E-03	900	45.0	25.4	21.2
5	42.9	280	20	317.51	1164.01	334.02	7.76E-03	860	43.0	24.2	19.2
6	42.6	300	20	253.41	1111.44	271.57	8.53E-03	880	44.0	24.8	20.6

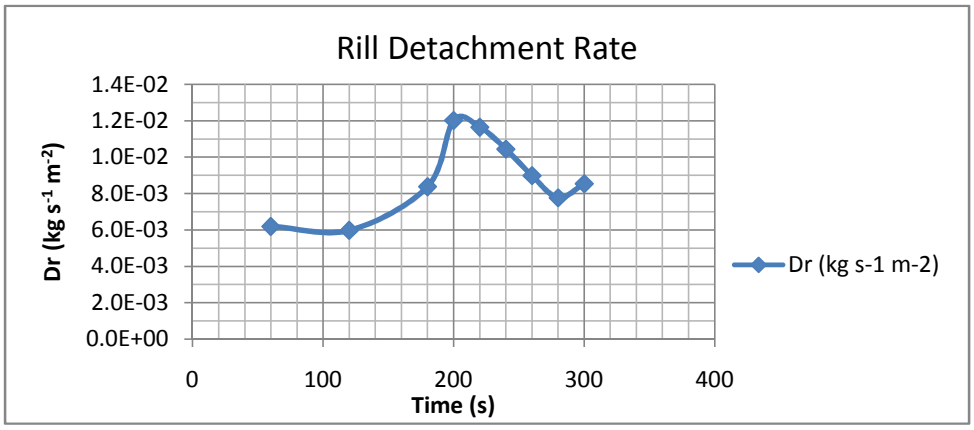

Simulation No.:											
		Soil	Okana						Date		14.8.13
Width (mm)	60										
Depth (Q) (mm)	1.3812										
Depth (h) (mm)	2.25	1	2	3	2	2					
Channel L (mm)	1325										
Inclination (°) start	30.222	31	28	29	30	31	31	32	29	31	
Inclination (°) end	28.444	29	28	31	29	30	25	25	30	29	
Gradient (-) start	0.5825										
Gradient (-) end	0.5417										
In-/Outflow (ml s^{-1})	42.463	72.54									
Hydr. R (Q) (mm)	1.3204										
Hydr. R (h) (mm)	2.093										
Surface (mm^2)	79500										
Time (sec)	4.31	4.31									
Velocity (mm s-1)	307.42										
Intensity (mm/h)	3284.9										
Hydr. Shear (Q) (Pa)	7.2814										
Hydr. Shear (h) (Pa)	11.542	start	11.961	end	11.123						
Dr (kg s^{-1} m^2)	0.0211										

Container #	Inflow (ml s^{-1})	Time Change	Time Step (s)	emp plast (g)	full plast (g)	dried plastic (g)	Dr (kg s^{-1} m^{-2})	Water amount (ml)	Outflow (ml s^{-1})	Intensity (mm min^{-1})	Concentration (g/l)
4	42.1	60	60	167.79	2644.53	321.79	3.23E-02	1850	30.8	23.3	83.2
5	42.4	120	60	163.29	2774.90	321.81	3.32E-02	2300	38.3	28.9	68.9
1.1	42.5	140	20	290.89	1171.44	324.88	2.14E-02	2370	118.5	89.4	14.3
1.2	42.5	160	20	261.34	1095.17	293.62	2.03E-02	2050	102.5	77.4	15.7
1.3	42.5	180	20	314.22	1171.61	340.45	1.65E-02				
1.4	42.6	200	20	303.96	1190.40	335.25	1.97E-02				
1.5	42.7	220	20	327.34	1199.27	361.45	2.15E-02				
1.6	42.4	240	20	280.34	1127.69	315.64	2.22E-02				

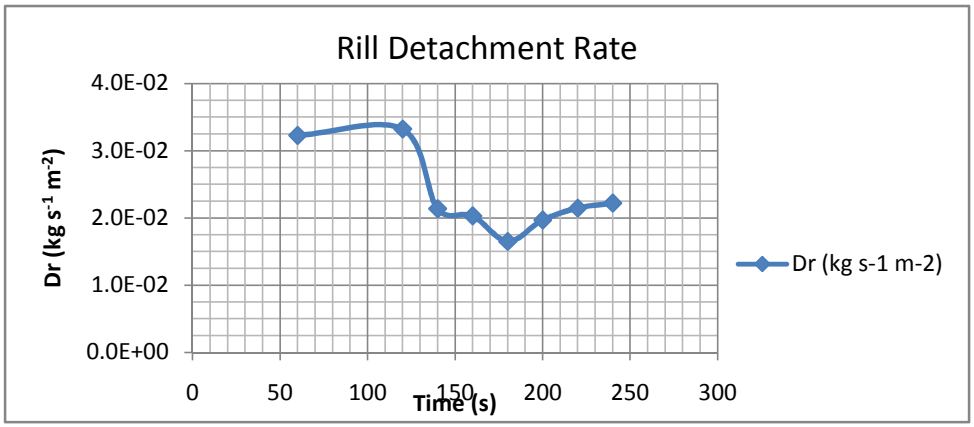

Appendix C. Particle Size Analysis

Caton1		
Clay	**10.62**	%
Silt	**83.90**	%
Sand	**5.48**	%

CatonBay1.1			CatonBay1.2			CatonBay1.3		
Clay	10.37	%	Clay	10.75	%	Clay	10.75	%
Silt	83.86	%	Silt	83.77	%	Silt	84.07	%
Sand	5.77	%	Sand	5.48	%	Sand	5.19	%

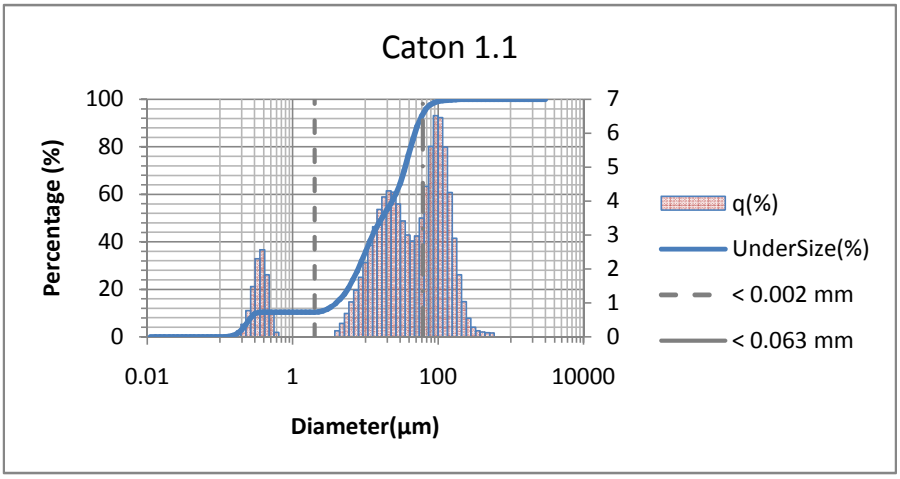

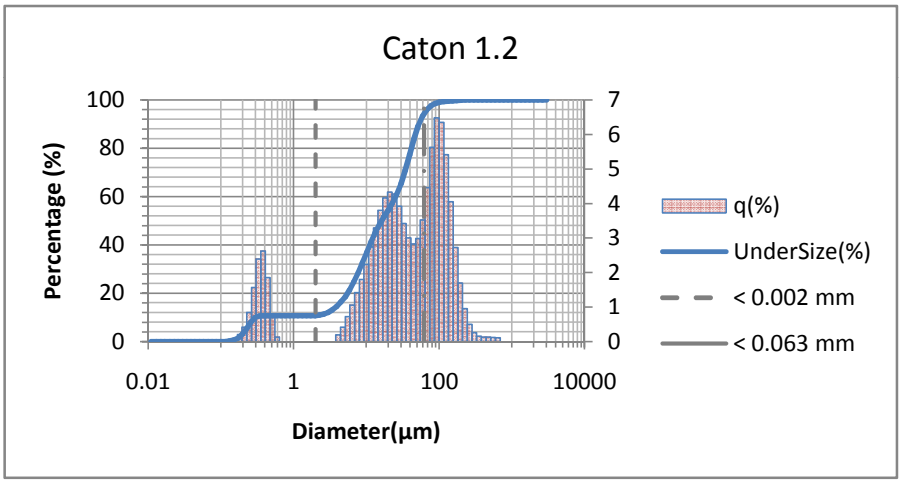

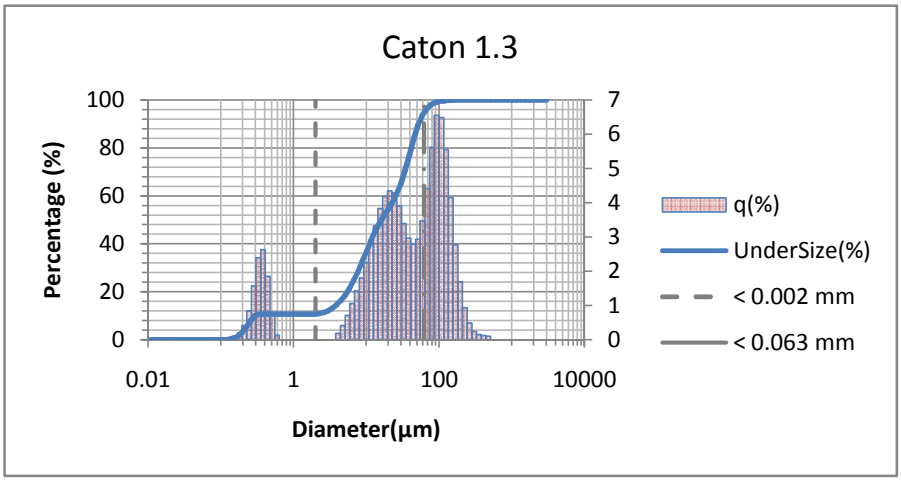

Caton3		
Clay	**9.44**	%
Silt	**79.69**	%
Sand	**10.87**	%

CatonBay3.1			CatonBay3.2			CatonBay3.3			CatonBay3.4		
Clay	9.14	%	Clay	9.32	%	Clay	9.51	%	Clay	9.78	%
Silt	79.33	%	Silt	79.56	%	Silt	79.58	%	Silt	80.29	%
Sand	11.53	%	Sand	11.12	%	Sand	10.91	%	Sand	9.93	%

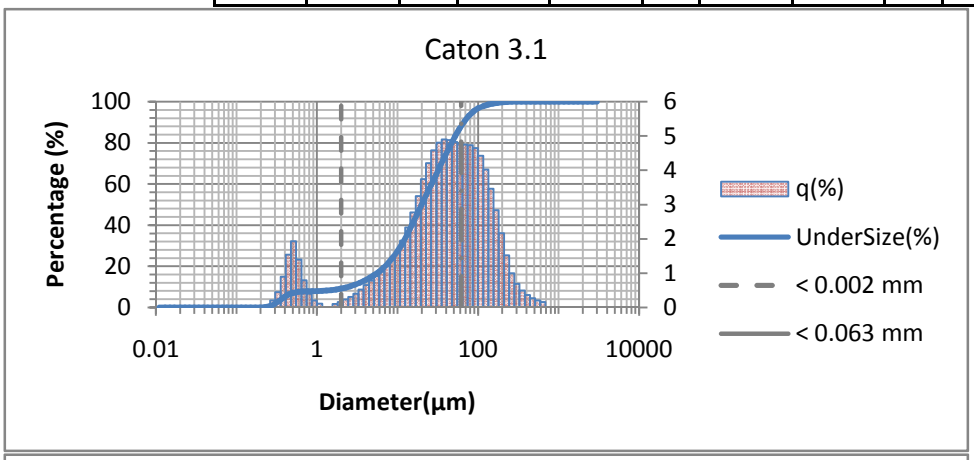

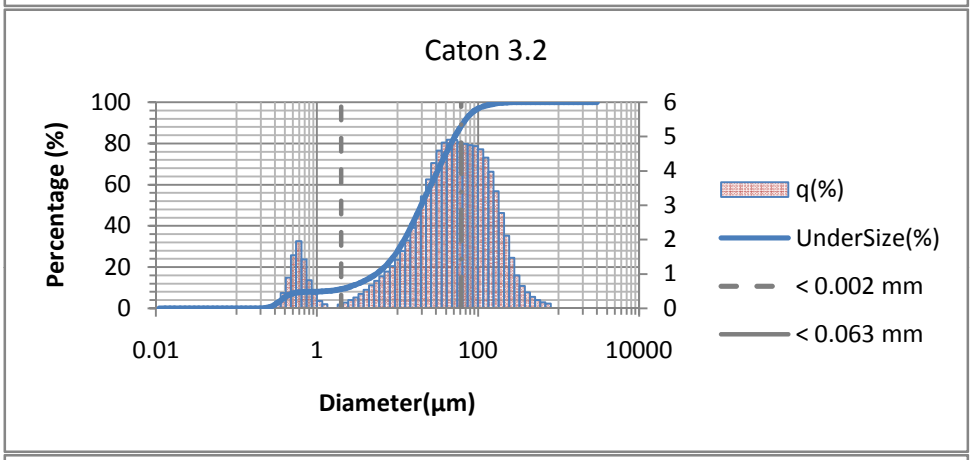

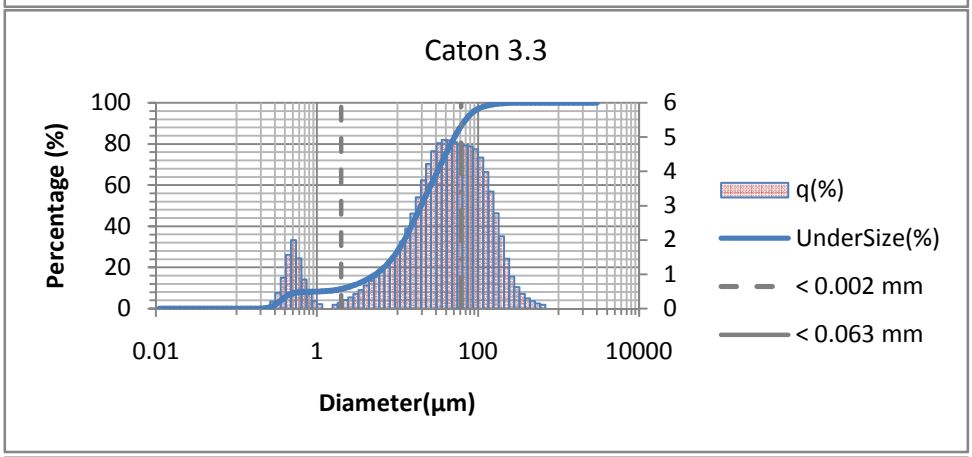

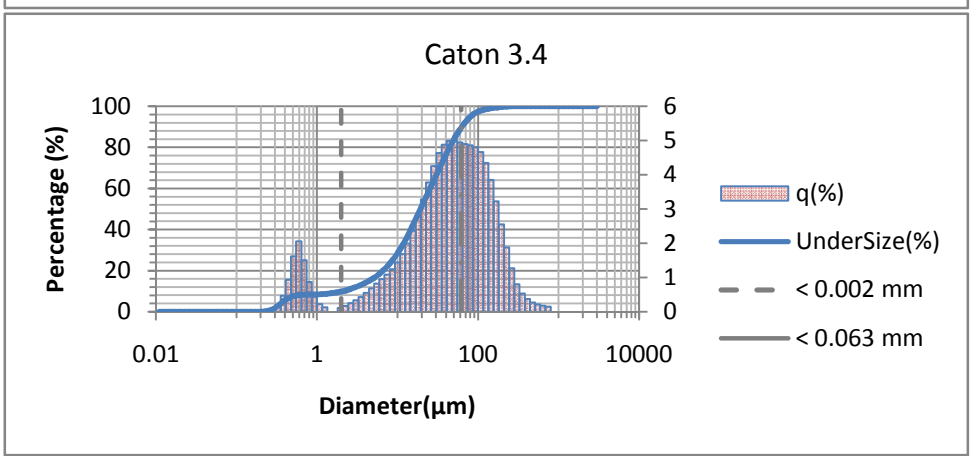

Caton4		
Clay	**9.20**	%
Silt	**78.35**	%
Sand	**12.45**	%

CatonBay4.1			CatonBay4.3			CatonBay4.3		
Clay	9.07	%	Clay	9.19	%	Clay	9.34	%
Silt	78.30	%	Silt	78.11	%	Silt	78.64	%
Sand	12.63	%	Sand	12.70	%	Sand	12.02	%

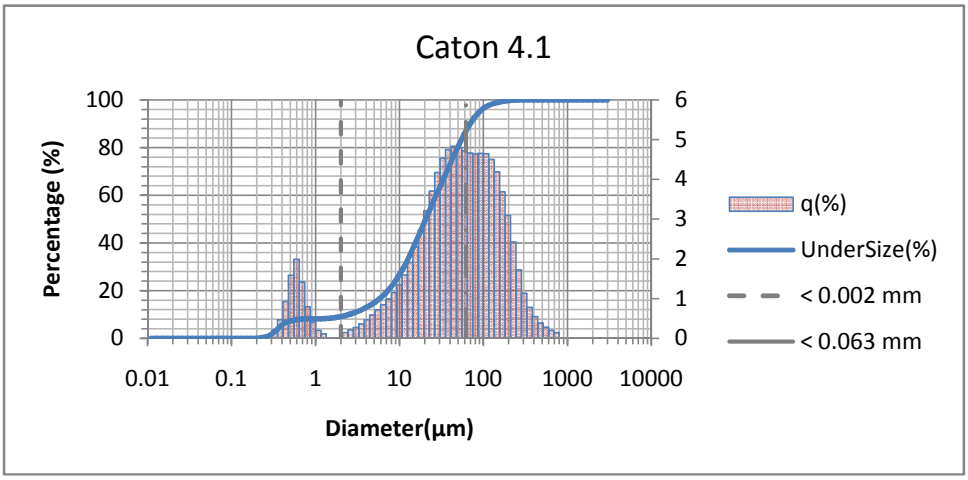

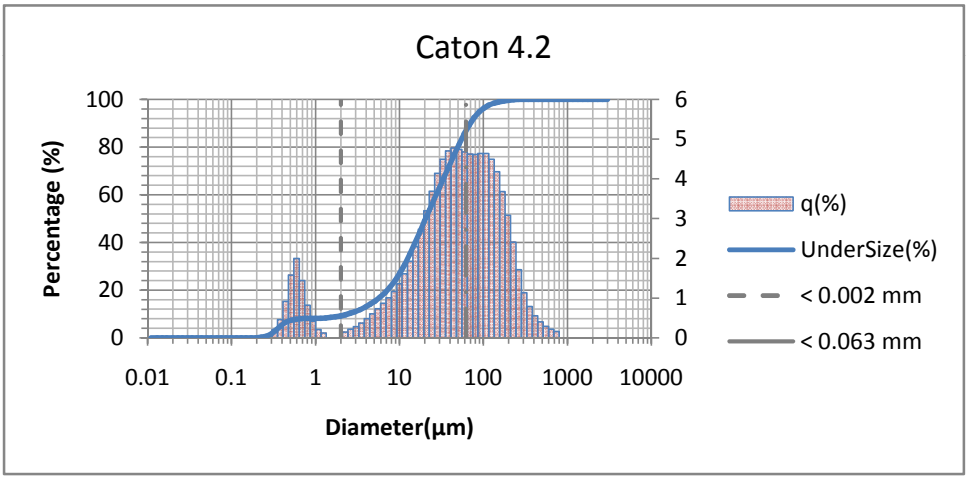

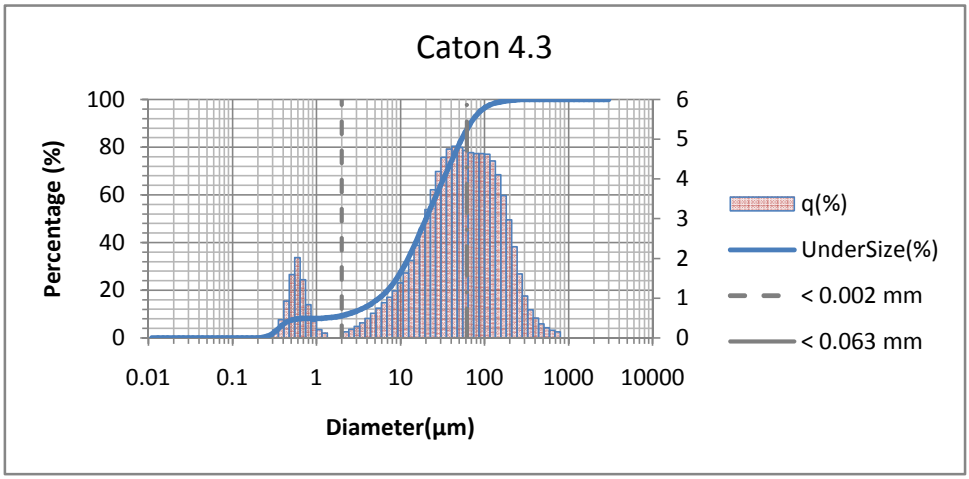

Okana1		
Clay	**5.30**	%
Silt	**78.36**	%
Sand	**16.34**	%

Okana1.4			Okana1.6			Okana1.7		
Clay	5.11	%	Clay	5.27	%	Clay	5.52	%
Silt	77.09	%	Silt	78.61	%	Silt	79.38	%
Sand	17.80	%	Sand	16.12	%	Sand	15.10	%

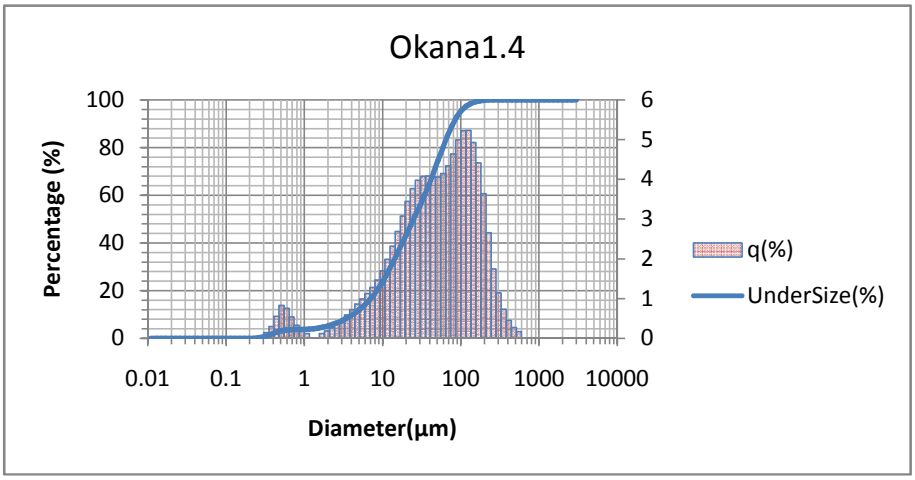

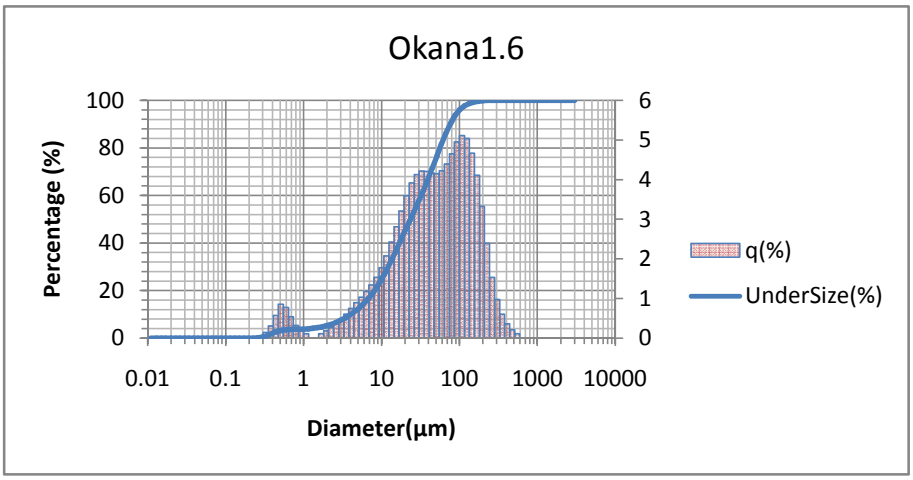

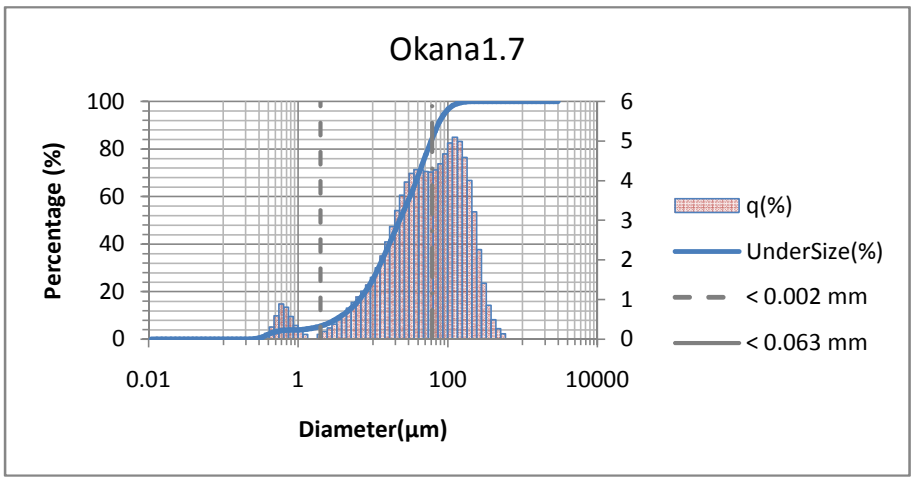

Okana2		
Clay	**5.30**	%
Silt	**78.36**	%
Sand	**16.34**	%

Okana2.2			Okana2.3			Okana2.4		
Clay	5.11	%	Clay	5.27	%	Clay	5.52	%
Silt	77.09	%	Silt	78.61	%	Silt	79.38	%
Sand	17.80	%	Sand	16.12	%	Sand	15.10	%

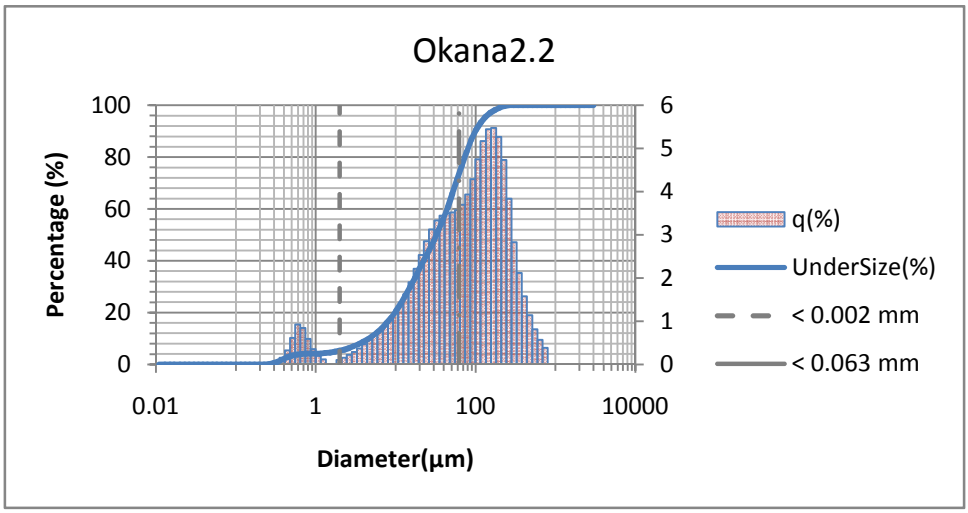

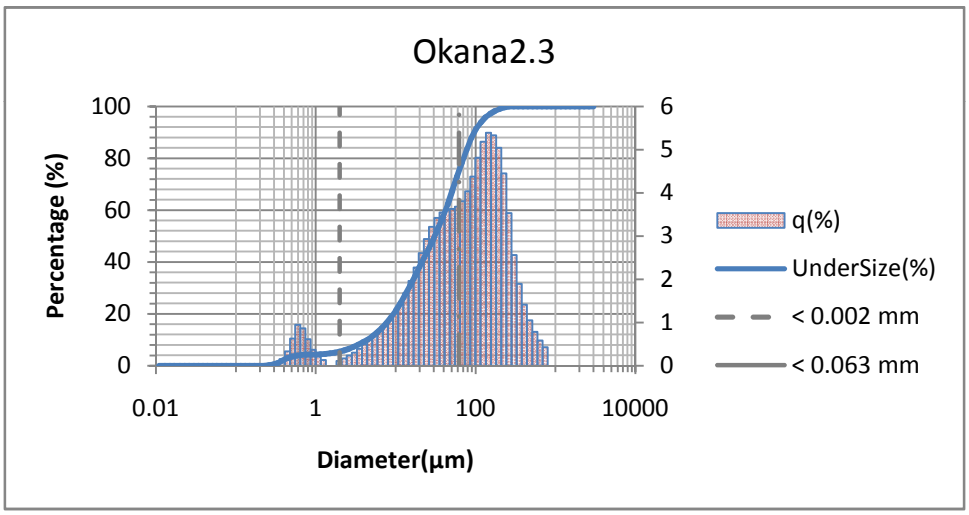

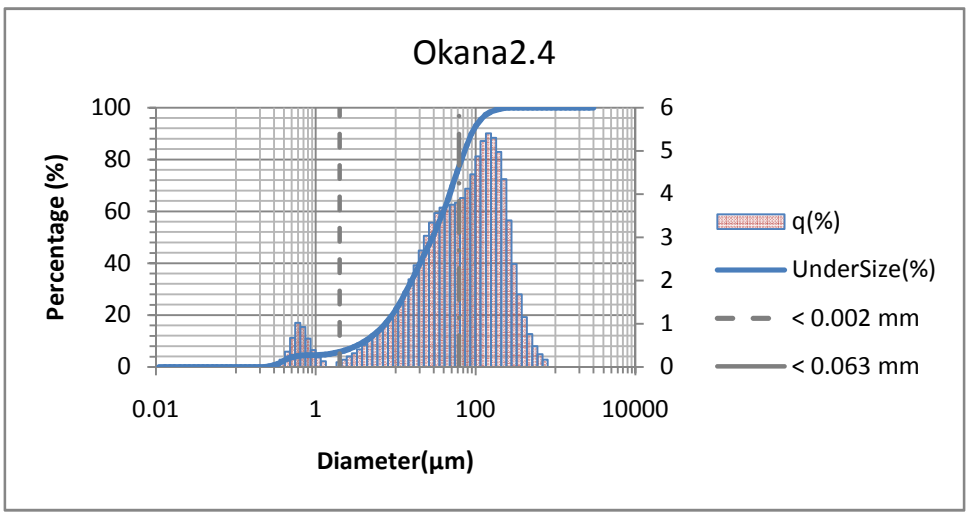

Okana2		
Clay	**5.30**	%
Silt	**78.36**	%
Sand	**16.34**	%

Okana2.2			Okana2.3			Okana2.4		
Clay	5.11	%	Clay	5.27	%	Clay	5.52	%
Silt	77.09	%	Silt	78.61	%	Silt	79.38	%
Sand	17.80	%	Sand	16.12	%	Sand	15.10	%